

Utah State University

DigitalCommons@USU

All Graduate Theses and Dissertations, Fall
2023 to Present

Graduate Studies

12-2024

Analysis of an Outdoor Pilot-Scale Rotating Algae Biofilm Reactor for Power Optimization, Ash-Enhanced Productivity, And Nutrient Uptake

Peter F. Jeppesen
Utah State University

Follow this and additional works at: <https://digitalcommons.usu.edu/etd2023>



Part of the [Biological Engineering Commons](#), and the [Biology Commons](#)

Recommended Citation

Jeppesen, Peter F., "Analysis of an Outdoor Pilot-Scale Rotating Algae Biofilm Reactor for Power Optimization, Ash-Enhanced Productivity, And Nutrient Uptake" (2024). *All Graduate Theses and Dissertations, Fall 2023 to Present*. 335.

<https://digitalcommons.usu.edu/etd2023/335>

This Thesis is brought to you for free and open access by the Graduate Studies at DigitalCommons@USU. It has been accepted for inclusion in All Graduate Theses and Dissertations, Fall 2023 to Present by an authorized administrator of DigitalCommons@USU. For more information, please contact digitalcommons@usu.edu.



ANALYSIS OF AN OUTDOOR PILOT-SCALE ROTATING ALGAE BIOFILM
REACTOR FOR POWER OPTIMIZATION, ASH-ENHANCED
PRODUCTIVITY, AND NUTRIENT UPTAKE

by

Peter F. Jeppesen

A thesis submitted in partial fulfillment
of the requirements for the degree

of

MASTER OF SCIENCE

in

Biological Engineering

Approved:

Ronald C. Sims, Ph.D.
Major Professor

Phillip E. Heck, Ph.D.
Committee Member

Luguang Wang, Ph.D.
Committee Member

D. Richard Cutler, Ph.D.
Vice Provost of Graduate
Studies

UTAH STATE UNIVERSITY
Logan, Utah

2024

ABSTRACT

Analysis of an Outdoor Pilot-Scale Rotating Algae Biofilm Reactor for Power
Optimization, Ash-Enhanced Productivity, and Nutrient Uptake

by

Peter Jeppesen, Master of Science

Utah State University, 2024

Major Professor: Dr. Ronald C. Sims
Department: Biological Engineering

An outdoor pilot-scale rotating algae biofilm reactor (RABR) was successfully implemented for nutrient uptake and productivity testing. Power reduction was performed by modulating duty cycle and rotational speed. Optimal power consumption values for nutrient removal were 1.36 kWh/kg_{TKN} (nitrogen) and 20.1 kWh/kg_{TP} (phosphorus). Maximum average footprint productivity was 7.09 g/m²-day. Comprehensive statistical analyses of productivity, ash content, liquid nutrients, and pH validated continuous flow stirred tank reactor (CFSTR) behavior and affirmed effects of operating parameters on reactor performance. Further statistical analysis delineated productivity differences due to light attenuation. Multiple linear regression established high correlation between light/temperature levels and productivity, ash content, and pH. Elemental balances showed a biomass nitrogen content within 1% of known stoichiometry of microalgae and elevated phosphorus, providing real-world evidence of luxury phosphorus uptake. Analysis of inorganic salts was performed, showing 0.68% w/w of the dry biofilm was comprised of struvite.

(119 pages)

PUBLIC ABSTRACT

Analysis of an Outdoor Pilot-Scale Rotating Algae Biofilm Reactor for Power
Optimization, Ash-Enhanced Productivity, and Nutrient Uptake

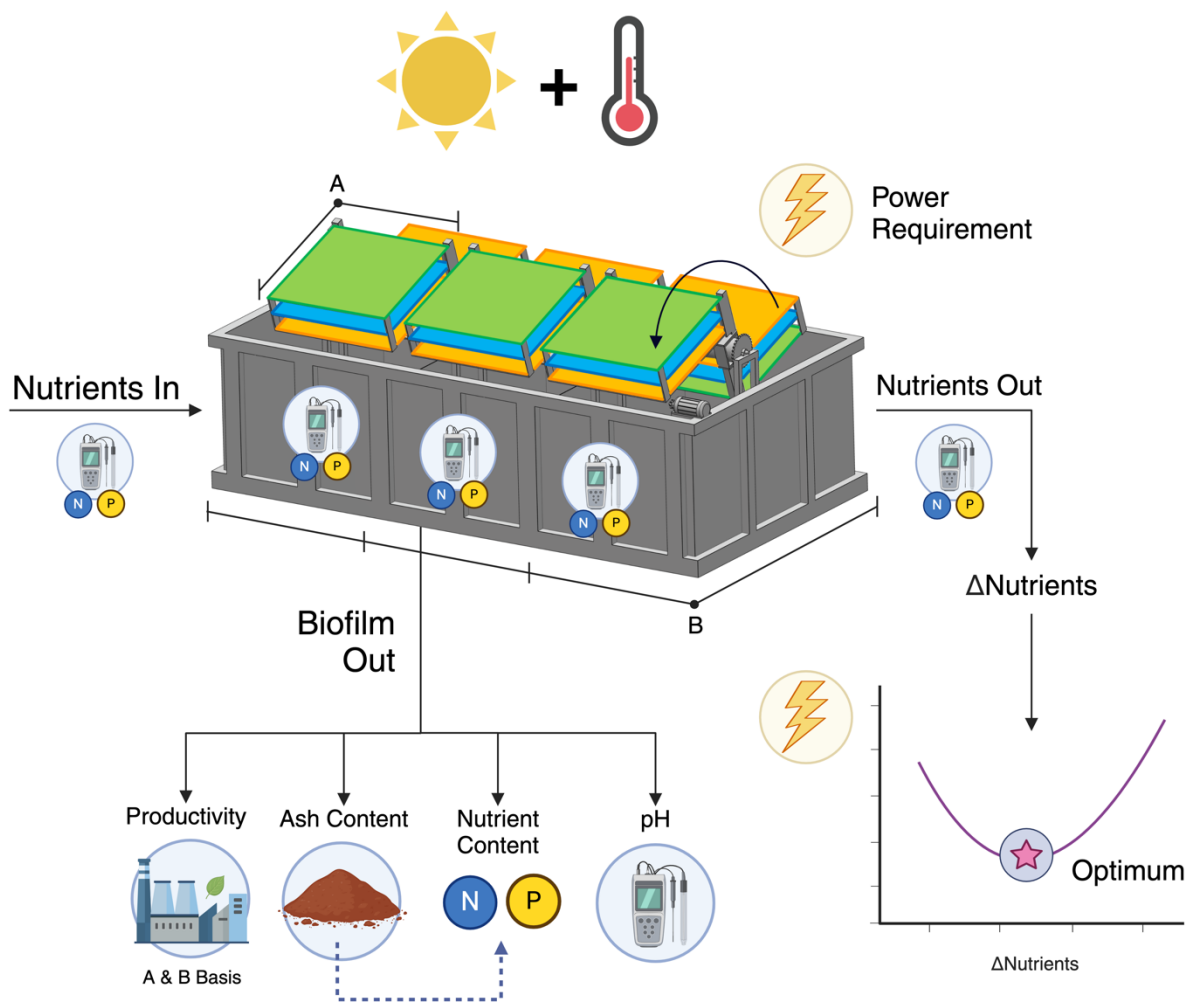
Peter Jeppesen

Outdoor testing of a rotating algae biofilm reactor (RABR) was performed to see how well it could remove nutrients from water and produce algae. By adjusting the operation settings, we found the lowest power needed to remove nitrogen and phosphorus. The lowest power values needed were 1.36 kWh per kilogram of nitrogen and 20.1 kWh per kilogram of phosphorus. The algae production rate reached a maximum of 7.09 grams per square meter per day. Detailed analysis showed that the reactor worked like a continuous flow system, and the performance was influenced by factors including light and temperature. The results also indicated that the algae absorbed more phosphorus than usual, which could be evidence of a phenomenon known as luxury phosphorus uptake. Additionally, a small amount (0.68%) of the biofilm's dry weight was made up of a compound called struvite.

DEDICATION

To my wife, Kate. I quite literally could not have finished this thesis without you.

FRONTISPIECE



ACKNOWLEDGMENTS

This research was funded by the U.S. Department of Energy Bioenergy Technology Office under award 446 number DE-EE0009271 to Utah State University. The views expressed in this article do not necessarily represent the views of the U.S. DOE or the United States Government. Neither the U.S. Government nor any agency thereof, nor any of their employees, makes any warranty, expressed, or implied, or assumes any legal liability or responsibility for the accuracy, completeness, or usefulness of any information, apparatus, product, or process disclosed, or represents that its use would not infringe privately owned rights.

Special thanks to Dr. Phil Heck, manager of CVWRF, for providing the host site and staff to assist with RABR maintenance. Additional thanks to Jim Judd from WesTech Engineering for his essential role in pilot construction and power draw measurements. Thanks to Joshua Wintch for development of standard curves for nitrogen and phosphorus quantification. Additional thanks to Dietr Storrer for help in drafting the introduction to this thesis, in addition to assistance harvesting, drying, and ashing biofilm.

Thanks to my parents, Anne and Ty Jeppesen, for their constant support and love of learning. Final thanks to my wife, Kate, and our son, William, for being my motivation and inspiration.

Peter Jeppesen

CONTENTS

Page

ABSTRACT	ii
PUBLIC ABSTRACT	iii
DEDICATION	iv
FRONTISPIECE.....	v
ACKNOWLEDGMENTS	vi
LIST OF TABLES	ix
LIST OF FIGURES	x
CHAPTER 1: INTRODUCTION	2
Literature Review.....	2
Scope of Work	5
References.....	9
CHAPTER 2: MAIN BODY	13
1. Introduction.....	13
2. Material and methods.....	16
2.1 RABR Structure	16
2.2 Power Measurement.....	19
2.2.1 Power Considerations in Operation	20
2.2.2 Power Requirements for Nutrient Removal.....	20
2.3 Biomass Harvesting	21
2.4 Dry Weight and Ash-Free Dry Weight.....	21
2.4.1 Footprint and Substratum Productivity	22
2.4.2 Ash Percentage Collection	23
2.5 Filtrate, Liquid Sampling, and Analysis	23
2.6 Light and Temperature Measurements	24
2.7 Biofilm and Ash Constituents.....	25
2.7.1 Total Phosphorus and Total Kjeldahl Nitrogen	25
2.7.2 Element Scan	26
2.8 Statistical Analyses	26
3. Results and Discussion	29
3.1 Power Reduction using Duty Cycle.....	29
3.2 Productivity.....	30
3.2.1 Bay Statistical Analysis	30

3.2.2 Section Statistical Analysis	31
3.2.3 Shelf Statistical Analyses	32
3.2.3.1 Combined Shelf Comparison	33
3.2.3.2 Individual Shelf Comparison	35
3.2.4 Light and Temperature Correlation	36
3.2.5 Biofilm Weight	39
3.3 Ash Content	39
3.3.1 Ash Content Statistical Analyses	40
3.3.2 Light and Temperature Correlation	41
3.4 Nutrient Uptake.....	43
3.4.1 Zero-Order Kinetics	43
3.4.2 Liquid Nutrient Statistical Analyses.....	44
3.4.3 Nutrient Uptake Power Requirements.....	45
3.4.4 Inorganic Salt Quantification.....	47
3.4.5 Nitrogen and Phosphorus Balances	50
3.5 pH Measurements	51
3.5.1 pH Statistical Analyses	52
3.5.2 Light, Temperature, and Productivity Correlation.....	53
4. Engineering Management Options	57
6. Conclusions and Future Work	60
7. References.....	63
APPENDIX.....	65

LIST OF TABLES

	Page
Table 1. Advantages and disadvantages of algae biofilm systems.....	2
Table 2. Pilot-scale algae biofilm reactor productivities.....	3
Table 3. Pilot-scale rotating algae biofilm reactor nutrient uptake and power requirements.....	5
Table 4. Average productivity values.....	30
Table 5. Productivity multiple linear regression tests.....	37
Table 6. Average ash content values.....	39
Table 7. Ash content multiple linear regression tests.....	41
Table 8. Average liquid nutrient reduction.....	43
Table 9. Summary of expected power consumption using empirical liquid-phase nutrient removal data.....	46
Table 10. Struvite (NH ₄ MgPO ₄) quantification for 25% duty cycle.....	47
Table 11. Struvite (NH ₄ MgPO ₄) quantification for 50% duty cycle.....	48
Table 12. Biofilm inorganic phosphorus quantification.....	49
Table 13. Nitrogen and phosphorus balances for algae biomass.....	50
Table 14. Average pH values.....	52
Table 15. Simple linear regression for pH.....	53
Table 16. Multiple linear regression for pH.....	56

LIST OF FIGURES

	Page
Figure 1. Outdoor pilot-scale rotating algae biofilm reactor.....	6
Figure 2. Three-dimensional model of the pilot-scale rotating algae biofilm reactor.....	17
Figure 3. Three-dimensional model of the pilot-scale rotating algae biofilm reactor under scaled-section operation.....	18
Figure 4. Complete rotating algae biofilm reactor system.....	19
Figure 5. Algae biofilm growth using the outdoor pilot-scale rotating algae biofilm reactor.....	21
Figure 6. Representation of statistical analyses performed using empirical data obtained from the pilot-scale rotating algae biofilm reactor.....	28
Figure 7. Power reduction of the pilot-scale rotating algae biofilm reactor.....	29
Figure 8. Visualization of productivity multiple regression tests.....	38
Figure 9. Visualization of ash content multiple regression tests.....	42
Figure 10. Visualization of simple linear regression tests to correlate rotating algae biofilm reactor pH values with average daily light integral.....	54
Figure 11. Visualization of simple linear regression tests to correlate rotating algae biofilm reactor pH values with average air temperature.....	55
Figure 12. Visualization of pH multiple regression tests.....	57

CHAPTER 1: INTRODUCTION

There is evidence microalgae have been used in wastewater remediation for over 3000 years (US, 2011; Vaz et al., 2023). Due to increasing environmental, societal, and regulatory pressure, the past 50 years have seen increased innovation in microalgae cultivation (Ubando et al., 2020). Two noteworthy algae cultivation methods include attached and suspended growth (Katarzyna et al., 2015).

Attached-growth systems, also known as biofilm reactors, hold potential for commercialization (Richard Kingsley et al., 2023). With lower moisture content than suspended-growth systems, attached-growth algae cultivation systems require less energy to be converted into value-added bioproducts (Barlow et al., 2016; Johnson and Wen, 2010; Kannah et al., 2021; Patwardhan et al., 2022; Ubando et al., 2020).

Literature Review

Biofilm reactors have additional advantages over suspended-growth systems. Biofilm reactors hold operational potential for use as biorefineries in downstream generation of biocrude, bioplastic, biodiesel, and biofertilizer (Katarzyna et al., 2015; Roostaei et al., 2018; Zhuang et al., 2020). However, biofilm reactors are not without operational disadvantages compared to suspended-growth systems. These advantages and disadvantages are summarized in Table 1.

Table 1. Advantages and disadvantages of algae biofilm systems, compared to suspended growth systems. Interpreted from (Wang et al., 2017; Zhuang et al., 2020).

Advantages	Disadvantages
<ul style="list-style-type: none"> • Simple harvesting and dewatering • High cell density • Potential higher productivity <ul style="list-style-type: none"> ○ Improved CO₂ and O₂ transfer • Increased microalgae resilience 	<ul style="list-style-type: none"> • Substratum spacing limits light availability • Nutrient over-depletion • Substratum deterioration • Labor intensive <ul style="list-style-type: none"> ○ High operating cost

As shown in Table 1, biofilm reactor systems can generate biomass with lower moisture levels than suspended growth systems. Biofilm reactor systems also increase microalgae hardiness. Extreme light, nutrient, pH, and temperature conditions affect biofilm productivity for a time, but when favorable conditions return, attached-growth algae cultivation systems can return to maximum productivity (Blanken et al., 2014; Patwardhan et al., 2022; Sebestyén et al., 2016).

In addition, microalgae consortia cultured using biofilm reactors provide diverse ecosystems which readily regrow during routine harvesting. This resilience contributes to higher productivity as the biofilm matures (Cheah and Chan, 2021; Schnurr et al., 2016). Additionally, some species of microalgae can exhibit heterotrophic metabolic activity under low-light conditions (Fica and Sims, 2016; Roostaei et al., 2018; Zhuang et al., 2020). This study can benefit from these advantages, while considering the disadvantages which would hinder an attached-growth system's performance for biofilm productivity and nutrient uptake. Because this study focuses on the productivity and nutrient uptake of

attached-growth microalgae, Table 2 provides best-case data for pilot-scale biofilm reactors. The pilot-scale biofilm reactors in Table 2 comprise several embodiments for comparison to results of this study.

Table 2. Pilot-scale algae biofilm reactor productivities (Gross et al., 2015; Hoh et al., 2016; Wang et al., 2017).

Biofilm Reactor Type	Culture Medium	Algal Species	Substratum Material	Footprint Productivity (g/m ² -day)	Substratum Productivity (g/m ² -day)	Institution	Reference
Revolving algal biofilm (RAB) cultivation system	Synthetic	<i>Chlorella vulgaris</i>	Cotton duck	46.8	NA	Iowa State University	(Gross et al., 2015)
RAB cultivation system	Synthetic	<i>Chlorella vulgaris</i>	Cotton duck	21.5 18.9 (ash-free)	5.8 5.1 (ash-free)	Iowa State University	(Gross and Wen, 2014)
RAB-enhanced open-pond	Synthetic	<i>Chlorella vulgaris</i>	Cotton duck	12.8	4.3	Iowa State University	(Gross et al., 2013)
RAB-enhanced open-pond	Synthetic	<i>Chlorella vulgaris</i>	Cotton duck	6.8	2.0	Iowa State University	(Gross et al., 2013)
RABR with spool harvester	Municipal wastewater	Consortium	Cotton rope	31	NA	Utah State University	(Christenson and Sims, 2012)
Hybrid high-rate pond biofilm reactor	Municipal wastewater	Consortium	Cotton Interlace	NA	9.99	Federal University of Viçosa	(De Assis et al., 2017)
Algal turf scrubber	Eutrophic riverine	Consortium	3D mesh screen	53.7	NA	University of Maryland	(Witarsa et al., 2020)
Algal turf scrubber	Dairy manure wastewater	Consortium	Mesh nylon netting	24	NA	United States Department of Agriculture	(Mulbry et al., 2008)
Hypothetical algal turf scrubber	Dairy manure wastewater	Consortium	Polyethylene liner	22 ^a	NA	University of Maryland	(Pizarro et al., 2006)
Algadisk system	Synthetic	<i>Chlorella sorokiniana</i>	Polyvinyl chloride	8.4	4.7 ^b	Bay Zoltán Nonprofit Ltd. for Applied Research	(Sebestyén et al., 2016)
Phototrophic biofilm reactor	Municipal wastewater	Consortium	Polyethylene-based woven geotextile	NA	4.5	Wageningen University	(Boelee et al., 2014)
Attached cultivation method with vertical planar matrix bioreactor	Synthetic	<i>Scenedesmus obliquus</i>	Filter paper mounted on glass	50	NA	Chinese Academy of Sciences, Qingdao	(Liu et al., 2013)
Twin-layer biofilm photobioreactor	Synthetic	<i>Halochlorella rubescens</i>	Printing paper	50 ^a	12.5 ^{a,b}	Universität zu Köln	(Schultze et al., 2015)
Rotating drum biofilm reactor	Synthetic	<i>Chlorella vulgaris</i> FACH B-31	Canvas	54.5	NA	Fuzhou University	(Shen et al., 2016)
Pilot-Scale RABR	Anaerobic Digester Effluent	Consortium	Polyethylene Carpet	8.8 4.5 (ash-free)	2.8 1.4 (ash-free)	Utah State University	This study

a. Predicted data

b. Values calculated using empirical data

The pilot-scale biofilm reactors referenced in Table 2 report productivity values using footprint and/or substratum bases. The footprint productivity basis is especially relevant when comparing biofilm reactors to suspended-growth systems. Suspended-growth systems tend to require a much larger land and water footprint than biofilm reactors (Wang et al., 2017). This difference gives biofilm reactors an advantage due to their higher cell densities and vertical growth capabilities.

Despite advantages in cell density and vertical growth, biofilm reactors are still inconsistent in real-world applications. Many manuscripts show inconsistency in productivity and nutrient uptake when systems are operated in pilot-scale configurations (Lutzu et al., 2021). However, the abundance of literature regarding lab-scale algae biofilm reactors is helpful for investigating new pilot-scale reactor configurations. There exists a gap in literature for power requirements of rotating biofilm reactors. Several studies discuss power requirements associated with pumping nutrients into a biofilm reactor and energy output from algae biomass productivity (Choudhary et al., 2022; Ennaceri et al., 2023; Gerardo et al., 2015; Mendoza et al., 2013; Morales et al., 2020; Rezvani et al., 2022; Sims and Peterson, 2021). However, only one study was found which offered an indication of power required to rotate the reactor (Table 3). Standardization of power requirements is vital for normalization of data and scaleup of biofilm reactors.

Table 3. Pilot-scale rotating algae biofilm reactor nutrient uptake and power requirements (Kesaano and Sims, 2014).

Biofilm Reactor Type	Instantaneous Power Draw (W)	Flow (L/min)	Influent Nitrogen (mg/L)	Average Percent Nitrogen Removal	Influent Phosphorus (mg/L)	Average Percent Phosphorus Removal	Optimal Power Consumption (kWh/kg)	Institution	Reference
RABR with spool harvester	6	11.4	4.5 ^a	75.6%	2.1 ^a	23.8%	TDP: 17.5 ^b TDN: 2.6 ^b	Utah State University	(Christenson and Sims, 2012)
Pilot-Scale RABR	28.3/18.9 ^c	367	15.5	21.4%	15.5	38.0%	TDP: 20.1 ^b TDN: 1.4 ^b	Utah State University	This study

a. Influent values estimated from graphs
b. Values calculated using empirical data
TDP = Total dissolved phosphorus
TN = Total dissolved nitrogen
c. Empirically measured using two separate operating conditions

Using optimal power consumption values, this study can satisfy the gap in literature by reporting power requirements (kWh/kg) for removal of dissolved nitrogen and phosphorus in liquid samples.

Scope of Work

The aim of this study is to optimize the energy consumption and biorefinery capabilities of a pilot-scale rotating algae biofilm reactor (RABR). This RABR, located at Central Valley Water Reclamation Facility (CVWRF) in Salt Lake City, Utah, removes highly concentrated nutrients from anaerobic digester effluent. This anaerobic digester effluent, known as “filtrate,” flows from a dewatering belt press to the headworks of CVWRF. Because the RABR is situated on a return stream, the testing conditions provide a low-risk proof of concept of the RABR’s capabilities.

The RABR used in this study is a modified continuous flow stirred tank reactor (CFSTR) (Figure 1). The RABR is comprised of a 11.6-m³ tank divided into three equally sized bays. By adjusting the rate of filtrate flow into the RABR, the system can

accommodate a predetermined hydraulic retention time (HRT) across the bays. The RABR is further comprised of a central shaft which spans the three bays and is attached to six shelves per bay. Each shelf is equipped with 2 m² recycled polyethylene (PET) carpet substratum which facilitate the growth of algae biofilm.



Fig. 1. Outdoor pilot-scale rotating algae biofilm reactor, located at CVWRF in Salt Lake City, Utah (40°42'19.9"N 111°54'35.3"W).

Filtrate from the anaerobic digester serves as influent to the first bay. The nutrients found in the filtrate are taken up by microalgae grown on the PET carpet. The rotating shaft allows the adherent microalgae to uptake sunlight and carbon dioxide while not submerged in the filtrate. The primary nutrients of interest to this project are nitrogen and phosphorus.

Four main benefits to using the algae biofilm reactor are as follows: Uptake of nutrients using naturally occurring microalgae, production of precursors to value-added

bioproducts, operation using a relatively small footprint, and productivity of low-moisture biomass (Katarzyna et al., 2015; Roostaei et al., 2018; Zhuang et al., 2020).

This project seeks to maintain nutrient uptake and biomass generation, while minimizing the system's power requirements. As such, this project explores variability of duty cycle (percentage of time rotating to time stationary) and rotational speed (RPM) to decrease the RABR's instantaneous power draw to drive the rotating assembly. When the optimal duty cycle and RPM pairings are obtained, the pairing is applied in operation for productivity and nutrient uptake testing. If productivity can be correlated to variation in duty cycle, the system can optimize net energy output.

Standards for reducing the RABR's power draw are provided by the United States Department of Energy (DOE). To begin, the DOE imposed a reduction of 15% from a baseline power consumption, reported in units of kWh/kg total phosphorus (TP) dissolved in the liquid filtrate. Upon realization of this reduction, the DOE set a reduction of 20% from the baseline power consumption, reported in kWh/kg TP, as used previously. In addition to optimization using TP, this study optimizes power consumption responsible for removal of total Kjeldahl nitrogen (TKN) from the liquid phase.

Through advances in bioprocessing, microalgae have become more attractive for use in biofuels, biopolymers, livestock feed, and pharmaceuticals (Katarzyna et al., 2015; Lutzu et al., 2021). If biofilm reactors can be optimized in industrial settings, costs of wastewater treatment can be offset through the sale of bioproducts (Kesaano and Sims, 2014; Zamalloa et al., 2013). By coupling value-added bioproducts with environmental sustainability, attached-growth microalgae cultivation systems hold significant industrial potential (Ubando et al., 2020).

This thesis is an expanded version of work described in a manuscript under current revision for refereed publication. This manuscript, found in the Appendix section of this document, was submitted to *Bioresource Technology* on June 4, 2024.

This research was funded by the U.S. Department of Energy Bioenergy Technology Office under award 446 number DE-EE0009271 to Utah State University. The views expressed in this article do not necessarily represent the views of the U.S. DOE or the United States Government. Neither the U.S. Government nor any agency thereof, nor any of their employees, makes any warranty, expressed, or implied, or assumes any legal liability or responsibility for the accuracy, completeness, or usefulness of any information, apparatus, product, or process disclosed, or represents that its use would not infringe privately owned rights.

References

- Barlow, J., Sims, R.C., Quinn, J.C., 2016. Techno-economic and life-cycle assessment of an attached growth algal biorefinery. *Bioresour. Technol.* 220, 360–368. <https://doi.org/10.1016/j.biortech.2016.08.091>
- Blanken, W., Janssen, M., Cuaresma, M., Libor, Z., Bhajji, T., Wijffels, R.H., 2014. Biofilm growth of *Chlorella sorokiniana* in a rotating biological contactor based photobioreactor. *Biotechnol. Bioeng.* 111, 2436–2445. <https://doi.org/10.1002/bit.25301>
- Boelee, N.C., Janssen, M., Temmink, H., Shrestha, R., Buisman, C.J.N., Wijffels, R.H., 2014. Nutrient Removal and Biomass Production in an Outdoor Pilot-Scale Phototrophic Biofilm Reactor for Effluent Polishing. *Appl. Biochem. Biotechnol.* 172, 405–422. <https://doi.org/10.1007/s12010-013-0478-6>
- Cheah, Y.T., Chan, D.J.C., 2021. Physiology of microalgal biofilm: a review on prediction of adhesion on substrates. *Bioengineered* 12, 7577–7599. <https://doi.org/10.1080/21655979.2021.1980671>
- Choudhary, S., Tripathi, S., Poluri, K.M., 2022. Microalgal-Based Bioenergy: Strategies, Prospects, and Sustainability. *Energy Fuels* 36, 14584–14612. <https://doi.org/10.1021/acs.energyfuels.2c02922>
- Christenson, L.B., Sims, R.C., 2012. Rotating algal biofilm reactor and spool harvester for wastewater treatment with biofuels by-products. *Biotechnol. Bioeng.* 109, 1674–1684. <https://doi.org/10.1002/bit.24451>
- De Assis, L.R., Calijuri, M.L., Do Couto, E.D.A., Assemany, P.P., 2017. Microalgal biomass production and nutrients removal from domestic sewage in a hybrid high-rate pond with biofilm reactor. *Ecol. Eng.* 106, 191–199. <https://doi.org/10.1016/j.ecoleng.2017.05.040>
- Ennaceri, H., Ishika, T., Mkpuma, V.O., Moheimani, N.R., 2023. Microalgal biofilms: Towards a sustainable biomass production. *Algal Res.* 72, 103124. <https://doi.org/10.1016/j.algal.2023.103124>
- Fica, Z.T., Sims, R.C., 2016. Algae-based biofilm productivity utilizing dairy wastewater: effects of temperature and organic carbon concentration. *J. Biol. Eng.* 10, 18. <https://doi.org/10.1186/s13036-016-0039-y>
- Gerardo, M.L., Van Den Hende, S., Vervaeren, H., Coward, T., Skill, S.C., 2015. Harvesting of microalgae within a biorefinery approach: A review of the developments and case studies from pilot-plants. *Algal Res.* 11, 248–262. <https://doi.org/10.1016/j.algal.2015.06.019>
- Gross, M., Henry, W., Michael, C., Wen, Z., 2013. Development of a rotating algal biofilm growth system for attached microalgae growth with in situ biomass harvest. *Bioresour. Technol.* 150, 195–201. <https://doi.org/10.1016/j.biortech.2013.10.016>
- Gross, M., Mascarenhas, V., Wen, Z., 2015. Evaluating algal growth performance and water use efficiency of pilot-scale revolving algal biofilm (RAB) culture systems. *Biotechnol. Bioeng.* 112, 2040–2050. <https://doi.org/10.1002/bit.25618>
- Gross, M., Wen, Z., 2014. Yearlong evaluation of performance and durability of a pilot-scale Revolving Algal Biofilm (RAB) cultivation system. *Bioresour. Technol.* 171, 50–58. <https://doi.org/10.1016/j.biortech.2014.08.052>

- Hoh, D., Watson, S., Kan, E., 2016. Algal biofilm reactors for integrated wastewater treatment and biofuel production: A review. *Chem. Eng. J.* 287, 466–473. <https://doi.org/10.1016/j.cej.2015.11.062>
- Johnson, M.B., Wen, Z., 2010. Development of an attached microalgal growth system for biofuel production. *Appl. Microbiol. Biotechnol.* 85, 525–534. <https://doi.org/10.1007/s00253-009-2133-2>
- Kannah, R.Y., Kavitha, S., Banu, J.R., Sivashanmugam, P., Gunasekaran, M., Kumar, G., 2021. A Mini Review of Biochemical Conversion of Algal Biorefinery. *Energy Fuels* 35, 16995–17007. <https://doi.org/10.1021/acs.energyfuels.1c02294>
- Katarzyna, L., Sai, G., Singh, O.A., 2015. Non-enclosure methods for non-suspended microalgae cultivation: literature review and research needs. *Renew. Sustain. Energy Rev.* 42, 1418–1427. <https://doi.org/10.1016/j.rser.2014.11.029>
- Kesaano, M., Sims, R.C., 2014. Algal biofilm based technology for wastewater treatment. *Algal Res.* 5, 231–240. <https://doi.org/10.1016/j.algal.2014.02.003>
- Liu, T., Wang, J., Hu, Q., Cheng, P., Ji, B., Liu, J., Chen, Y., Zhang, W., Chen, X., Chen, L., Gao, L., Ji, C., Wang, H., 2013. Attached cultivation technology of microalgae for efficient biomass feedstock production. *Bioresour. Technol.* 127, 216–222. <https://doi.org/10.1016/j.biortech.2012.09.100>
- Lutzu, G.A., Ciurli, A., Chiellini, C., Di Caprio, F., Concas, A., Dunford, N.T., 2021. Latest developments in wastewater treatment and biopolymer production by microalgae. *J. Environ. Chem. Eng.* 9, 104926. <https://doi.org/10.1016/j.jece.2020.104926>
- Mendoza, J.L., Granados, M.R., De Godos, I., Acién, F.G., Molina, E., Banks, C., Heaven, S., 2013. Fluid-dynamic characterization of real-scale raceway reactors for microalgae production. *Biomass Bioenergy* 54, 267–275. <https://doi.org/10.1016/j.biombioe.2013.03.017>
- Morales, M., Bonnefond, H., Bernard, O., 2020. Rotating algal biofilm versus planktonic cultivation: LCA perspective. *J. Clean. Prod.* 257, 120547. <https://doi.org/10.1016/j.jclepro.2020.120547>
- Mulbry, W., Kondrad, S., Pizarro, C., Kebede-Westhead, E., 2008. Treatment of dairy manure effluent using freshwater algae: Algal productivity and recovery of manure nutrients using pilot-scale algal turf scrubbers. *Bioresour. Technol.* 99, 8137–8142. <https://doi.org/10.1016/j.biortech.2008.03.073>
- Patwardhan, S.B., Pandit, S., Ghosh, D., Dhar, D.W., Banerjee, S., Joshi, S., Gupta, P.K., Lahiri, D., Nag, M., Ruokolainen, J., Ray, R.R., Kumar Kesari, K., 2022. A concise review on the cultivation of microalgal biofilms for biofuel feedstock production. *Biomass Convers. Biorefinery.* <https://doi.org/10.1007/s13399-022-02783-9>
- Pizarro, C., Mulbry, W., Blerch, D., Kangas, P., 2006. An economic assessment of algal turf scrubber technology for treatment of dairy manure effluent. *Ecol. Eng.* 26, 321–327. <https://doi.org/10.1016/j.ecoleng.2005.12.009>
- Rezvani, S., Saadaoui, I., Al Jabri, H., Moheimani, N.R., 2022. Techno-economic modelling of high-value metabolites and secondary products from microalgae cultivated in closed photobioreactors with supplementary lighting. *Algal Res.* 65, 102733. <https://doi.org/10.1016/j.algal.2022.102733>

- Richard Kingsley, P., Braud, L., Kumar Mediboyina, M., McDonnell, K., Murphy, F., 2023. Prospects for commercial microalgal biorefineries: Integrated pilot demonstrations and process simulations based techno-economic assessment of single and multi-product value chains. *Algal Res.* 74, 103190. <https://doi.org/10.1016/j.algal.2023.103190>
- Roostaei, J., Zhang, Y., Gopalakrishnan, K., Ochocki, A.J., 2018. Mixotrophic Microalgae Biofilm: A Novel Algae Cultivation Strategy for Improved Productivity and Cost-efficiency of Biofuel Feedstock Production. *Sci. Rep.* 8, 12528. <https://doi.org/10.1038/s41598-018-31016-1>
- Schnurr, P.J., Molenda, O., Edwards, E., Espie, G.S., Allen, D.G., 2016. Improved biomass productivity in algal biofilms through synergistic interactions between photon flux density and carbon dioxide concentration. *Bioresour. Technol.* 219, 72–79. <https://doi.org/10.1016/j.biortech.2016.06.129>
- Schultze, L.K.P., Simon, M.-V., Li, T., Langenbach, D., Podola, B., Melkonian, M., 2015. High light and carbon dioxide optimize surface productivity in a Twin-Layer biofilm photobioreactor. *Algal Res.* 8, 37–44. <https://doi.org/10.1016/j.algal.2015.01.007>
- Sebestyén, P., Blanken, W., Bacsa, I., Tóth, G., Martin, A., Bhaiji, T., Dergez, Á., Kesserű, P., Koós, Á., Kiss, I., 2016. Upscale of a laboratory rotating disk biofilm reactor and evaluation of its performance over a half-year operation period in outdoor conditions. *Algal Res.* 18, 266–272. <https://doi.org/10.1016/j.algal.2016.06.024>
- Shen, Y., Zhu, W., Chen, C., Nie, Y., Lin, X., 2016. Biofilm formation in attached microalgal reactors. *Bioprocess Biosyst. Eng.* 39, 1281–1288. <https://doi.org/10.1007/s00449-016-1606-9>
- Sims, R., Peterson, B., 2021. Waste to value: algae-based biofuel utilizing oil and gas extraction wastewater. *Acad. Lett.* <https://doi.org/10.20935/AL4460>
- Ubando, A.T., Felix, C.B., Chen, W.-H., 2020. Biorefineries in circular bioeconomy: A comprehensive review. *Bioresour. Technol.* 299, 122585. <https://doi.org/10.1016/j.biortech.2019.122585>
- US, E., 2011. Principles of design and operation of wastewater treatment pond systems for plant operators, engineers, and managers.
- Vaz, S.A., Badenes, S.M., Pinheiro, H.M., Martins, R.C., 2023. Recent reports on domestic wastewater treatment using microalgae cultivation: Towards a circular economy. *Environ. Technol. Innov.* 30, 103107. <https://doi.org/10.1016/j.eti.2023.103107>
- Wang, J., Liu, W., Liu, T., 2017. Biofilm based attached cultivation technology for microalgal biorefineries—A review. *Bioresour. Technol.* 244, 1245–1253. <https://doi.org/10.1016/j.biortech.2017.05.136>
- Witarsa, F., Yarberry, A., May, P., Kangas, P., Lansing, S., 2020. Complementing energy production with nutrient management: Anaerobic digestion system for algal turf scrubber biomass. *Ecol. Eng.* 143, 105618. <https://doi.org/10.1016/j.ecoleng.2019.105618>
- Zamalloa, C., Boon, N., Verstraete, W., 2013. Decentralized two-stage sewage treatment by chemical–biological flocculation combined with microalgae biofilm for

nutrient immobilization in a roof installed parallel plate reactor. *Bioresour. Technol.* 130, 152–160. <https://doi.org/10.1016/j.biortech.2012.11.128>

Zhuang, L.-L., Li, M., Hao Ngo, H., 2020. Non-suspended microalgae cultivation for wastewater refinery and biomass production. *Bioresour. Technol.* 308, 123320. <https://doi.org/10.1016/j.biortech.2020.123320>

CHAPTER 2: MAIN BODY

1. Introduction

Due to increasing environmental, societal, and regulatory pressure, the past 50 years have seen increased innovation in microalgae cultivation (Ubando et al., 2020). With advances in bioprocessing, microalgae cultivation has become more attractive for application in environmental and manufacturing industries (Katarzyna et al., 2015; Lutz et al., 2021). The two most prominent algae cultivation methods include attached- and suspended-growth (Katarzyna et al., 2015). Attached-growth systems, often represented as algae biofilm reactors, hold potential for commercialization (Kesaano and Sims, 2014; Richard Kingsley et al., 2023; Zamalloa et al., 2013). Algae biofilm reactors hold potential for use in a variety of applications. In addition to the immediate benefit of biological nutrient uptake from wastewater, biofilm reactors can serve as biologically induced chemical reactors. This biological induction by algae biomass is a new area of research which can facilitate production of chemical precipitates such as struvite in various industrial or space applications (Espinosa-Ortiz et al., 2023; Goldsberry et al., 2023; Hillman and Sims, 2020).

Biofilm reactors have distinct advantages over suspended-growth systems. Algae biofilm reactors benefit from small footprint areas, simple harvesting and dewatering, high cell density, and enhanced resilience (Cheah and Chan, 2021; Schnurr et al., 2016; Wang et al., 2017; Zhuang et al., 2020). Algae biofilm reactors also hold operational potential for use as biorefineries in sustainable generation of value-added bioproducts, including biocrude, bioplastic, biodiesel, and biofertilizer (Katarzyna et al., 2015; Roostaei et al., 2018; Zhuang et al., 2020). These value-added bioproducts can help offset

costs of wastewater remediation and prove economical for municipal and industrial entities (Barlow et al., 2016; Christenson and Sims, 2011; Johnson and Wen, 2010; Kannah et al., 2021; Patwardhan et al., 2022; Ubando et al., 2020). Algae biofilm reactors, however, are not without flaws. One major drawback of biofilm reactors is light attenuation due to self-shading. This self-shading, caused by spacing of growth substratum, has yet to be investigated quantitatively or statistically through productivity analysis (Wang et al., 2017; Zhuang et al., 2020).

The United States Department of Energy (DOE) is invested in circular engineering through water treatment and bioproduct generation. In the context of this study, the DOE is specifically interested in power requirements for nutrient removal, reported in units of kWh/kg total nutrient removed. However, there remains a gap in literature regarding power requirements for algae biofilm cultivation in an outdoor pilot-scale setting. Only one study has reported a power requirement associated with operating an algae biofilm reactor (Christenson and Sims, 2012). This power requirement, when converted to power consumptions (kWh/kg total nutrient removed), yielded 2.6 kWh/kg_{TKN} (nitrogen) and 17.5 kWh/kg_{TP} (phosphorus). Power requirements associated with real-world algae biofilm reactors are of great importance for scale-up and commercialization of attached-growth algae cultivation technology (Choudhary et al., 2022; Ennaceri et al., 2023; Gerardo et al., 2015; Mendoza et al., 2013; Morales et al., 2020; Rezvani et al., 2022; Sims and Peterson, 2021).

Many studies have been performed using attached-growth microalgae cultivation at a laboratory scale. However, fewer studies have investigated attached-growth microalgae systems at a pilot scale. Of these few pilot-scale studies, many show

inconsistency in productivity and nutrient uptake (Lutzu et al., 2021). One potential cause of the inconsistency associated with outdoor pilot-scale testing of algae biofilm systems (and photosynthetic organisms en masse) is the challenge of determining whether operational parameters or seasonal effects have a greater influence on pilot performance.

This study optimizes the energy consumption and biorefinery capabilities of an outdoor pilot-scale rotating algae biofilm reactor (RABR). This RABR, located at Central Valley Water Reclamation Facility (CVWRF) in Salt Lake City, Utah, removes nitrogen and phosphorus from nutrient-rich anaerobic digester effluent. This anaerobic digester effluent, referred to throughout this document as “filtrate,” flows from a dewatering belt press to the headworks of CVWRF. Because the RABR is situated on a return stream, the testing conditions provide a low-risk proof of concept of the RABR’s capabilities for biofilm productivity and nutrient uptake. The microalgae used in this study is a consortium obtained from a trickling filter located at CVWRF. This study correlates pilot performance parameters, including productivity, ash content, and pH, with light and temperature levels under both seasonal- and operational-specific conditions. This study investigates both dry weight (DW) and ash-free dry weight (AFDW) biofilm productivity using footprint and substratum bases. These productivity values are tested statistically to find spatial productivity differences between growth substrata of the pilot-scale RABR. Additionally, this study presents empirical data to correlate power requirements with removal of nitrogen and phosphorus. Lastly, this study establishes elemental balances using nitrogen and phosphorus to validate biomass stoichiometry and quantify struvite-containing ash content.

This chapter is an expanded version of work described in a manuscript under current revision for refereed publication. This manuscript, found in the Appendix section of this document, was submitted to *Bioresource Technology* on June 4, 2024.

2. Material and methods

The purpose of this section is to describe the structural, operational, and analytical methods for the pilot-scale rotating algae biofilm reactor (RABR). Experimental work consisted of harvesting, drying, ashing, and quantifying nutrient concentrations of algae biofilm cultivated using the RABR. Additionally, experimental work included taking liquid samples for pH, nitrogen, and phosphorus quantification. The experimental period associated with these methods was the fall season of 2023.

2.1 RABR Structure

The RABR was comprised of a steel tank (4.72 m × 2.44 m × 1.22 m interior dimensions, containing 11.5 m³ anaerobic digester effluent), a 0.2-m diameter steel shaft (4.06 m long), and six three-shelved sections (1.15 m × 1.19 m × 0.34 m) (Figure 2). The tank was divided into three bays, with each bay containing two sections. For growth substratum, 2-m² post-consumer recycled carpets were fastened to each shelf (Goldsberry et al., 2023). The rotating assembly, weighing ~785 kg in total, was rotated by a 7.38-kW electric gearbox (172.17:1 box ratio) via a chain to a sprocket (12:1 gear ratio). The electric gearbox allowed for modulation of rotational speed (RPM) and duty cycle (ratio of time rotating to time stationary).

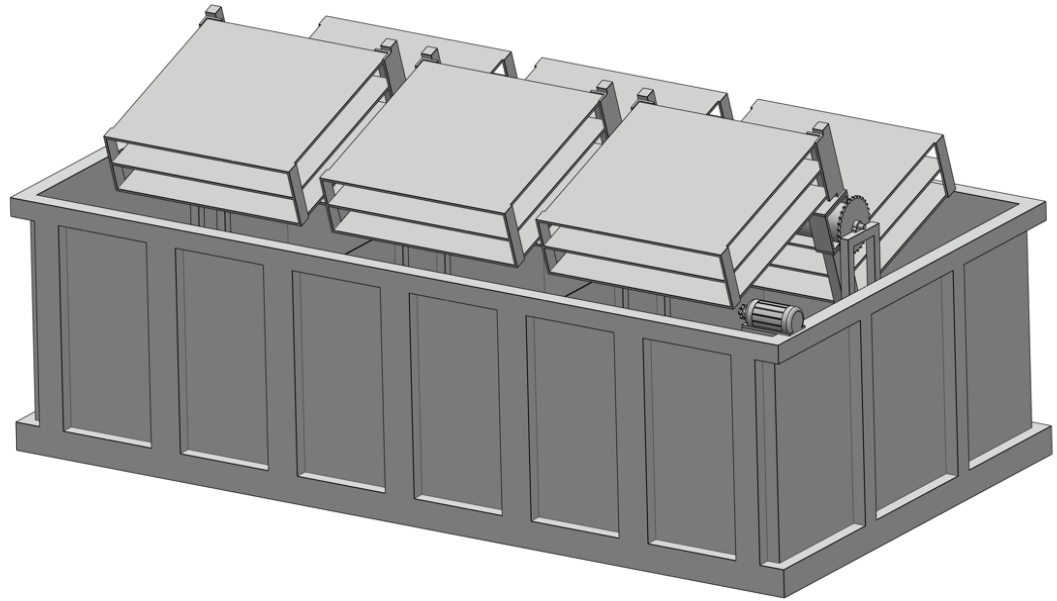


Fig. 2. Three-dimensional model of the pilot-scale rotating algae biofilm reactor.

As shown in Figure 2, the RABR used six 3-shelved sections, while future embodiments could accommodate up to 12 sections. Using 6 sections, the packing factor was 3.1/m. With 12 sections, 36 shelves would be available for algae cultivation (Figure 3), yielding a packing factor of 6.3/m. Full scaleup could allow installation of 5 shelves per section, yielding 60 shelves and a packing factor of 10.5/m.

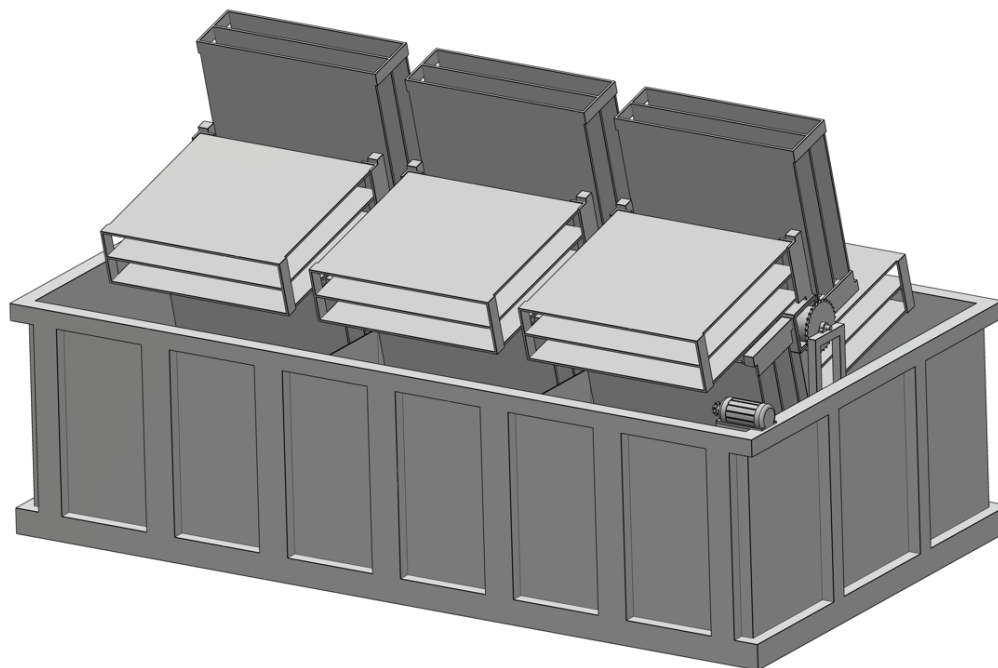


Fig. 3. Three-dimensional model of the pilot-scale rotating algae biofilm reactor under scaled-section operation. An additional two shelves could be added to each section.

To further separate the bays, two polycarbonate sheets were fastened between bays 1 and 2 and bays 2 and 3, attempting to convert the system from a continuous flow stirred tank reactor (CFSTR) to a plug-flow reactor (PFR). Lastly, the RABR system was equipped with a polycarbonate roof and optional polycarbonate walls. These walls were installed at the beginning of December 2023 to prevent the biofilm from freezing. The liquid influent to the RABR system was anaerobic digester effluent. This anaerobic digester effluent, delivered to the system from a filter press, is known throughout this document as “filtrate.” Influent filtrate flow was set to accommodate a 2-day hydraulic retention time (HRT) across bay 1 of the RABR. This HRT translated to a 6-day HRT across the entire RABR, or a flow of approximately 1.33 L/min. To successfully use this filtrate, the RABR system required a clarification step. The RABR’s operation system, coupled with a photograph of the system, is summarized in Figure 4.

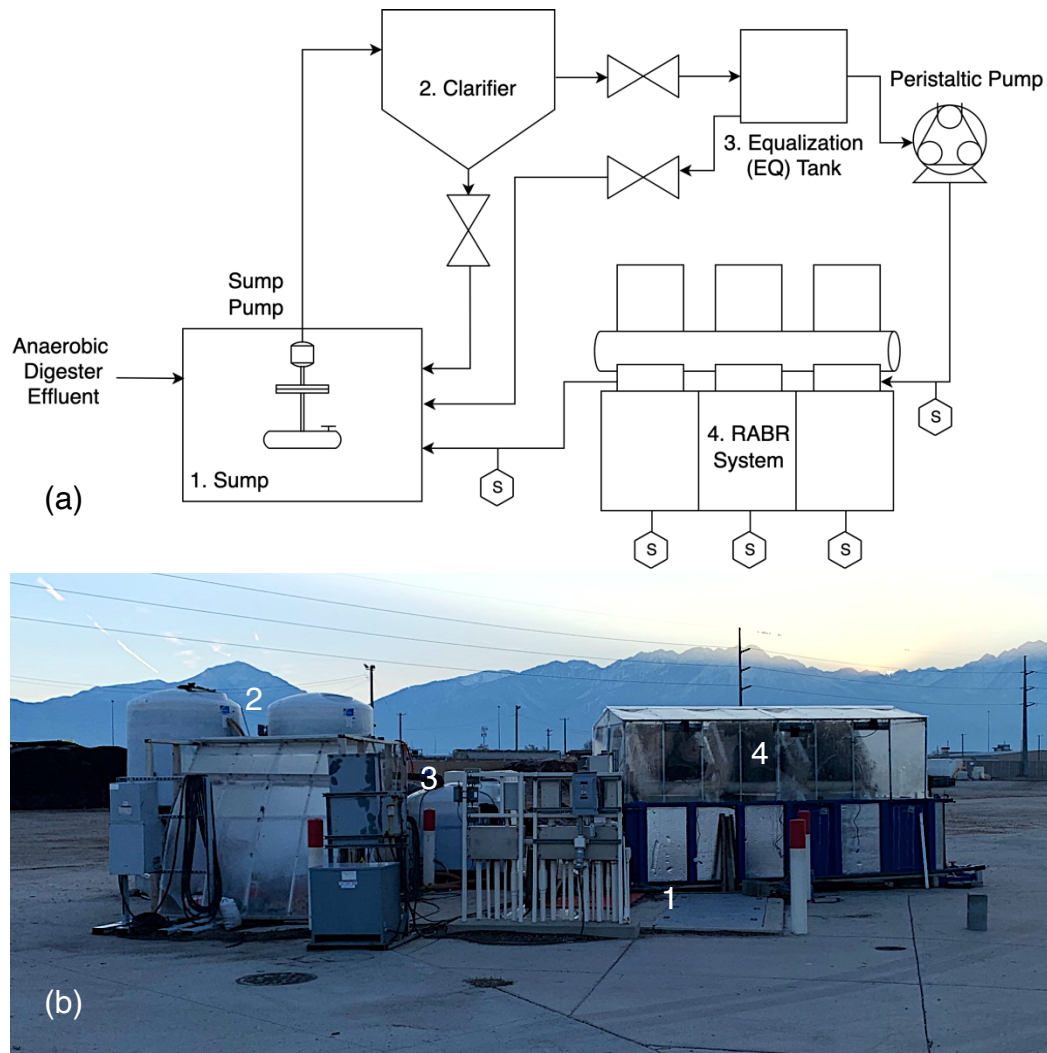


Fig. 4. Complete rotating algae biofilm system, represented by (a) diagram and (b) photograph, located at Central Valley Water Reclamation Facility in Salt Lake City, Utah ($40^{\circ}42'19.9''\text{N}$ $111^{\circ}54'35.3''\text{W}$). In (a), “S” represents liquid sampling points.

2.2 Power Measurement

Power readings were obtained using a Fluke® 39 Power Meter. Readings were taken at the variable frequency drive (VFD) that controlled the electric gearbox. The experimental procedure involved manipulating the rotational speed (RPM) using the VFD and modulating the duty cycle, alternating intervals rotating and stationary, using the system control panel. Power measurements were recorded at twenty 1-min intervals for a

100% duty cycle and forty 15-s intervals for 50% and 25% duty cycles. Preliminary results showed the lowest power draw at 25% and 50% duty cycles using 0.896 RPM; hence, productivity testing was prioritized for these two duty cycle and RPM combinations.

2.2.1 Power Considerations in Operation

The optimal duty cycles found through power measurements were coupled with the optimal RPM and implemented for productivity testing during the fall season of 2023. These duty cycles, 25% and 50%, were both tested in multiple months during the fall season to ensure operating parameters were responsible for variability of RABR output, instead seasonal differences being the driving factor. By implementing optimized duty cycle-RPM combinations, the testing ensured power savings before productivity testing had commenced.

2.2.2 Power Requirements for Nutrient Removal

The nutrients investigated for power optimization were nitrogen and phosphorus (see Material and Methods 2.5). The influent and effluent liquid nutrient concentrations, sampled weekly during the fall season of 2023 using sampling points shown in Figure 4a, were first converted to a mass-flow rate using the flow rate associated with a 6-day HRT for the RABR system. Second, the difference between influent and effluent nutrient mass-flow rates was calculated, constituting a nutrient removal rate. Third, the nutrient removal rate was extended to determine the operation time required to remove 1 kg of the nutrient of interest according to the nutrient removal rate at the time of liquid sampling. Fourth, the rotational power measurements obtained as explained in the previous section

were used to determine the power requirement for removal of 1 kg nutrient. This power requirement, referred to as “expected power consumption,” provides a metric for pilot performance under operation-specific power draws and nutrient removal rates, assuming the operation-specific parameters were allowed to continue until 1 kg nutrient is removed from the liquid phase by the RABR.

2.3 Biomass Harvesting

The algae biomass was harvested weekly during fall 2023. Using conventional garden hoes, biomass from both sides of the eighteen shelves was harvested into water-tight plastic containers (Figure 5). Each container was given identifiers specific to the bay, section, and shelf location. Within 8 h of harvesting, the biomass samples were transported to a freezer set at -10°C .



Fig. 5. Algae biofilm growth using the outdoor pilot-scale rotating algae biofilm reactor. The left image is before harvesting and the right image is after harvesting.

2.4 Dry Weight and Ash-Free Dry Weight

The individual shelf samples were moved from the -10°C freezer to 25-cm baking tins, weighed for wet weight analysis, and dried at 60°C for 48 h. After drying, these

shelf samples were placed in a desiccator and allowed to cool to room temperature. After cooling, the dry biomass was weighed for dry weight (DW) analysis and ground using a mortar and pestle (Udom et al., 2013).

Ensuring homogeneity of the dry biomass, a 1-g sample of each shelf sample was combusted in a muffle furnace at 550°C for 2 h (Boelee et al., 2014). When cooled in a desiccator and weighed, this sample constituted the ash weight (AW) content of the shelf. The ash-free dry weight (AFDW) was then calculated by subtracting the AW from the 1-g dry sample. The AFDW content was then used to determine total AFDW for the individual shelf sample.

2.4.1 Footprint and Substratum Productivity

Productivity values were determined by dividing either the DW or AFDW by the product of the days since the previous harvest and the area under analysis. This calculation yielded units of g/m²-day.

Footprint productivity values were determined based on either the area of a single bay in the RABR or the total tank area (11.5 m²). This differentiation is crucial because a single shelf occupies the same area as an entire bay. By employing bay areas for comparison, the analysis facilitates a more comprehensive assessment among different spatial arrangements of the shelves. Substratum productivity values were calculated using 2 m² for each shelf. This area represented the top and bottom area of the carpet substratum attached to each shelf. Unlike footprint productivity, the substratum area used increases proportionally to the number of shelves in the analysis.

In this study, four productivity values were monitored through weekly harvests of the eighteen shelves of the RABR: DW footprint, DW substratum, AFDW footprint, and

AFDW substratum productivity. These productivity values, monitored during the fall season of 2023, furnished an extensive data set, and enabled comprehensive statistical analyses. The productivity values were combined in total, bay, section, and shelf analyses.

2.4.2 Ash Percentage Collection

To calculate AFDW productivity, ashing procedures were performed, as outlined in Material and Methods 2.4. By recording the AW values for the eighteen shelves harvested weekly, AW percentages of the observed DW were obtained. These percentages were used in statistical tests to explore operational, seasonal, and spatial variations in ash content.

2.5 Filtrate, Liquid Sampling, and Analysis

The filtrate used in the system exited the belt press with a total suspended solids (TSS) concentration of approximately 1000 mg/L. The clarification step reduced the TSS concentration to an estimated 200 mg/L. The filtrate pH ranged from 7.85 to 8.45 during the testing period during fall 2023.

Liquid samples were obtained for analysis of nitrogen and phosphorus concentrations. Samples were taken weekly from system influent, bay 1, bay 2, bay 3, and effluent locations (Figure 4a). These locations were also used for weekly pH measurements using an Oakton® WD-35614-20 field pH probe calibrated before each weekly session of data collection. For the month of October, a single sample was taken at each of these locations once a week before harvesting. For the month of December, a pseudo-composite sampling procedure was adopted once a week before harvesting.

In the pseudo-composite sampling procedure, a 50-mL flask was filled one-third of the way with liquid medium, and set aside for 2 min. This process was repeated at each of the five sampling locations until 50 mL were obtained for each location. Analyses of the liquid samples for total Kjeldahl nitrogen (TKN) and total phosphorus (TP) were performed using Hach TNT828 and TNT845 kits, respectively (Hach Co., Loveland, CO) (Barlow et al., 2016). Five-point standard curves were used for these analyses.

In addition to liquid pH samples, biofilm pH samples were taken each week before harvesting. The biofilm pH samples were measured in corresponding shelves of the three bays from the same section. In so doing, both liquid and biofilm pH values were available for statistical analyses.

2.6 Light and Temperature Measurements

Light levels were quantified using an Apogee Instruments DLI-500. In addition to a daily light integral (DLI), photosynthetic photon flux density (PPFD) readings were obtained weekly (Goldsberry et al., 2023). These PPFD measurements, obtained from the center of the RABR shelves, were used to determine light attenuation among the three-shelved sections of the RABR.

Air temperature readings were logged using the National Weather Service's climate weather data. The temperature data, taken 8.61 km from the RABR, reported values for minimum, maximum, and average daily temperatures. These values were obtained using NOAA Online Weather Data (National Weather Service, 2023). By correlating light and air temperature with RABR outputs, this study offers a basis of comparison which further studies can build upon.

2.7 Biofilm and Ash Constituents

Biofilm and ash constituents were quantified using procedures for nitrogen, phosphorus, solids, and element scanning. These constituents were used in elemental balances, nutrient uptake, and bioproduct analyses.

2.7.1 Total Phosphorus and Total Kjeldahl Nitrogen

Measurements for total phosphorus (TP), total Kjeldahl nitrogen (TKN), and total solids (TS) of the biofilm were collected by an independent certified laboratory, located at Central Valley Water Reclamation Facility (CVWRF) in Salt Lake City, Utah.

Methods used for TP, TKN, and TS were EPA 365.1, EPA 351.2, and SM 2540G-1997, respectively (APHA, 1997; EPA, 1993a, 1993b). In this study, TKN is used for total nitrogen because the filtrate used in the RABR comes from an anaerobic digester.

In addition, TP and TKN procedures were performed using the AW obtained from the RABR biofilm. These procedures used EPA 365.1 and EPA 351.2 (EPA, 1993a, 1993b). However, the CVWRF laboratory used 100 mL deionized water for suspension of 5-g AW samples. The laboratory then digested the suspended AW, followed by the EPA procedures for TP and TKN (EPA, 1993a, 1993b).

It was assumed that organic phosphorus compounds, like organic nitrogen compounds, have sufficiently low boiling points to be released as gaseous oxides under the combustion conditions used (Vassilev et al., 2023). Hence, the nitrogen and phosphorus elemental balances were closed for the biofilm as follows:

$$N_{Biofilm} = N_{Biomass} + N_{Ash}$$

$$P_{Biofilm} = P_{Biomass} + P_{Ash}$$

By quantifying the nutrient concentrations in the biofilm and the AW, the nutrient content in the biomass was calculated. The nitrogen-containing AW, assumed to be primarily struvite, was also interpreted for struvite productivity and struvite mass percentage of the biofilm using simple chemical conversions (Hillman and Sims, 2020). The struvite quantities, calculated using TKN concentrations of AW, were used to calculate struvite-bound inorganic phosphorus. Subsequently, the concentration of struvite-bound inorganic phosphorus was subtracted from the TP concentration in the AW to analyze non-struvite-bound inorganic phosphorus.

2.7.2 Element Scan

Element scans were obtained for dried biofilm samples taken from the RABR. These scans were performed by the Utah State University Analytical Laboratory using a Thermo Scientific® Electron iCAP 6300 ICP instrument. After obtaining the scans, the solid element concentrations were converted to liquid concentrations using the moisture content evaporated in the drying step.

These liquid concentrations were then modeled using Visual MINTEQ modeling software (Goldsberry et al., 2023). This modeling yielded simulated mineral precipitates based on the biofilm's elemental profile. Of particular interest in this study, the presence of struvite was validated using MINTEQ modeling of the biofilm AW constituents.

2.8 Statistical Analyses

Statistical tests were performed for productivity, ash content, liquid nutrients, and pH measurements. These tests were performed using five analysis groupings: Total, intra-duty-cycle, inter-duty-cycle, intra-month, and inter-month testing. For statistical analysis

of both productivity and ash content, one-way analysis of variance (ANOVA) was used. In ANOVA tests of productivity, DW and AF productivity values were analyzed using a footprint basis. Also, the ANOVA analysis of the RABR shelves was performed using combined shelf productivity values and individual shelf productivity values. Unlike the individual-shelf method, the combined-shelf method averaged shelf productivity values for corresponding shelves within the same bay of the RABR. For ANOVA testing using shelf productivity or ash values, pairwise comparison was performed using the Tukey Adjustment.

Following ANOVA tests for productivity and ash content, multiple linear regression was performed to investigate the effects of weekly averages of light and temperature. In multiple linear regression tests of productivity, DW and AF productivity values were analyzed using both footprint and substratum bases. For statistical analysis of liquid nutrient concentrations, one-way ANOVA was performed for influent; bays 1, 2, 3; and effluent samples. Lastly, statistical analysis using pH measurements was executed using one-way ANOVA tests, followed by simple and multiple linear regression. The one-way ANOVA tests compared pH between and across liquid and biofilm pH measurements from various locations in the RABR system. The linear regression tests were performed to establish correlation of pH values with light, temperature, and productivity. All ANOVA tests were performed using a 95% confidence interval (CI). Statistical analyses were performed in SAS® Studio and Microsoft Excel, while data visualization was performed in Python and Microsoft Excel. The statistical analyses employed throughout this study are summarized in Figure 6.

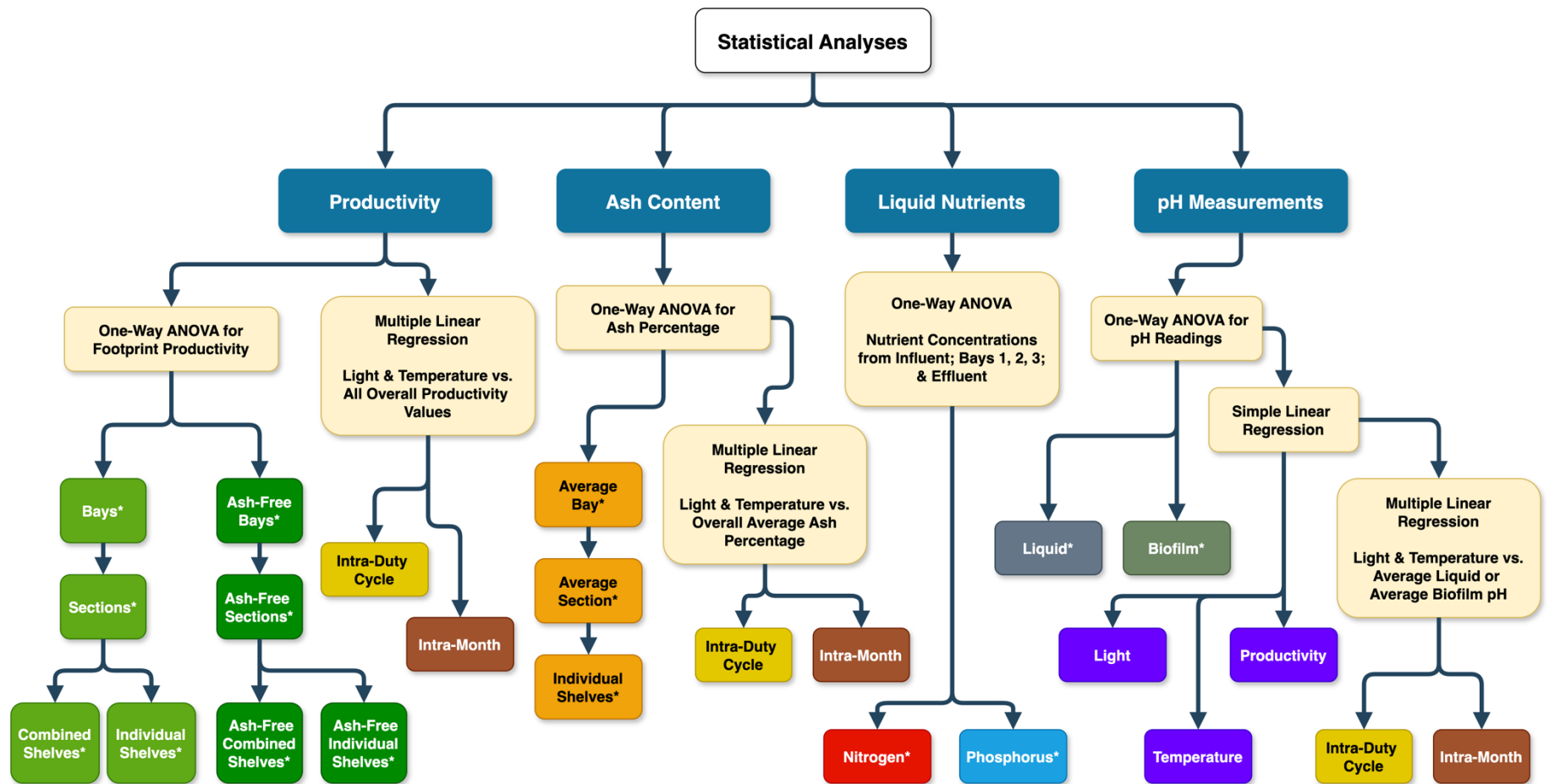


Fig. 6. Representation of statistical analyses performed using empirical data obtained from the pilot-scale rotating algae biofilm reactor. Asterisks denote repeated tests using total, intra-duty-cycle, inter-duty-cycle, intra-month, and inter-month analysis groupings.

3. Results and Discussion

3.1 Power Reduction using Duty Cycle

Results from the power reduction experiments are found in Figure 7. As expected, the lowest instantaneous power draw occurred at the lowest RPM and duty cycle.

Because the two lowest power draws occurred at 25% and 50% duty cycles, these two duty cycles were chosen for testing in the fall of 2023. To maintain consistency between duty cycles, both 25% and 50% were assigned a 20 min continuous cycle. As such, the 25% duty was programmed to rotate for 5 min and remain stationary for 15 min, while the 50% duty was programmed to rotate for 10 min and remain stationary for 10 min. To further reduce power draw, the RPM was held constant at 0.896 RPM.

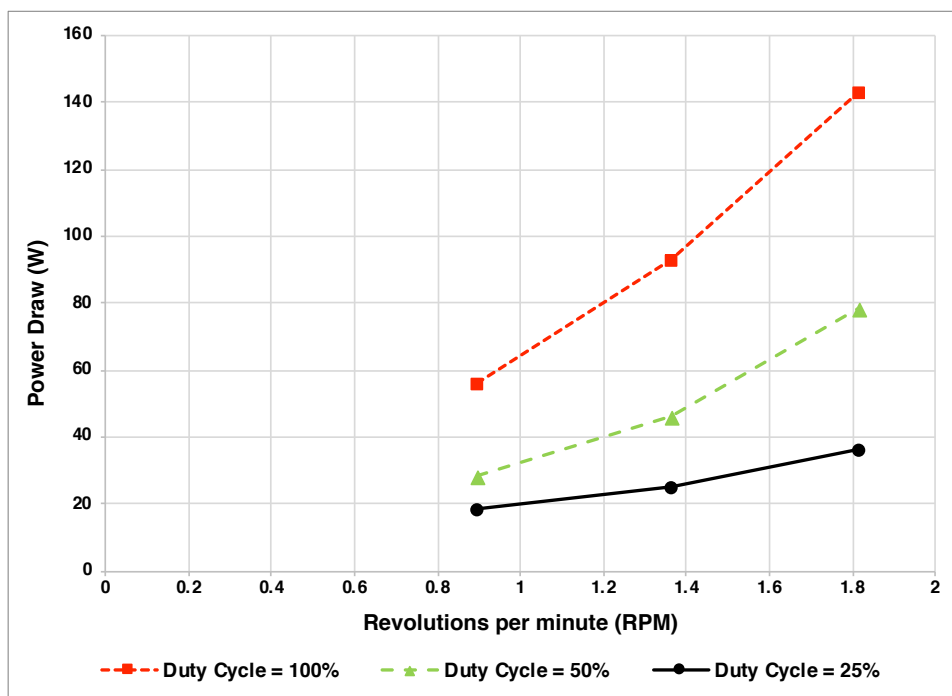


Fig. 7. Power reduction of pilot-scale rotating algae biofilm reactor, obtained by modulating duty cycle and RPM of rotating assembly.

3.2 Productivity

The complete results for productivity are reported in Table 4. Of note, the harvests associated with 50% duty cycle testing yielded maximum productivity across all productivity bases. The harvests associated with 25% duty cycle tests, conversely, yielded the lowest productivity across all productivity bases. With an additional 5 cyclical minutes of stationary operation compared with a 50% duty cycle, the algae biofilm was more nutrient-starved using a 25% duty cycle. As shown in previous studies, greater algae biomass growth contributed to ash-enhanced productivity (Hillman and Sims, 2020).

Table 4. Average productivity values, obtained using mathematical combinations of 18 shelf yields harvested weekly during the fall season of 2023.

	Dry Weight Productivity		Ash-Free Dry Weight Productivity	
	Footprint Basis (g/m ² -day)	Substratum Basis (g/m ² -day)	Footprint Basis (g/m ² -day)	Substratum Basis (g/m ² -day)
Total	5.85	1.88	3.27	1.05
25% Duty Cycle	4.30	1.40	2.58	0.84
50% Duty Cycle	7.09	2.26	3.83	1.22
October	5.49	1.78	3.31	1.07
December	6.29	2.01	3.23	1.03

3.2.1 Bay Statistical Analysis

Using a 95% confidence interval (CI), one-way ANOVA tests using productivity yielded no statistically significant differences between the three RABR bays using intra-duty-cycle, intra-month, and total tests. This lack of statistical significance held true irrespective of DW and AFDW productivity analysis. The lowest p-value observed of eight ANOVA tests was $p = 0.2744$, observed at the test involving all AFDW bay productivities observed during the fall of 2023. This lack of difference between bays is

indicative of continuous flow stirred tank reactor (CFSTR) behavior. The intended purpose of the two polycarbonate sheets serving as dividers between the three bays to retrofit the RABR to plug-flow operation was not realized; the RABR's performance is not indicative of plug-flow reactor (PFR) behavior. Had productivity values between the three bays been statistically distinct, PFR behavior would have been validated.

The only statistically significant results observed from bay comparisons were for inter-duty-cycle tests. In comparing all bays from 25% and 50% duty cycle tests, AFDW productivity yielded a p-value = 0.0255 and DW productivity yielded a p-value = 0.0041. Because duty cycle yielded productivity differences and months tested did not yield productivity differences, it is concluded the duty cycles had a greater effect on productivity than seasonal effects.

3.2.2 Section Statistical Analysis

As with bay comparisons, one-way ANOVA tests for section productivity using intra-duty-cycle, intra-month, and total testing yielded no significant differences. These sections, housing the shelves containing the growth substrata, were exposed to the same liquid medium, and the only structural difference was placement on the RABR's rotating shaft. The lack of statistical distinction between sections makes intuitive sense, as the treatment conditions were identical. As in the bay comparisons, section productivity ANOVA yielded statistical significance for inter-duty-cycle testing, while inter-month testing yielded no statistical significance. The tests between 25% and 50% duty cycles showed significance using both DW and AFDW productivity ($p = 0.0005$ and 0.0066 , respectively).

3.2.3 Shelf Statistical Analyses

Statistical analyses were performed for shelf productivity using both combined and individual shelf productivities. The rationale for using combined shelf comparison stems from the section comparison testing. In this testing, no difference was found between sections directly across from one other on the rotating assembly. Hence, in combined shelf comparison, the productivity values of the shelves directly across from one another were averaged, having received identical treatment conditions.

However, individual shelf comparison provides a more precise assessment of the shelves. Because section comparisons only compare overall productivity values, the true productivity difference between shelves remains unknown. By analyzing productivity using individual shelf productivity values, a more nuanced understanding of the RABR's performance is achieved.

In all combined and individual shelf comparison tests, the highest productivity was observed from the highest shelf, followed by the middle and bottom shelves. This difference, due to light attenuation between shelves, was shown to be significant in many testing groups. However, intuition suggests the bottom shelf would produce comparably to the top shelf, as the bottom shelf receives high light conditions during the upward rotation of the section (Figure 2). However, mechanical constraints caused the bottom shelf to receive minimal exposure to the liquid filtrate. Specifically, the bottom shelf was closest to the axis of rotation, and therefore received the least contact with the filtrate. This lack of contact may have contributed to nutrient starvation and subsequent hindered growth, causing the bottom shelf to underperform in productivity analysis compared to the top and middle shelf.

3.2.3.1 Combined Shelf Comparison

Using the combined-shelf method, the three RABR shelves showed strong statistical differences across total, intra-duty-cycle, and intra-month testing. Within all one-way ANOVA tests, the top shelf showed the highest productivity, followed by the middle and bottom shelves. In most tests, significant differences were observed for both the top and bottom shelves and the middle and bottom shelves. Additionally, for October testing, the top and middle shelves almost showed statistically significant differences for DW and AFDW productivity ($p = 0.0670$ and $p = 0.0565$, respectively). These differences suggest the shelves tested in October performed distinctively from one another. However, for 25% duty cycle and the December month analyses, the only significant differences observed were between the top and bottom shelves. This lack of distinction between shelves would suggest that the 25% duty cycle and December month caused the middle and bottom shelves to produce biomass indistinguishably from one another.

As shown in bay and section analyses, combined shelf ANOVA yielded statistical significance for inter-duty-cycle testing, while inter-month testing yielded no statistical significance. The tests between all shelves from 25% and 50% duty cycles showed significance using both DW and AFDW productivity ($p = 0.0003$ and $p = 0.0071$ respectively). This distinction between duty cycle and month testing is further evidence the operating parameters had a greater effect on the RABR's performance than time of year.

Further ANOVA testing compared all shelves, coupling combined shelf values with the associated duty cycle or month tested. In comparing all shelves and both duty

cycles, the mean shelf productivity values were ranked as follows: 50% top, 50% middle, 25% top, 25% middle, 50% bottom, and 25% bottom shelves. In addition to the intra-duty-cycle differences referenced previously, there were additional insights gained regarding differences of combined shelf productivities using inter-duty-cycle testing. Specifically, DW productivity analysis yielded statistical significance distinguishing the 25% middle and 50% top, 25% bottom and 50% top, and 25% bottom and 50% middle shelves. Unlike DW productivity analysis, AFDW productivity did not show statistical significance distinguishing the 25% middle and 50% middle shelves. This discrepancy could be attributed to artifact associated with AFDW productivity calculations. In the ANOVA testing using coupled shelf values with associated duty cycle, the combined-method successfully preserved all intra-duty-cycle statistical differences.

In comparing all combined shelves and both months tested, the mean shelf productivity values were ranked as follows: October top, December top, December middle, October middle, December bottom, and October bottom. As shown in inter-duty-cycle testing, there were additional insights gained regarding differences of combined shelf productivities between months tested. Specifically, DW productivity analysis yielded statistical significance distinguishing the October top and December bottom and October bottom and December top shelves. Interestingly, results from AFDW and DW productivity analysis for inter-month shelf comparison remained consistent. Also, months showed fewer inter-month distinction between shelf productivities. This difference from inter-duty-cycle analysis could be due to the continuing evidence that operating parameters had greater influence on the RABR's performance than the time of year. Different duty cycles had a higher likelihood of creating statistically distinct shelf

productivities. Lastly, the ANOVA testing using coupled shelf values with associated duty cycles did not successfully preserve intra-duty cycle statistical differences; specifically, the DW analysis lost October middle and bottom shelf distinction; and the AFDW analysis lost December top and bottom shelf distinction, and October middle and bottom shelf distinction.

3.2.3.2 Individual Shelf Comparison

The individual-shelf method showed similar statistical differences to the combined-shelf method. However, the individual-shelf ANOVA tests showed additional statistical differences for the December month testing. Specifically, using the individual-shelf method for December month testing showed statistically significant differences for DW and AFDW productivity between the middle and bottom shelves ($p = 0.0240$ and $p = 0.0229$, respectively). These statistically significant differences highlight the merit of the individual-shelf comparison. These findings disprove the combined-shelf method's assertion that middle shelves produced biomass indistinguishably from one another in December 2023.

Further ANOVA testing coupled individual shelf values with the associated duty cycle or month tested. In comparing all shelves and both duty cycles, the mean shelf productivity values followed the same ranking as the combined-shelf method. In addition to the inter-duty-cycle testing differences shown in the combined-shelf method, the individual-shelf method showed statistically significant differences between the top shelves of 25% and 50% duty cycles using DW productivity. For inter-month comparisons, the mean shelf productivity values followed the same ranking and same statistical differences as the combined-shelf method. This inter-month ANOVA testing

using the individual-shelf method yielded no further statistical distinctions compared to the combined-shelf method. Additionally, the individual-shelf method did not successfully preserve DW or AFDW differences between the December middle and bottom shelves, nor did the method preserve AFDW differences between the December top and bottom shelves. However, unlike the combined-shelf method, both DW and AFDW analysis performed using the individual-shelf method preserved differences between the October middle and bottom shelves.

For the ANOVA testing which coupled individual shelf value and the duty cycle or month tested, the individual-shelf method preserved intra-month shelf differences better than the combined-shelf method. Despite the lack of statistical distinction between shelves shown by the section comparisons, the individual-shelf method is recommended for future research due to its higher precision analyses.

3.2.4 Light and Temperature Correlation

Multiple linear regression (MLR) of productivity values vs. light and temperature yielded varied correlation for duty cycles and months tested. All MLR tests for productivity are summarized in Table 5.

Table 5. Productivity multiple linear regression tests of average daily light integral (DLI) and average air temperature vs. productivity values from the RABR system.

Analysis Grouping	Testing Period	Biofilm Analysis	Productivity Basis	Adjusted R-squared	Correlation Interpretation
Month	October	DW	Footprint	-0.5940	Insignificant
			Substratum	-0.5395	Insignificant
		AFDW	Footprint	-0.4373	Insignificant
			Substratum	-0.3829	Insignificant
	December	DW	Footprint	-1.2846	Insignificant
			Substratum	-1.2846	Insignificant
		AFDW	Footprint	-1.2484	Insignificant
			Substratum	-1.2484	Insignificant
Duty Cycle	25%	DW	Footprint	0.8721	High
			Substratum	0.9382	High
		AFDW	Footprint	0.8895	High
			Substratum	0.9487	High
	50%	DW	Footprint	-0.0275	Insignificant
			Substratum	-0.0275	Insignificant
		AFDW	Footprint	0.1674	Low
			Substratum	0.1674	Low

As shown in Table 5, grouping productivity values using months produced the least significant correlation. Conversely, grouping productivity values using duty cycles produced more significant correlation. Correlation was highest using the 25% duty cycle testing period, with the highest fidelity regression occurring using the AFDW analysis. It is likely the AFDW analysis provided slightly higher correlation than the DW analysis because, of the organic and inorganic phases of the biofilm, the organic phase is more directly influenced by light and temperature. The MLR analysis for the 25% duty cycle testing is visualized in Figure 8.

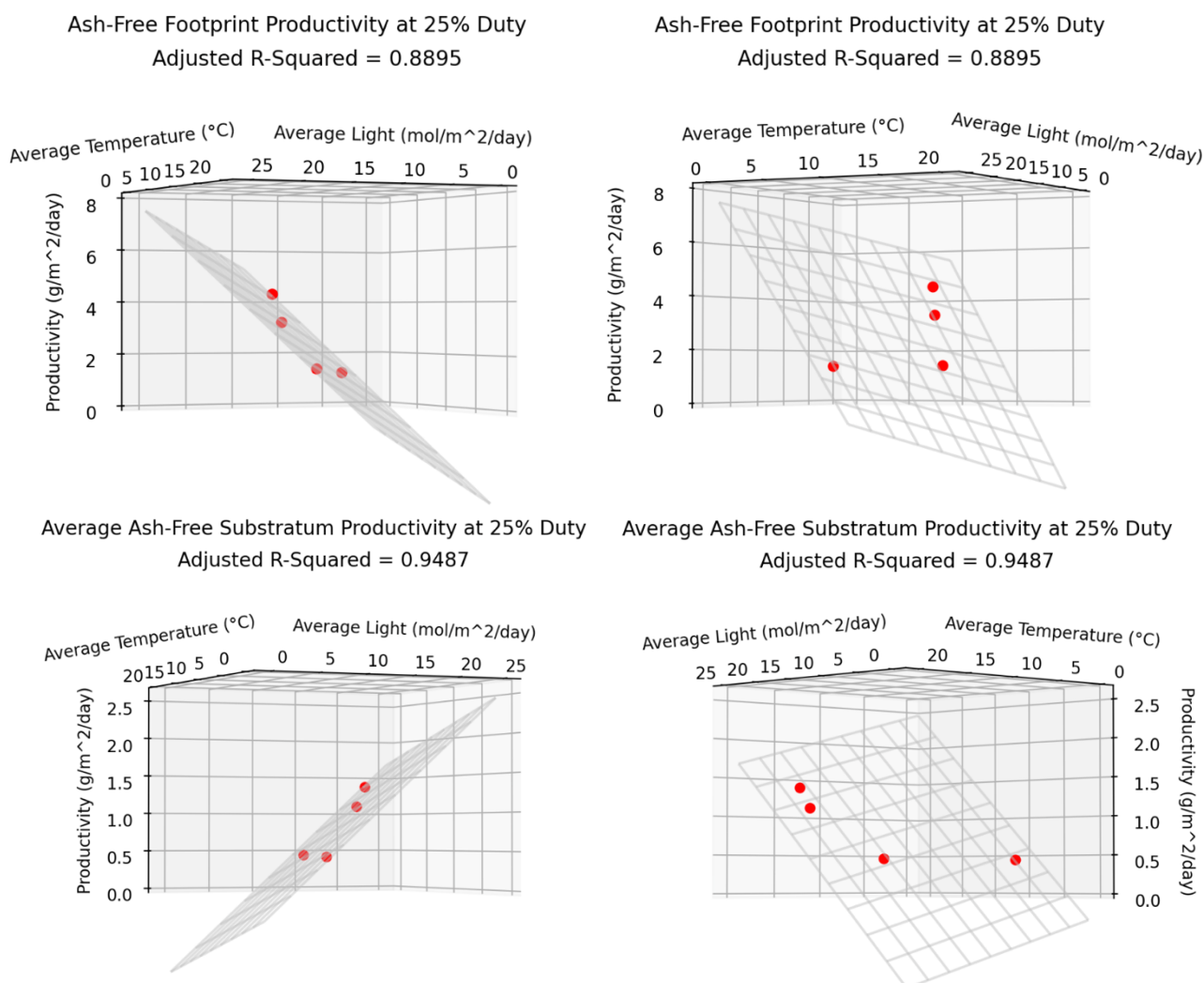


Fig. 8. Visualization of multiple linear regression tests to correlate RABR productivity with average daily light integral (DLI) and average air temperature. The top two graphs use a footprint basis while the bottom two graphs use a substratum basis.

As shown by ANOVA testing for productivity, the duty cycle used in operation had a greater effect on productivity than the month tested. For this reason, the duty cycle grouping in MLR had stronger correlation with the data than the month grouping. However, the 50% duty cycle MLR had considerably lower correlation than the 25% duty cycle. This lack of correlation could be attributed to the freezing temperatures. With the onset of freezing temperatures, the RABR was equipped with polycarbonate walls,

causing greater light attenuation and heat insulation within the RABR. These factors may have caused the lack of fidelity from the 50% duty cycle MLR testing.

3.2.5 Biofilm Weight

The highest wet biofilm weight harvested from the pilot-RABR was 24 kg. This weight contributed to less than 3% of the total rotating assembly weight. Biofilm weight's insignificance is favorable for scale-up and further optimization. Unlike rotating biological contactors (RBC), the current and future embodiments of the RABR can avoid mechanical fatigue associated with biomass overloading (Mba et al., 1999).

3.3 Ash Content

The overall average ash content values are shown in Table 6. These average values were obtained using AW values, observed from weekly harvests of the 18 shelves of RABR. Since each shelf ash content was monitored, the ash content values were used in further comparisons of RABR bays, sections, and shelves. The highest average ash content, 48.0%, was recorded for the month of December.

Table 6. Average ash content values, obtained by averaging ashed RABR biofilm samples from 18 shelves harvested weekly during the fall season of 2023.

	Average Ash Percentage (%)
Total	42.6
25% Duty	40.6
50% Duty	44.2
October	38.2
December	48.0

3.3.1 Ash Content Statistical Analyses

One-way ANOVA tests of bay ash content percentages yielded no statistically significant differences between bays for total testing, intra-duty-cycle testing, and intra-month testing. This lack of distinction is further evidence of the RABR's CFSTR behavior. For inter-duty-cycle testing, there was statistical significance between the bays ($p = 0.0069$). Likewise, the inter-duty-cycle testing yielded statistical significance between the bays ($p < 0.0001$). In these tests, the 50% duty cycle and December bays exhibited higher ash percentages, as shown in Table 6. These results are indicative of ash-enhanced productivity at a 50% duty cycle. However, with statistical significance from bay comparison tests for both inter-duty-cycle and inter-month testing, it remains unclear if the duty cycle or time of year had greater influence on ash content from this analysis alone. As with the analysis of productivity and pH measurements, linear regression was employed to better understand the influences of duty cycle and time of year.

As shown in the bay comparisons, section comparisons yielded no statistically significant differences between sections for total, intra-duty-cycle, and intra-month testing. Additionally, inter-duty-cycle and inter-month testing yielded statistical significance between sections ($p < 0.0001$ for both).

Because the productivity analyses that employed the individual-shelf method showed more precise results, the individual-shelf method was used in the ash content statistical analyses. For total and intra-duty-cycle testing, there were no statistically significant differences between the shelves' ash content. Similarly, there were no statistically significant differences between the shelves for October testing. This lack of statistical difference suggests non-freezing temperatures and high light conditions of

October yielded uniformity of ash content between the shelves. For intra-month testing of December, however, there was statistically significant differences between the top and middle shelves, and the top and bottom shelves. The top shelves had the highest average ash content, followed by the middle and bottom shelves. Lower light conditions and freezing temperatures were likely the causes for this distinction.

3.3.2 Light and Temperature Correlation

Since all inter-duty and inter-month tests yielded statistical significance, it would seem both duty cycle and month tested were predictors for ash content. Yet, further analysis using MLR showed duty cycle better fit the overall ash content data. The average ash content MLR testing for the different analysis groupings is found in Table 7.

Table 7. Ash content multiple linear regression tests of average daily light integral (DLI) and average air temperature vs. ash percentage averages in the RABR system.

Analysis Grouping	Testing Period	Adjusted R-squared	Correlation Interpretation
Month	October	0.5848	Moderate
	December	-1.4631	Insignificant
Duty Cycle	25%	0.9919	Very High
	50%	0.9950	Very High

As shown in Table 7, month grouping of the average ash content data was not a favorable model for MLR. Grouping with respect to duty cycle provided a higher-fidelity linear model. The duty cycle MLR models, visualized in Python, are shown in Figure 9.

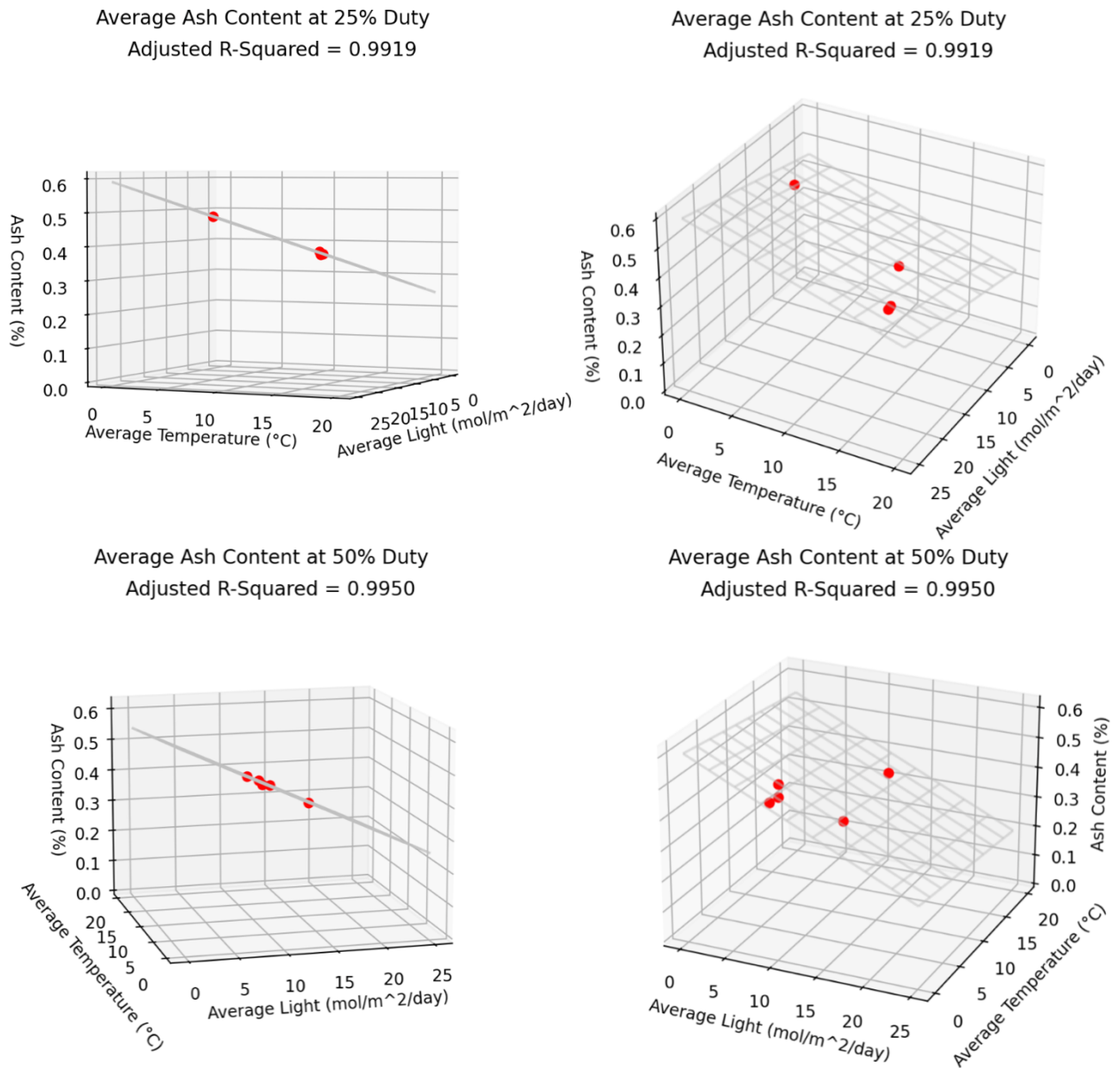


Fig. 9. Visualization of multiple linear regression tests to correlate rotating algae biofilm reactor ash content with average daily light integral (DLI) and average air temperature. The top two graphs use a footprint basis while the bottom two graphs use a substratum basis.

Interestingly, the 50% duty cycle grouping had virtually identical correlation to the 25% duty cycle grouping. This similarity between 50% and 25% duty cycle testing is

contrary to what was observed for productivity using MLR. It is noted despite non-linear productivity values, the 50% duty cycle yielded very linear ash content with respect to light and temperature. Though productivity lacked MLR consistency between duty cycles, ash content proved highly predictable using duty cycle grouping.

3.4 Nutrient Uptake

Nutrient uptake of nitrogen and phosphorus occurred through both biological metabolism and chemical precipitation. The average nitrogen concentration measured from the RABR's influent was 367 mg/L. The average phosphorus concentration in the influent was 15.5 mg/L. Average nutrient removals are summarized in Table 8.

Table 8. Average liquid nutrient reduction, measured using influent and effluent samples from the pilot-scale RABR.

Nutrient Reduction Dataset	Average Reduction (%)	Reduction Standard Deviation (%)	Maximum Reduction (%)
Nitrogen	21.4	25.7	58.0
Nitrogen*	28.8	18.0	58.0
Phosphorus	38.0	28.3	76.3
Phosphorus*	44.4	24.1	76.3

* - Liquid samples with no apparent nutrient removal removed from average calculation

3.4.1 Zero-Order Kinetics

As shown by high standard deviations in Table 8, nutrient reduction from the liquid phase was highly variable. Hence, an understanding of Michaelis-Menten (MM) kinetics of algae is important for understand nutrient uptake and biofilm productivity (Aslan and Kapdan, 2006). For mixed microalgae grown using anaerobic liquid digestate under batch conditions, $K_{mN} = 29.3$ mg/L (nitrogen) and $K_{mP} = 2.94$ mg/L (phosphorus) (Ermis and Altinbas, 2019). The average filtrate concentrations of nitrogen and phosphorus in the RABR system were much higher than these K_m values; consequently,

the microalgae were continuously operating under zero-order enzyme kinetics. With variable temperature and light conditions, the system's ability to biologically uptake nitrogen and phosphorus was unpredictable. For this system, it is clear MM kinetics may be insufficient to predict nutrient uptake.

3.4.2 Liquid Nutrient Statistical Analyses

Using the sampling points shown in Figure 4a, five liquid samples were taken weekly for the RABR. These five samples allow overall and bay nutrient reduction analysis. For one-way ANOVA testing of all five samples, no significant differences were observed. This lack of significance was consistent for total, intra-duty-cycle, intra-month, inter-duty-cycle, and inter-month testing. Since no statistical distinctions could be made between nutrient sampling points, statistical analyses compared the bay nutrient reductions with the effluent nutrient reductions. These analyses yielded no statistical significance, strengthening the understanding of the RABR as a CFSTR. Then, the original analyses were repeated combining all bay samples with the effluent samples and comparing these "RABR samples" with the influent samples.

For nitrogen, the RABR samples showed a statistically significant difference from the influent samples ($p = 0.0372$). This statistical significance, shown using all liquid samples obtained, validated nutrient removal had occurred. Using these RABR samples for nutrient removal, the average nitrogen removal was 30.9%. Further nitrogen analysis yielded no significant differences in inter-duty-cycle and inter-month testing.

As with nitrogen, RABR samples for phosphorus showed a statistically significant difference from the influent samples ($p = 0.0209$). This statistical significance, shown using all liquid samples obtained, validated nutrient removal had occurred. Using these

RABR samples for nutrient removal, the average phosphorus removal was 35.0%. As shown using RABR samples for nitrogen, RABR samples for phosphorus yielded no significant differences in inter-month testing. But unlike RABR samples for nitrogen, the RABR samples for phosphorus showed significant differences in inter-duty-cycle testing ($p = 0.0190$). There are multiple interpretations to be made from this statistically significant result. First, the 50% duty cycle had higher phosphorus removal efficiency than the 25% duty cycle. Also, phosphorus removal from the liquid phase proved more predictable than nitrogen. Nitrogen was present in much higher concentrations in the filtrate influent but was unable to chemically precipitate as readily as phosphorus, nitrogen likely only precipitating in struvite. The phosphorus removal presumably occurred through the solid phase precipitation of calcium- and magnesium-phosphate inorganic salts, enhanced through the higher biological induction of chemical precipitation associated with the 50% duty cycle. Additionally, phosphorus removal from the liquid phase could have occurred through biological luxury uptake (see Results and Discussion 3.4.5). Lastly, the significance of inter-duty-cycle testing for phosphorus favors operational effects over seasonal effects of nutrient removal.

3.4.3 Nutrient Uptake Power Requirements

Using power draws required to rotate the RABR assembly, power consumption for nutrient removal using 25% and 50% duty cycles were summarized in Table 9. For these calculations, liquid nutrient reductions were correlated to power requirements to rotate at the associated duty cycle. Hence, Table 9 offers a representation of power requirements to remove 1 kg liquid nutrient if the RABR were to continue performing as

observed during liquid sampling. Average values do not include liquid sampling events where no apparent nutrient was observed.

Table 9. Summary of expected power consumption using empirical liquid-phase nutrient removal data, where the rotating algae biofilm reactor (RABR) was operated at 25% and 50% duty cycles.

Nutrient Power Requirement	Associated Duty Cycle	Expected nitrogen power consumption (kWh/kg _{TKN})	Expected phosphorus power consumption (kWh/kg _{TP})
Minimum for nitrogen removal	25%	1.36	-
Minimum for phosphorus removal	50%	-	20.1
Average values	25%	1.89	106
Average values	50%	6.38	55.7
Percent Reduction using Average Power Consumption	25 to 50%	-	47.5%
	50 to 25%	70.4%	-

Of note, the power consumption was optimized for nitrogen at a 25% duty cycle. Conversely, the power consumption was optimized for phosphorus using a 50% duty cycle. The 25% duty cycle may have efficiently removed nitrogen by operating in a stationary position and thereby encouraging evaporation of NH_3^+ . The 25% duty cycle also failed to remove phosphorus as efficiently as the 50% duty cycle. Phosphorus would likely require more contact with the filtrate to be taken up or precipitated; it is therefore plausible, relative to the 25% duty cycle, the 50% duty cycle's prolonged contact with the filtrate facilitated this enhanced phosphorus uptake.

Overall, the optimal expected power consumption for nitrogen, 1.36 kWh/kg_{TKN}, occurred during 25% duty cycle testing. Likewise, the optimal expected power consumption for phosphorus, 20.1 kWh/kg_{TP}, was observed during the 50% duty cycle testing. In relation to the only other study to specify power requirements for nutrient

removal using an attached-growth algae cultivation system, this system proved very comparable. The RABR used in this study removed nitrogen slightly more efficiently (1.36 kWh/kg vs. 2.6 kWh/kg) and removed phosphorus slightly less efficiently (20.1 kWh/kg vs. 17.5 kWh/kg) under best-case operation (Christenson and Sims, 2012). If further studies report analogous power requirements, there is strong potential for innovation in power optimization of attached-growth algae cultivation systems.

3.4.4 Inorganic Salt Quantification

Struvite quantities from within the algae biofilm are summarized in Tables 10 and 11. Due to inconsistencies in the digestion of the ash for TKN, the results for struvite quantities obtained for the 25% duty cycle were inconsistent and therefore represent low-confidence data. These values for struvite quantification are found in Table 10. Conversely, inconsistencies related to the digestion of the ash were mitigated for analysis of 50% duty cycle testing. Table 11 summarizes struvite quantities for the 50% duty cycle.

Table 10. Struvite (NH_4MgPO_4) quantification for 25% duty cycle, using dry weight values for RABR shelves and TKN values of ashed biofilm from the same location of the rotating algae biofilm reactor.

	Struvite Weight (g)	Struvite Percent of Dry Weight (%)	Theoretical Productivity ($\text{g/m}^2\text{-day}$) [^]
	0.326*	0.70*	0.037*
	0.377*	0.70*	0.049*
	0.004	0.05	0.001
	0.502	1.42	0.038
Average	0.302	0.72	0.031
Standard Deviation	0.184	0.48	0.018

* - Values obtained using average TKN content from all ash samples taken

[^] - Calculated using struvite percent of total solids multiplied by RABR's overall DW footprint productivity (Hillman and Sims, 2020)

As shown in Table 10, the average struvite percent DW was 0.72% when operating at the 25% duty cycle. Additionally, the average theoretical productivity for production of struvite was 0.031 g/m²-day.

Table 11. Struvite (NH₄MgPO₄) quantification for 50% duty cycle, using DW values for RABR shelves and TKN values of ashed biofilm from the same location of the rotating algae biofilm reactor (RABR) operating at a 50% duty cycle.

	Struvite Harvested (g)	Struvite Percent of Dry Weight (%)	Theoretical Productivity (g/m ² -day) [^]
	0.152	0.22	0.018
	0.176	0.42	0.012
	0.816	1.14	0.093
	0.292	0.94	0.051
	0.507	0.71	0.062
Average	0.389	0.68	0.049
Standard Deviation	0.248	0.33	0.028

[^] - Calculated using struvite percent of total solids multiplied by RABR's overall DW footprint productivity (Hillman and Sims, 2020)

Shown in Table 11, the average struvite percentage of the biofilm DW was 0.68%. The average theoretical struvite productivity, assuming all shelves of the RABR produced struvite as efficiently as the shelf sampled for struvite analysis, was 0.049 g/m²-day. This value is meaningful because it translates the RABR from strictly a water remediation tool to a veritable biorefinery for production of struvite-rich biofilm.

Comparisons between data found in Tables 10 and 11 should be done with caution. Since digestion of the ash proved using inconsistent, we cannot definitively make conclusions regarding differences of struvite quantities. However, the data would suggest theoretical productivity is higher for the 50% duty cycle, even though struvite percentage was slightly higher using the 25% duty cycle. It is possible the higher biofilm productivity from the 50% duty cycle testing compensated for any difference of struvite

concentration, causing the 50% duty cycle to produce more struvite than the 25% duty cycle.

Due to the lack of confidence in the 25% duty cycle ash nutrient content, inorganic salt analysis for 25% duty cycle testing is stopped here. Therefore, struvite percentages obtained from 50% duty cycle tests only. Obtained from TKN ash content, struvite quantities were converted into struvite-bound inorganic phosphorus. This struvite-bound inorganic phosphorus, when subtracted from the AW TP concentrations, yielded non-struvite-bound inorganic phosphorus. These inorganic phosphorus values are summarized in Table 12.

Table 12. Biofilm inorganic phosphorus quantification, using biofilm struvite concentrations from shelves of ashed biofilm from the same location of the rotating algae biofilm reactor operating at a 50% duty cycle.

	Total Inorganic Phosphorus Harvested (g)	Inorganic Phosphorus Percent as Struvite (%)	Inorganic Phosphorus* Percent of Dry Weight (%)	Inorganic Theoretical Phosphorus* Productivity (g/m ² -day) [^]
50% Duty Cycle Tests	1.763	1.98	2.52	0.386
	0.567	7.52	1.26	0.118
	3.366	5.79	4.43	0.711
	1.131	3.20	6.60	0.461
	1.983	6.12	2.61	0.488
Average	1.762	4.92	3.48	0.361
Standard Deviation	1.054	2.27	2.08	0.260

* - Non-struvite-bound inorganic phosphorus

[^] - Calculated using struvite percent of total solids multiplied by RABR's overall DW footprint productivity (Hillman and Sims, 2020)

By quantifying total inorganic nitrogen- and phosphorus-containing salts, the analysis accounts for all nutrient uptake of nitrogen and phosphorus through chemical precipitation. From Table 12, it is observed the percent inorganic phosphorus observed as struvite-bound inorganic phosphorus is less than 5%. This means most of the inorganic

phosphorus in the DW is composed of calcium-, magnesium-, or sodium-phosphates.

While these non-struvite-bound phosphorus salts are not empirically measured, this analysis provides an understanding of total inorganic phosphorus compounds.

Results from this study suggest an increase of ash productivity using a 50% duty cycle.

Further studies can explore operating parameters to enhance mineral productivity as algae systems are integrated as biologically induced chemical reactors.

3.4.5 Nitrogen and Phosphorus Balances

Results from DW and AW quantification of nitrogen and phosphorus were used to generate elemental balances. These balances, summarized in Table 13, offer validation of the elemental composition of the algae biomass harvested from the RABR.

Table 13. Nitrogen and phosphorus balances for algae biomass, calculated using biofilm samples obtained from bay 1 of the outdoor pilot-scale rotating algae biofilm reactor (RABR).

Analyses Biomass Sample Date	Dry Weight (DW)			Ash Weight (AW)			Biomass Nutrient Calculation		Biomass Percent Nutrient		Percent Difference of Average from Algae Stoichiometry	
	TP (mg/kg)	TKN (mg/kg)	DW (%)	TP (mg/kg)	TKN (mg/kg)	AW (%)	TP (mg/kg)	TKN (mg/kg)	TP (%)	TKN (%)	Percent Difference for P (%)	Percent Difference for N (%)
10/5/23	33700	52300	3.6	70800	-	37.0	7478	-	0.7	-		
10/12/23	31500	56200	2.7	-	-	39.4	-	-	-	-		
10/19/23	34000	63200	2.6	11600	51.9	36.1	29813	63181	3.0	6.3		
10/26/23	30600	63500	3.4	25700	226	35.7	21436	63419	2.1	6.3		
11/2/23	69800	57900	2.2	13500	427	44.5	63787	57710	6.4	5.8		
12/7/23	60300	60900	5.5	46900	1160	50.4	36667	60315	3.7	6.0		
12/14/23	52400	53600	4.5	36200	954	47.8	35083	53144	3.5	5.3		
12/20/23	51100	77600	4.7	27700	722	48.9	37555	77247	3.8	7.7		
12/28/2023 [^]	50800	63250	2.9	45200	1450	49.3	28523	62535	2.9	6.3		
Average	46000	61000	3.6	34700	713	43.2	33000	63000	3.3	6.3	273*	-0.9*
Standard Deviation	13300	7110	1.0	18000	471	5.8	15000	6910	1.5	0.7		

[^] - Averages of samples from bay 2 used for dry weight analyses

* - Percent difference compares biomass percent nutrient to algae stoichiometry of C₁₀₆H₂₆₃O₁₁₀N₁₆P (Stumm and Morgan, 2012)

As shown in Table 13, the elemental balance for nitrogen was within one percent of the known algae stoichiometry. This precision is favorable for validation of AW nutrient concentrations discussed previously. Because the elemental balance closed favorably for nitrogen, the analysis successfully accounted for all nitrogen found in the organic and inorganic phases of the biofilm.

The phosphorus elemental balance did not match the algae stoichiometry as favorably as the nitrogen elemental balance. The biomass percentage of phosphorus observed was 3.3% w/w, while the stoichiometry percentage of phosphorus is approximately 1% w/w. However, this elevated level of phosphorus could be evidence of luxury phosphorus uptake (Solovchenko et al., 2019). This would be the first pilot-scale observation of luxury phosphorus uptake using an outdoor attached-growth algae cultivation system. However, with influent phosphorus levels well above K_m for microalgae, it seems unlikely the microalgae would store excess polyphosphate (Ermis and Altinbas, 2019). With high levels of bioavailable phosphorus, it is not possible to know definitively if luxury phosphorus uptake occurred. The possibility of luxury phosphorus uptake is favorable for attached-growth microalgae cultivation, and further studies should seek to validate these findings using outdoor pilot-scale systems.

3.5 pH Measurements

The average pH of the influent of the RABR was 8.14 (standard deviation = 0.20). This average value, along with all other average pH values obtained for various testing of the analysis groupings, are found in Table 14. Due to lack of statistical significance between bay and effluent pH samples, these pH samples were combined, constituting liquid “RABR samples,” as used in the liquid nutrient analysis (see Results and

Discussion 3.4.2). The lack of distinction between bays and effluent pH values are further evidence of CFSTR behavior.

Table 14. Average pH values, obtained from weekly influent, bays, and effluent sampling of the RABR during the fall season of 2023.

	Influent pH		Liquid pH		Biofilm pH	
	Average	Standard Deviation	Average	Standard Deviation	Average	Standard Deviation
Total	8.14	0.20	8.00	0.35	7.57	0.56
25% Duty Cycle	8.25	0.17	7.78	0.34	7.32	0.53
50% Duty Cycle	8.08	0.19	8.18	0.24	7.77	0.50
October	8.07	0.14	7.73	0.21	7.16	0.39
December	8.21	0.23	8.35	0.06	8.08	0.21

The observed decrease of pH from influent to liquid and biofilm pH could be attributed to evaporation of ammonia (NH_3^+). As ammonia exits the aqueous phase, the pH becomes more acidic. The pH change is not fully counteracted by the algae's absorption of CO_2 , which would cause the filtrate within the RABR system to become more basic.

3.5.1 pH Statistical Analyses

For ANOVA testing of all liquid samples taken from the five sampling points of the RABR (see Figure 4a), there was little statistical significance observed at a 95% CI. Only pH samples from the month of October showed distinction between liquid samples from within the RABR and the influent (p -value = 0.0069). However, ANOVA testing between biofilm pH and influent pH showed statistical significance for total, October, and 25% intra-duty-cycle testing. In these statistically significant tests, it was shown that influent pH was consistently higher than the biofilm pH. Additionally, ANOVA testing between liquid and biofilm pH samples yielded highly significant results. In all tests

performed, the average liquid pH was higher than the average biofilm pH. This difference suggests precipitation of organic salts such as struvite was more likely to occur in the liquid phase of the RABR, if only pH parameters are considered.

As with statistical analyses used for ash content, the inter-duty-cycle and inter-month testing both yielded statistical significance. For inter-duty-cycle testing, both the liquid and biofilm pH of the 50% duty cycle testing were higher than the liquid and biofilm pH of the 25% duty cycle testing. Similarly, both the liquid and biofilm pH of the December testing were higher than the liquid and biofilm pH of the October testing.

During the 50% duty cycle testing, it is likely the biofilm was more biologically active. Both the liquid and biofilm pH were significantly raised as more CO₂ was absorbed for biological metabolism by the algae biomass.

3.5.2 Light, Temperature, and Productivity Correlation

Simple linear regression yielded varied levels of correlation. The highest correlation using simple linear regression was observed using average air temperature vs. average biofilm pH. This and other tests are summarized in Table 15.

Table 15. Simple Linear Regression for pH, using average daily light integral (DLI), average air temperature, and productivity values vs. pH averages in the RABR system.

Simple Linear Test Description	r-squared	Correlation Interpretation
Average DLI vs. Average Biofilm pH	0.3521	Low
Average DLI vs. Average RABR Samples Liquid pH	0.7105	Moderate
Average Air Temp vs. Average Biofilm pH	0.4333	Slight
Average Air Temp vs. Average RABR Samples Liquid pH	0.7687	Moderate
Productivity vs. ANY pH	-	Insignificant for all productivity types

As evidenced by Table 15, Productivity was not strong enough to manifest a significant change of pH in liquid or in biofilm samples. This lack of correlation is

evidence light and temperature had greater influence on pH within the RABR system.

Using simple linear regression, moderate correlation was observed, as shown in Figures 10 and 11.

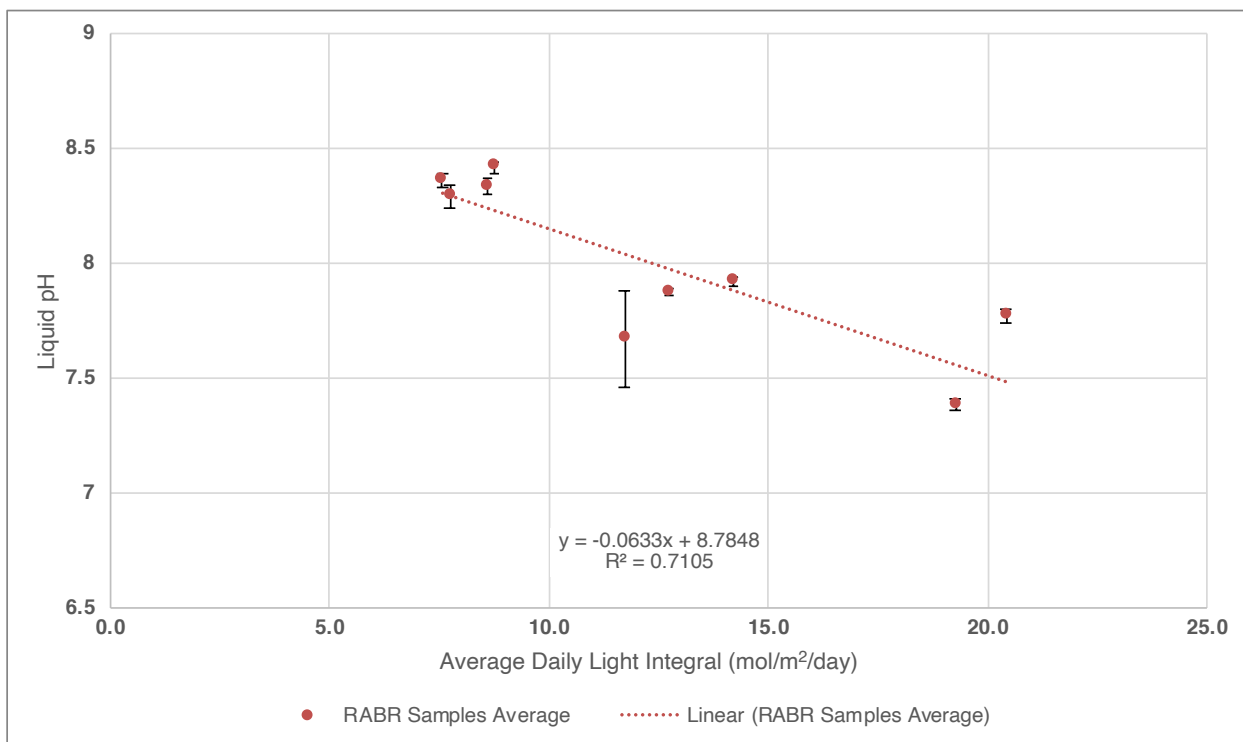


Fig. 10. Visualization of simple linear regression tests to correlate rotating algae biofilm reactor pH values with average daily light integral (DLI).

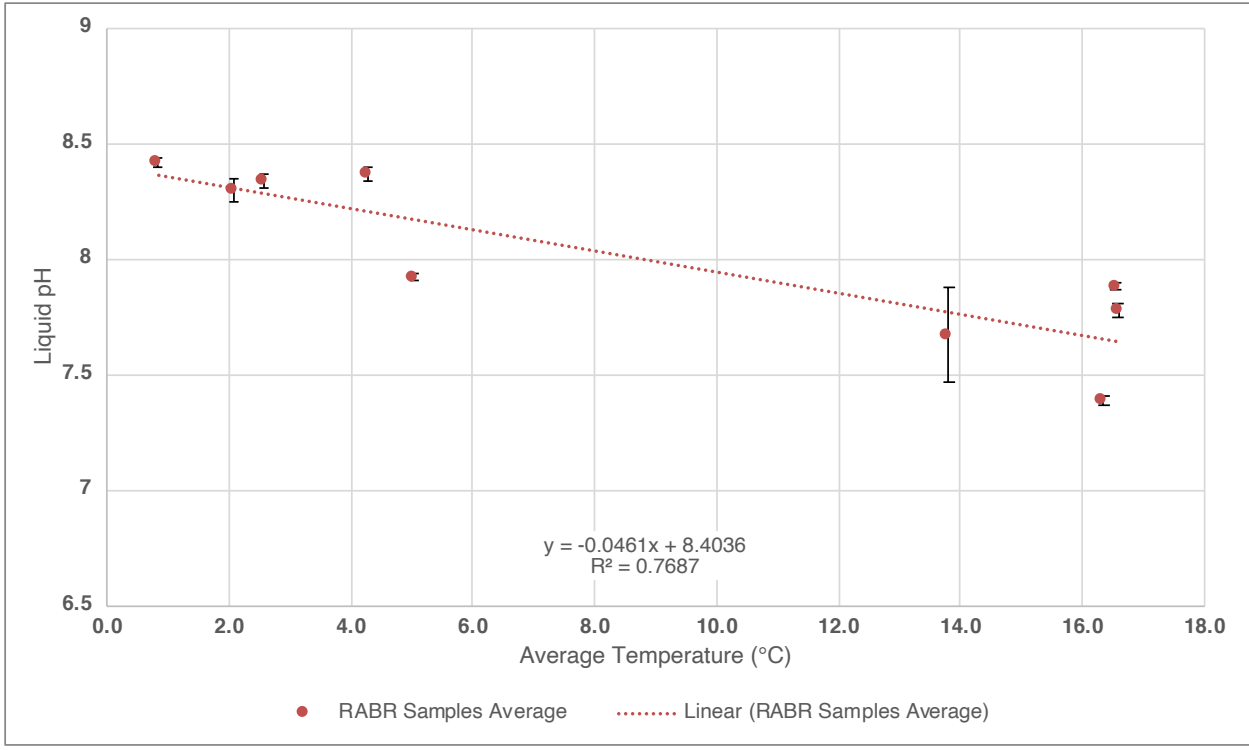


Fig. 11. Visualization of simple linear regression tests to correlate rotating algae biofilm reactor pH values with average air temperature.

As shown in Figures 10 and 11, simple linear regression provided moderate correlation at best for pH as a function of light or temperature. Hence, multiple linear regression (MLR) was performed for the various analysis groupings to understand combined correlation of light and temperature levels with pH. The MLR tests are outlined in Table 16.

Table 16. Multiple linear regression for pH, using average daily light integral (DLI) and average air temperature vs. pH averages in the RABR system.

pH Average	Testing Period	Adjusted R-squared	Correlation Interpretation
Biofilm	Total	0.2605	Low
	25%	0.1798	Low
	50%	0.9159	High
	Oct	-0.5330	Insignificant
	Dec	0.9930	High
Liquid	Total	0.6954	Moderate
	25%	0.1943	Low
	50%	0.8430	High
	Oct	-0.5675	Insignificant
	Dec	0.8710	High

Greater fluctuations in light and temperature, as seen in October testing, may have caused the inconsistency seen in pH. Ammonia evaporation may have also skewed results. By contrast, the walls installed in December, coupled with more consistent light and temperature conditions, may have eliminated drastic pH fluctuations. This normalization likely contributed to more predictable pH results using the multiple linear regression model. Additionally, the 50% duty cycle testing may have fostered more consistent biological activity in the biofilm, contributing to more predictable pH values using the MLR model. Interestingly, for the December and 50% duty cycle testing, the testing periods that appear to have best fit the MLR model, the correlation is higher for biofilm pH averages. This difference from liquid pH averages suggests the algae biomass was more predictable in its response to light and temperature than was the liquid filtrate.

Visualizations of the liquid and biofilm pH MLR were performed in Python. The visualizations for the December testing period are shown in Figure 12.

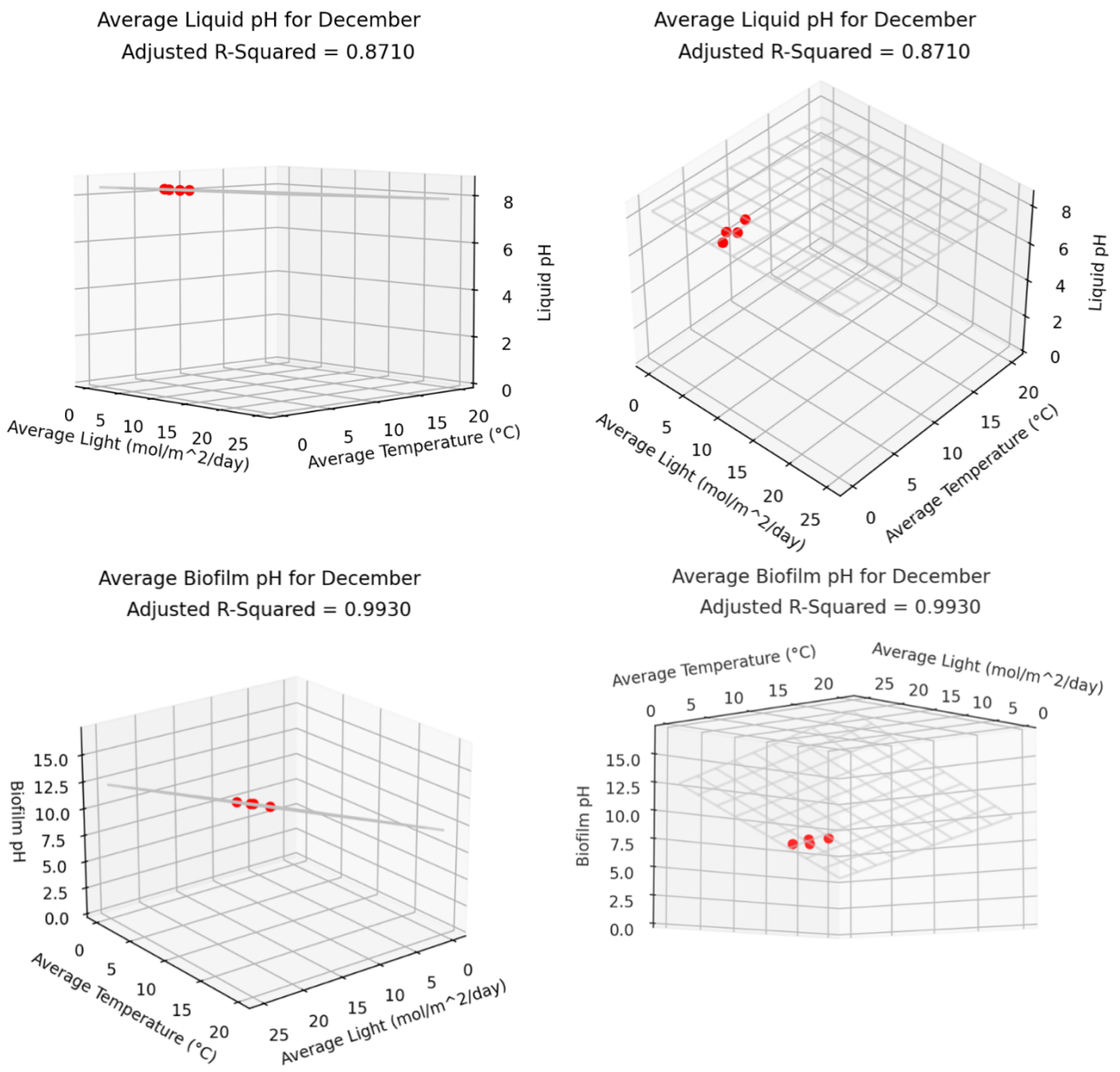


Fig. 12. Visualization of multiple linear regression tests to correlate rotating algae biofilm reactor pH values with average daily light integral (DLI) and average air temperature. The top two graphs use a liquid pH while the bottom two graphs use biofilm pH.

4. Engineering Management Options

Using results from this study, engineering management options for the RABR are outlined for use in future research. These management options, associated with operating parameters of the RABR, are as follows: duty cycle, RPM, direction of rotation,

temperature, UV screening, chemical additives, biostimulation, and bioaugmentation. Each of these management options is explained here.

For variation in duty cycle, results from this study suggest operation at higher duty cycles result in higher DW and AFDW productivity. For power savings associated with TKN uptake, a lower duty cycle was more energetically favorable. Conversely, for power savings associated with TP uptake, a higher duty cycle was more energetically favorable. Ash content was also higher at the higher duty cycle tested, suggesting a higher duty cycle contributed to a more biologically and chemically active biofilm. Rotational speed could be increased by modulating RPM, but increases in power associated with higher rotational speeds will likely negatively impact power requirements to removal 1 kg nutrient.

Direction of rotation can be changed to further decrease power requirements. Preliminary results show an approximate decrease of 30% for instantaneous power draw by reversing the RABR's direction of rotation. This is likely due to the mechanical design of the RABR. By reversing the rotation, the system minimizes shear forces by "gliding" through the filtrate, as opposed to the previous "scooping" behavior shown during testing. Level of filtrate through the system can also be raised. While this change would affect power requirements associated with rotating the assembly, raising the filtrate level would mitigate nutrient starvation experienced by the shelves closest to the axis of rotation, as explained in Results and Discussion section 3.2.3.

Temperature can be varied by heating the influent filtrate into the RABR system. From results of this study, productivity values are expected to increase with increases in the liquid temperature, especially during the winter months. This elevated liquid

temperature can be maintained using foam insulation attached to the RABR tank.

Additionally, changes in HRT, manifested by higher flow, can help maintain elevated liquid temperature, so long as nutrient removal rates are not compromised.

It is possible high light levels associated with summer months create photooxidation and UV damage. Hence, shade cloth coverings can be installed to the RABR system's roof to block out high levels of light. Additionally, UV-filtering screens can be installed to the walls and roof during high-light conditions. For low-light periods, light can be supplemented with standard grow lights, programmed to illuminate when light conditions during the daytime growth period reach a sufficiently low threshold. Productivity values, when coupled with these management options, are expected to increase.

Chemical additives can be added to the RABR system to select for desired ash constituents. Specifically, it is possible magnesium is the limiting reactant in the chemical precipitation of struvite (NH_4MgPO_4). By selectively sparging magnesium into the system, greater precipitation of struvite can occur within the biofilm. This enhanced inorganic precipitation is favorable for nitrogen uptake, phosphorus uptake, and biofertilizer production. In addition to introduction of magnesium to the system, gas sparging of carbon dioxide can be performed. This addition to the system would likely enhance the microalgae's autotrophic metabolism. It is expected the introduction of CO_2 to the liquid phase of the system would increase biological activity in the biofilm, which would in turn increase chemical precipitation in the biofilm.

If further work can identify species within the microalgae contributing to luxury uptake of phosphorus, these species can be biostimulated. By strategically varying

conditions for the biofilm, the RABR system could eventually be integrated into a feast-famine induction of luxury uptake of phosphorus. Similarly, the species found to contribute to luxury uptake of phosphorus can be harvested, cultured in a laboratory, and re-applied to the RABR system. This selective augmentation has the potential to increase luxury uptake of phosphorus and enhance nutrient uptake of the RABR system.

6. Conclusions and Future Work

An outdoor pilot-scale rotating algae biofilm reactor (RABR) was implemented for nutrient uptake and productivity testing. The 25% and 50% duty cycles showed minimal power draw at 0.896 revolutions per minute (RPM). Optimal power consumptions for nutrient uptake were 1.36 kWh/kg_{TKN} (nitrogen) and 20.1 kWh/kg_{TP} (phosphorus). Maximum average footprint productivity was 7.09 g/m²-day. Statistical analysis distinguished operating parameters from seasonal effects and quantified productivity differences due to light attenuation. Multiple linear regression established correlation between light/temperature levels and productivity, ash content, and pH. Nitrogen content was within 1% of microalgae stoichiometry, and phosphorus was elevated, suggesting luxury phosphorus uptake. Analysis of inorganic salts showed 0.68% w/w of the dry biofilm was struvite.

For the purposes of this study, TKN was used to quantify nitrogen in the liquid and biofilm phases. However, with the possibility of nitrification occurring in the RABR system, further nitrogen-containing compounds could be investigated. Specifically, tests for presence of nitrate and nitrate molecules in the liquid and biofilm phases could be performed.

The power requirements required to remove 1 kg nutrient could be compared to various water remediation systems. Specifically, energy and cost comparisons could be performed with high-rate algal ponds (HRAPs), traditional raceways, and traditional photobioreactors (PBRs). In addition to microalgae-based water remediation systems, energy and cost associated with the RABR can be compared to Annamox and Magprex systems. These comparisons can be used for better-informed scaleup of the RABR system.

To further retrofit the RABR into a PFR system, steel dividers could be installed into the RABR tank. More robust dividers within the tank could show statistically distinct productivity and nutrient uptake between RABR bays. Further scaleup could be performed by linking multiple RABR systems in series for maximum nutrient removal and polishing. To continue productivity and nutrient uptake testing, analysis using further duty cycle and RPM combinations should be performed. Of most importance to continuation of this study, 100% duty cycle testing should be performed using the current embodiment of the RABR. Since no statistical differences were shown between bays and sections in productivity analysis, harvests from each corresponding shelf can be combined to obtain separate top shelf, middle shelf, and bottom shelf yields. In addition to productivity testing, analysis should be performed to quantify yield of AFDW productivity per mol photosynthetically active photons. This calculation would be represented as g AFDW/day-mol.

Further work should validate the evidence of luxury uptake of phosphorus demonstrated in this study. Luxury uptake of phosphorus can be validated using staining and microscopy for observation of polyphosphate granules within the microalgae.

Additionally, validation of thermal properties of struvite should be validated by combusting pure struvite samples in a muffle furnace, ensuring negligible struvite decomposition in the ashing procedures used in this study.

7. References

- APHA, 1997. Standard Methods for the Examination of Water and Wastewater.
- Aslan, S., Kapdan, I.K., 2006. Batch kinetics of nitrogen and phosphorus removal from synthetic wastewater by algae. *Ecol. Eng.* 28, 64–70.
<https://doi.org/10.1016/j.ecoleng.2006.04.003>
- Barlow, J., Sims, R.C., Quinn, J.C., 2016. Techno-economic and life-cycle assessment of an attached growth algal biorefinery. *Bioresour. Technol.* 220, 360–368.
<https://doi.org/10.1016/j.biortech.2016.08.091>
- Boelee, N.C., Janssen, M., Temmink, H., Shrestha, R., Buisman, C.J.N., Wijffels, R.H., 2014. Nutrient Removal and Biomass Production in an Outdoor Pilot-Scale Phototrophic Biofilm Reactor for Effluent Polishing. *Appl. Biochem. Biotechnol.* 172, 405–422. <https://doi.org/10.1007/s12010-013-0478-6>
- Cheah, Y.T., Chan, D.J.C., 2021. Physiology of microalgal biofilm: a review on prediction of adhesion on substrates. *Bioengineered* 12, 7577–7599.
<https://doi.org/10.1080/21655979.2021.1980671>
- Choudhary, S., Tripathi, S., Poluri, K.M., 2022. Microalgal-Based Bioenergy: Strategies, Prospects, and Sustainability. *Energy Fuels* 36, 14584–14612.
<https://doi.org/10.1021/acs.energyfuels.2c02922>
- Christenson, L., Sims, R., 2011. Production and harvesting of microalgae for wastewater treatment, biofuels, and bioproducts. *Biotechnol. Adv.* 29, 686–702.
<https://doi.org/10.1016/j.biotechadv.2011.05.015>
- Christenson, L.B., Sims, R.C., 2012. Rotating algal biofilm reactor and spool harvester for wastewater treatment with biofuels by-products. *Biotechnol. Bioeng.* 109, 1674–1684. <https://doi.org/10.1002/bit.24451>
- Ennaceri, H., Ishika, T., Mkpuma, V.O., Moheimani, N.R., 2023. Microalgal biofilms: Towards a sustainable biomass production. *Algal Res.* 72, 103124.
<https://doi.org/10.1016/j.algal.2023.103124>
- EPA, 1993a. Method 365.1, Revision 2.0: Determination of Phosphorus by Semi-Automated Colorimetry.
- EPA, 1993b. Method 351.2, Revision 2.0: Determination of Total Kjeldahl Nitrogen by Semi-Automated Colorimetry.
- Ermis, H., Altinbas, M., 2019. Determination of biokinetic coefficients for nutrient removal from anaerobic liquid digestate by mixed microalgae. *J. Appl. Phycol.* 31, 1773–1781. <https://doi.org/10.1007/s10811-018-1671-3>
- Espinosa-Ortiz, E.J., Gerlach, R., Peyton, B.M., Roberson, L., Yeh, D.H., 2023. Biofilm reactors for the treatment of used water in space: potential, challenges, and future perspectives. *Biofilm* 6, 100140. <https://doi.org/10.1016/j.bioflm.2023.100140>
- Gerardo, M.L., Van Den Hende, S., Vervaeren, H., Coward, T., Skill, S.C., 2015. Harvesting of microalgae within a biorefinery approach: A review of the developments and case studies from pilot-plants. *Algal Res.* 11, 248–262.
<https://doi.org/10.1016/j.algal.2015.06.019>
- Goldsberry, P., Jeppesen, P., McLean, J., Sims, R., 2023. An attached microalgae platform for recycling phosphorus through biologically mediated fertilizer formation and biomass cultivation. *Clean. Eng. Technol.* 17, 100701.
<https://doi.org/10.1016/j.clet.2023.100701>

- Hillman, K.M., Sims, R.C., 2020. Struvite formation associated with the microalgae biofilm matrix of a rotating algal biofilm reactor (RABR) during nutrient removal from municipal wastewater. *Water Sci. Technol.* 81, 644–655. <https://doi.org/10.2166/wst.2020.133>
- Johnson, M.B., Wen, Z., 2010. Development of an attached microalgal growth system for biofuel production. *Appl. Microbiol. Biotechnol.* 85, 525–534. <https://doi.org/10.1007/s00253-009-2133-2>
- Kannah, R.Y., Kavitha, S., Banu, J.R., Sivashanmugam, P., Gunasekaran, M., Kumar, G., 2021. A Mini Review of Biochemical Conversion of Algal Biorefinery. *Energy Fuels* 35, 16995–17007. <https://doi.org/10.1021/acs.energyfuels.1c02294>
- Katarzyna, L., Sai, G., Singh, O.A., 2015. Non-enclosure methods for non-suspended microalgae cultivation: literature review and research needs. *Renew. Sustain. Energy Rev.* 42, 1418–1427. <https://doi.org/10.1016/j.rser.2014.11.029>
- Kesaano, M., Sims, R.C., 2014. Algal biofilm based technology for wastewater treatment. *Algal Res.* 5, 231–240. <https://doi.org/10.1016/j.algal.2014.02.003>
- Lutzu, G.A., Ciurli, A., Chiellini, C., Di Caprio, F., Concas, A., Dunford, N.T., 2021. Latest developments in wastewater treatment and biopolymer production by microalgae. *J. Environ. Chem. Eng.* 9, 104926. <https://doi.org/10.1016/j.jece.2020.104926>
- Mba, D., Bannister, R.H., Findlay, G.E., 1999. Mechanical redesign of the rotating biological contactor. *Water Res.* 33, 3679–3688. [https://doi.org/10.1016/S0043-1354\(99\)00086-X](https://doi.org/10.1016/S0043-1354(99)00086-X)
- Mendoza, J.L., Granados, M.R., De Godos, I., Acién, F.G., Molina, E., Banks, C., Heaven, S., 2013. Fluid-dynamic characterization of real-scale raceway reactors for microalgae production. *Biomass Bioenergy* 54, 267–275. <https://doi.org/10.1016/j.biombioe.2013.03.017>
- Morales, M., Bonnefond, H., Bernard, O., 2020. Rotating algal biofilm versus planktonic cultivation: LCA perspective. *J. Clean. Prod.* 257, 120547. <https://doi.org/10.1016/j.jclepro.2020.120547>
- National Weather Service, 2023. NOWData - NOAA Online Weather Data.
- Patwardhan, S.B., Pandit, S., Ghosh, D., Dhar, D.W., Banerjee, S., Joshi, S., Gupta, P.K., Lahiri, D., Nag, M., Ruokolainen, J., Ray, R.R., Kumar Kesari, K., 2022. A concise review on the cultivation of microalgal biofilms for biofuel feedstock production. *Biomass Convers. Biorefinery.* <https://doi.org/10.1007/s13399-022-02783-9>
- Rezvani, S., Saadaoui, I., Al Jabri, H., Moheimani, N.R., 2022. Techno-economic modelling of high-value metabolites and secondary products from microalgae cultivated in closed photobioreactors with supplementary lighting. *Algal Res.* 65, 102733. <https://doi.org/10.1016/j.algal.2022.102733>
- Richard Kingsley, P., Braud, L., Kumar Mediboyina, M., McDonnell, K., Murphy, F., 2023. Prospects for commercial microalgal biorefineries: Integrated pilot demonstrations and process simulations based techno-economic assessment of single and multi-product value chains. *Algal Res.* 74, 103190. <https://doi.org/10.1016/j.algal.2023.103190>
- Roostaei, J., Zhang, Y., Gopalakrishnan, K., Ochocki, A.J., 2018. Mixotrophic Microalgae Biofilm: A Novel Algae Cultivation Strategy for Improved

- Productivity and Cost-efficiency of Biofuel Feedstock Production. *Sci. Rep.* 8, 12528. <https://doi.org/10.1038/s41598-018-31016-1>
- Schnurr, P.J., Molenda, O., Edwards, E., Espie, G.S., Allen, D.G., 2016. Improved biomass productivity in algal biofilms through synergistic interactions between photon flux density and carbon dioxide concentration. *Bioresour. Technol.* 219, 72–79. <https://doi.org/10.1016/j.biortech.2016.06.129>
- Sims, R., Peterson, B., 2021. Waste to value: algae-based biofuel utilizing oil and gas extraction wastewater. *Acad. Lett.* <https://doi.org/10.20935/AL4460>
- Solovchenko, A.E., Ismagulova, T.T., Lukyanov, A.A., Vasilieva, S.G., Konyukhov, I.V., Pogosyan, S.I., Lobakova, E.S., Gorelova, O.A., 2019. Luxury phosphorus uptake in microalgae. *J. Appl. Phycol.* 31, 2755–2770. <https://doi.org/10.1007/s10811-019-01831-8>
- Stumm, W., Morgan, J.J., 2012. *Aquatic Chemistry: Chemical Equilibria and Rates in Natural Waters*, 3rd ed. ed. Wiley, Hoboken.
- Ubando, A.T., Felix, C.B., Chen, W.-H., 2020. Biorefineries in circular bioeconomy: A comprehensive review. *Bioresour. Technol.* 299, 122585. <https://doi.org/10.1016/j.biortech.2019.122585>
- Udom, I., Zaribaf, B.H., Halfhide, T., Gillie, B., Dalrymple, O., Zhang, Q., Ergas, S.J., 2013. Harvesting microalgae grown on wastewater. *Bioresour. Technol.* 139, 101–106. <https://doi.org/10.1016/j.biortech.2013.04.002>
- Vassilev, S.V., Vassileva, C.G., Bai, J., 2023. Content, modes of occurrence, and significance of phosphorous in biomass and biomass ash. *J. Energy Inst.* 108, 101205. <https://doi.org/10.1016/j.joei.2023.101205>
- Wang, J., Liu, W., Liu, T., 2017. Biofilm based attached cultivation technology for microalgal biorefineries—A review. *Bioresour. Technol.* 244, 1245–1253. <https://doi.org/10.1016/j.biortech.2017.05.136>
- Zamalloa, C., Boon, N., Verstraete, W., 2013. Decentralized two-stage sewage treatment by chemical–biological flocculation combined with microalgae biofilm for nutrient immobilization in a roof installed parallel plate reactor. *Bioresour. Technol.* 130, 152–160. <https://doi.org/10.1016/j.biortech.2012.11.128>
- Zhuang, L.-L., Li, M., Hao Ngo, H., 2020. Non-suspended microalgae cultivation for wastewater refinery and biomass production. *Bioresour. Technol.* 308, 123320. <https://doi.org/10.1016/j.biortech.2020.123320>

APPENDIX

Power Optimization of an Outdoor Pilot-Scale Rotating Algae Biofilm Reactor for Enhanced Productivity and Nutrient Uptake from Anaerobic Digestate

Authors: Peter F. Jeppesen*, J. Dietrich Storrer, Ronald C. Sims

* - Corresponding author, peter.f.jeppesen@gmail.com

Subject classification: 50.060 Optimization of bioprocess

All authors mutually agree this manuscript should be submitted to BITE.

The authors concur this study is the product of our original work.

This manuscript has not previously been submitted to BITE.

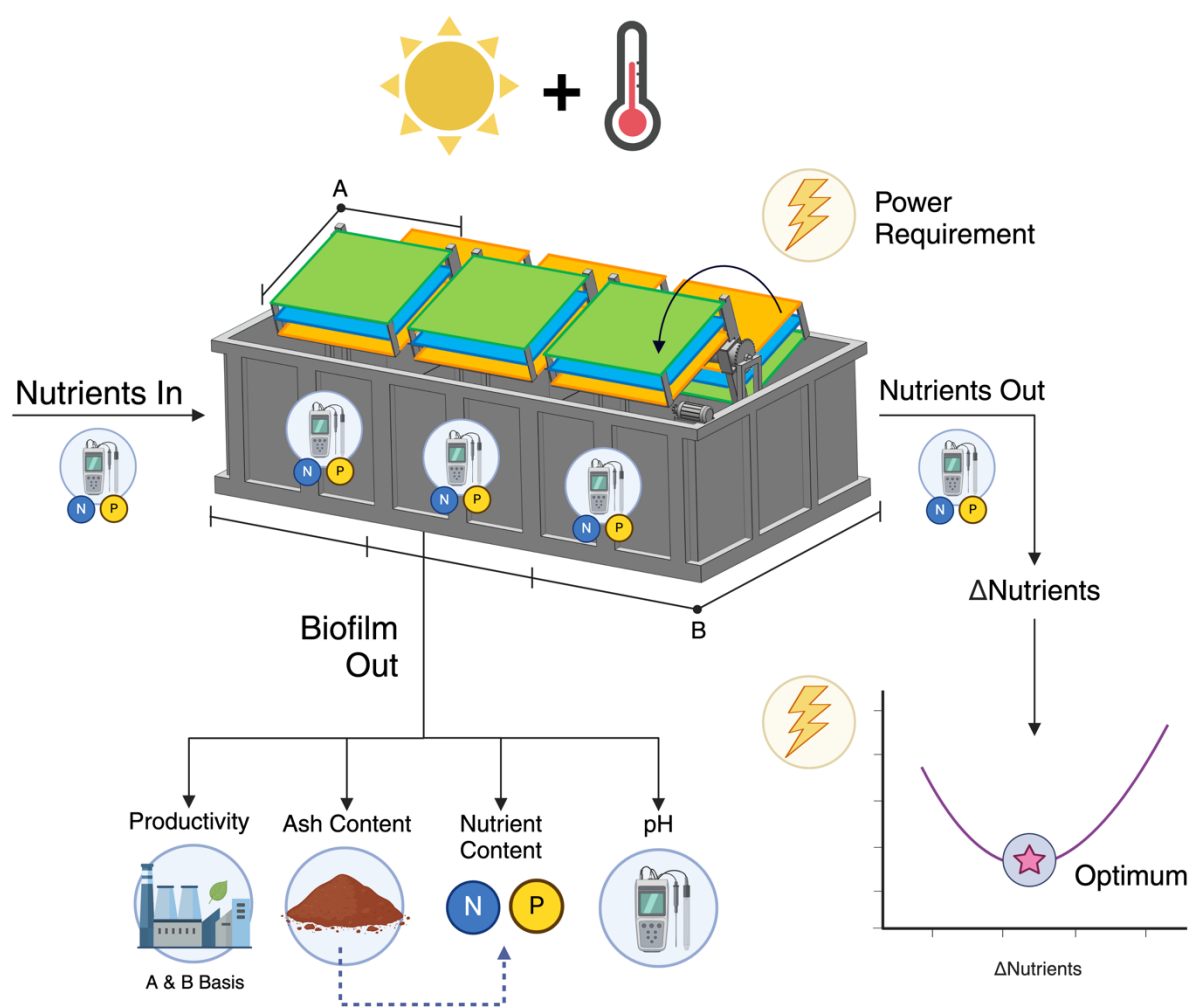
Novelty: Power optimization for nutrient uptake, which has never been performed using an outdoor attached-growth algae cultivation system, was addressed. This study offers methodology and results for quantification of power requirements per liquid kg nutrient removed. These findings will be vital to lateral testing and scaleup of future attached-growth algae systems. Furthermore, many studies have discussed the shortcomings of attached-growth productivity due to light attenuation caused by self-shading. Until now, no study has statistically analyzed productivity differences caused by this light attenuation, which is addressed in the testing reported here. Lastly, evidence of luxury uptake of phosphorus, which has never been observed using an outdoor attached-growth algae cultivation system, is demonstrated.

Power Optimization of an Outdoor Pilot-Scale Rotating Algae Biofilm Reactor for Enhanced Productivity and Nutrient Uptake from Anaerobic Digestate

Authors: Peter F. Jeppesen*, J. Dietrich Storrer, Ronald C. Sims

* - Corresponding author, peter.f.jeppesen@gmail.com

Graphical Abstract:



Power Optimization of an Outdoor Pilot-Scale Rotating Algae Biofilm Reactor for Enhanced Productivity and Nutrient Uptake from Anaerobic Digestate

Authors: Peter F. Jeppesen*, J. Dietrich Storrer, Ronald C. Sims

* - Corresponding author, peter.f.jeppesen@gmail.com

Highlights

- Footprint and substratum productivity values are contrasted
- Power consumption for nutrient removal is optimized
- Light attenuation affects productivity of attached-growth algae cultivation
- Pilot-scale evidence of luxury uptake of phosphorus

Power Optimization of an Outdoor Pilot-Scale Rotating Algae Biofilm Reactor for Enhanced Productivity and Nutrient Uptake from Anaerobic Digestate

Authors: Peter F. Jeppesen^{a*}, J. Dietrich Storrer^b, Ronald Sims^c

^a - 4105 Old Main Hill, Logan, UT 84322-2793 USA, peter.f.jeppesen@gmail.com

^b - 4105 Old Main Hill, Logan, UT 84322-2793 USA, a02398087@aggies.usu.edu

^c - 4105 Old Main Hill, Logan, UT 84322-2793 USA, ron.sims@usu.edu

* - Corresponding author, peter.f.jeppesen@gmail.com

Funding: This research was funded by the U.S. Department of Energy Bioenergy Technology Office under award 446 number DE-EE0009271 to Utah State University. The views expressed in this article do not necessarily represent the views of the U.S. DOE or the United States Government. Neither the U.S. Government nor any agency thereof, nor any of their employees, makes any warranty, expressed, or implied, or assumes any legal liability or responsibility for the accuracy, completeness, or usefulness of any information, apparatus, product, or process disclosed, or represents that its use would not infringe privately owned rights.

Competing Interests: The authors have no known competing interests to declare.

Data Statement: The data associated with this study will be made available upon request.

Acknowledgements

The United States DOE is responsible for the funding of this project (grant number DE-EE0009271). Special thanks to Dr. Phil Heck, manager of CVWRF, for providing the

host site and staff to assist with RABR maintenance. Additional thanks to Jim Judd from WesTech Engineering for his essential role in pilot construction and power draw measurements. Thanks to Joshua Wintch for development of standard curves for nitrogen and phosphorus quantification.

Abstract

An outdoor pilot-scale rotating algae biofilm reactor (RABR) was successfully implemented for nutrient uptake and productivity testing. Power reduction was performed by modulating duty cycle and rotational speed. Optimal power consumption values for nutrient removal were 1.36 kWh/kg_{TKN} (nitrogen) and 20.1 kWh/kg_{TP} (phosphorus). Maximum footprint productivity was 7.09 g/m²-day. Comprehensive statistical analyses of productivity, ash content, liquid nutrients, and pH validated continuous flow stirred tank reactor (CFSTR) behavior and affirmed effects of operating parameters on reactor performance. Further statistical analysis delineated productivity differences due to light attenuation. Multiple linear regression established high correlation between light/temperature levels and productivity, ash content, and pH. Elemental balances showed microalgae nitrogen content within 1% of known stoichiometry of microalgae and elevated phosphorus, providing real-world evidence of luxury phosphorus uptake. Analysis of inorganic salts was performed, showing 0.68% w/w of the dry biofilm was comprised of struvite. Keywords: Biofilm productivity; nutrient uptake; power optimization; struvite precipitation

1. Introduction

Due to increasing environmental, societal, and regulatory pressure, the past 50 years have seen increased innovation in microalgae cultivation (Ubando et al., 2020). With advances in bioprocessing, microalgae cultivation has become more attractive for application in environmental and manufacturing industries (Katarzyna et al., 2015; Lutz et al., 2021). The two most prominent algae cultivation methods include attached- and suspended-growth (Katarzyna et al., 2015). Attached-growth systems, often represented as algae

biofilm reactors, hold potential for commercialization (Kesaano and Sims, 2014; Richard Kingsley et al., 2023; Zamalloa et al., 2013). Algae biofilm reactors hold potential for use in a variety of applications. In addition to the immediate benefit of biological nutrient uptake from wastewater, biofilm reactors can serve as biologically induced chemical reactors. This biological induction by algae biomass is a new area of research which can facilitate production of chemical precipitates such as struvite in various industrial or space applications (Espinosa-Ortiz et al., 2023; Goldsberry et al., 2023; Hillman and Sims, 2020).

Biofilm reactors have distinct advantages over suspended-growth systems. Algae biofilm reactors benefit from small footprint area, simple harvesting and dewatering, high cell density, and enhanced resilience (Cheah and Chan, 2021; Schnurr et al., 2016; Wang et al., 2017; Zhuang et al., 2020). Algae biofilm reactors also hold operational potential for use as biorefineries in sustainable generation of value-added bioproducts, including biocrude, bioplastic, biodiesel, and biofertilizer (Katarzyna et al., 2015; Roostaei et al., 2018; Zhuang et al., 2020). These value-added bioproducts can help offset costs of wastewater remediation and prove economical for municipal and industrial entities (Barlow et al., 2016; Christenson and Sims, 2011; Johnson and Wen, 2010; Kannah et al., 2021; Patwardhan et al., 2022; Ubando et al., 2020). Algae biofilm reactors, however, are not without their flaws. One major drawback of biofilm reactors is light attenuation due to self-shading. This self-shading, caused by spacing of growth substratum, has yet to be investigated quantitatively or statistically through productivity analysis (Wang et al., 2017; Zhuang et al., 2020).

The United States Department of Energy (DOE) is invested in circular engineering through water treatment and bioproduct generation. In the context of this study, the DOE is specifically interested in power requirements for nutrient removal, reported in units of kWh/kg total nutrient removed. However, there remains a gap in literature regarding power requirements for algae biofilm cultivation in an outdoor pilot-scale setting. Only one study has reported a power requirement associated with operating an algae biofilm reactor (Christenson and Sims, 2012). This power requirement, when converted to power consumptions (kWh/kg total nutrient removed), yielded 2.6 kWh/kg_{TKN} (nitrogen) and 17.5 kWh/kg_{TP} (phosphorus). Power requirements associated with real-world algae biofilm reactors are of great importance for scale-up and commercialization of attached-growth algae cultivation technology (Choudhary et al., 2022; Ennaceri et al., 2023; Gerardo et al., 2015; Mendoza et al., 2013; Morales et al., 2020; Rezvani et al., 2022; Sims and Peterson, 2021).

Many studies have been performed using attached-growth microalgae cultivation at a laboratory scale. However, fewer studies have investigated attached-growth microalgae systems at a pilot scale. Of these few pilot-scale studies, many show inconsistency in productivity and nutrient uptake (Lutzu et al., 2021). One potential cause of the inconsistency associated with outdoor pilot-scale testing of algae biofilm systems (and photosynthetic organisms en masse) is the challenge of determining whether operational parameters or seasonal effects have a greater influence on pilot performance. This study optimizes the energy consumption and biorefinery capabilities of an outdoor pilot-scale rotating algae biofilm reactor (RABR). This RABR, located at Central Valley Water Reclamation Facility (CVWRF) in Salt Lake City, Utah, removes nitrogen and

phosphorus from nutrient-rich anaerobic digester effluent. This anaerobic digester effluent, referred to throughout this document as “filtrate,” flows from a dewatering belt press to the headworks of CVWRF. Because the RABR is situated on a return stream, the testing conditions provide a low-risk proof of concept of the RABR’s capabilities for biofilm productivity and nutrient uptake. The microalgae inoculum used in this study was a natural consortium obtained from a trickling filter at CVWRF. This study correlates pilot performance parameters, including productivity, ash content, and pH, with light and temperature levels under both seasonal- and operational-specific conditions. This study investigates both dry weight (DW) and ash-free dry weight (AFDW) biofilm productivity using footprint and substratum bases. These productivity values are tested statistically to find spatial productivity differences between growth substrata of the pilot-scale RABR. Additionally, this study presents empirical data to correlate power requirements with removal of nitrogen and phosphorus. Lastly, this study establishes elemental balances using nitrogen and phosphorus to validate biomass stoichiometry and quantify struvite-containing ash content.

2. Material and methods

The purpose of this section is to describe the structural, operational, and analytical methods for the pilot-scale rotating algae biofilm reactor (RABR). Experimental work consisted of harvesting, drying, ashing, and quantifying nutrient concentrations of algae biofilm cultivated using the RABR. Additionally, experimental work included taking liquid samples for pH, nitrogen, and phosphorus quantification. The experimental period associated with these methods was the fall season of 2023.

2.1 RABR Structure

The RABR was comprised of a steel tank (4.72 m × 2.44 m × 1.22 m interior dimensions, containing 11.5 m³ anaerobic digester effluent), a 0.2-m diameter steel shaft (4.06 m long), and six three-shelved sections (1.15 m × 1.19 m × 0.34 m) (Figure 2). The tank was divided into three bays, with each bay containing two sections. For growth substratum, 2-m² post-consumer recycled carpets were fastened to each shelf (Goldsberry et al., 2023). The rotating assembly, weighing ~785 kg in total, was rotated by a 7.38-kW electric gearbox (172.17:1 box ratio) via a chain to a sprocket (12:1 gear ratio). The electric gearbox allowed for modulation of rotational speed (RPM) and duty cycle (ratio of time rotating to time stationary). As shown in Figure 2, the RABR used six three-shelved sections, while future embodiments could accommodate up to twelve sections, totaling 36 shelves.

To further separate the bays, two polycarbonate sheets were fastened between bays 1 and 2 and bays 2 and 3, attempting to convert the system from a continuous flow stirred tank reactor (CFSTR) to a plug-flow reactor (PFR). Lastly, the RABR system was equipped with a polycarbonate roof and optional polycarbonate walls. These walls were installed at the beginning of December 2023 to prevent the biofilm from freezing.

The liquid influent to the RABR system was anaerobic digester effluent. This anaerobic digester effluent, delivered to the system from a filter press, is known throughout this document as “filtrate.” Influent filtrate flow was set to accommodate a 2-day hydraulic retention time (HRT) across bay 1 of the RABR. This HRT translated to a 6-day HRT across the entire RABR, or a flow of approximately 1.33 L/min. To successfully use this filtrate, the RABR system required a clarification step. The RABR’s operation system, coupled with a photograph of the system, is summarized in Figure 2.

2.2 Power Measurement

Power readings were obtained using a Fluke® 39 Power Meter. Readings were taken at the variable frequency drive (VFD) that controlled the gearbox. The experimental procedure involved manipulating the rotational speed (RPM) using the VFD and modulating the duty cycle, alternating intervals rotating and stationary, using the system control panel. Power measurements were recorded at twenty 1-min intervals for a 100% duty cycle and forty 15-s intervals for 50% and 25% duty cycles. Preliminary results showed the lowest power draw at 25% and 50% duty cycles using 0.896 RPM; hence, productivity testing was prioritized for these two duty cycle and RPM combinations.

2.2.1 Power Considerations in Operation

The optimal duty cycles found through power measurements were coupled with the optimal RPM and implemented for productivity testing during the fall season of 2023. These duty cycles, 25% and 50%, were both tested in multiple months during the fall season to ensure operating parameters were responsible for variability of RABR output, instead seasonal differences being the driving factor. By implementing optimized duty cycle-RPM combinations, the testing ensured power savings before productivity testing had commenced.

2.2.2 Power Requirements for Nutrient Removal

The nutrients investigated for power optimization were nitrogen and phosphorus (see Material and Methods 2.5). The influent and effluent liquid nutrient concentrations, sampled weekly during the fall season of 2023 using sampling points shown in Figure 2a, were first converted to a mass-flow rate using the flow rate associated with a 6-day HRT for the RABR system. Second, the difference between influent and effluent nutrient

mass-flow rates was calculated, constituting a nutrient removal rate. Third, the nutrient removal rate was extended to determine the operation time required to remove 1 kg of the nutrient of interest according to the nutrient removal rate at the time of liquid sampling. Fourth, the rotational power measurements obtained as explained in the previous section were used to determine the power requirement for removal of 1 kg nutrient. This power requirement, referred to as “expected power consumption,” provides a metric for pilot performance under operation-specific power draws and nutrient removal rates, assuming the operation-specific parameters were allowed to continue until 1 kg nutrient is removed from the liquid phase by the RABR.

2.3 Biomass Harvesting

The algae biomass was harvested weekly during fall 2023. Using conventional garden hoes, biomass from both sides of the eighteen shelves was harvested into water-tight plastic containers. Each container was given identifiers specific to the bay, section, and shelf location. Within 8 h of harvesting, the biomass samples were transported to a freezer set at -10°C .

2.4 Dry Weight and Ash-Free Dry Weight

The individual shelf samples were moved from the -10°C freezer to 25-cm baking tins, weighed for wet weight analysis, and dried at 60°C for 48 h. After drying, these shelf samples were placed in a desiccator and allowed to cool to room temperature. After cooling, the dry biomass was weighed for dry weight (DW) analysis and ground using a mortar and pestle (Udom et al., 2013). Ensuring homogeneity of the dry biomass, a 1-g sample of each shelf sample was combusted in a muffle furnace at 550°C for 2 h (Boelee et al., 2014). When cooled in a desiccator and weighed, this sample constituted the ash

weight (AW) content of the shelf. The ash-free dry weight (AFDW) was then calculated by subtracting the AW from the 1-g dry sample. The AFDW content was then used to determine total AFDW for the individual shelf sample, and the ash content was used in statistical tests to explore operational, seasonal, and spatial variations in ash content.

2.4.1 Footprint and Substratum Productivity

Productivity values were determined by dividing either the DW or AFDW by the product of the days since the previous harvest and the area under analysis. This calculation yielded units of g/m²-day. Footprint productivity values were determined based on either the area of a single bay in the RABR or the total tank area (11.5 m²). This differentiation is crucial because a single shelf occupies the same area as an entire bay. By employing bay areas for comparison, the analysis facilitates a more comprehensive assessment among different spatial arrangements of the shelves. Substratum productivity values were calculated using 2 m² for each shelf. This area represented the top and bottom area of the carpet substratum attached to each shelf. Unlike footprint productivity, the substratum area used increases proportionally to the number of shelves in the analysis.

In this study, four productivity values were monitored through weekly harvests of the eighteen shelves of the RABR: DW footprint, DW substratum, AFDW footprint, and AFDW substratum productivity. These productivity values, monitored during the fall season of 2023, furnished an extensive data set, and enabled comprehensive statistical analyses. The productivity values were combined in total, bay, section, and shelf analyses.

2.5 Filtrate, Liquid Sampling, and Analysis

The filtrate used in the system exited the belt press with a total suspended solids (TSS) concentration of approximately 1000 mg/L. The clarification step reduced the TSS concentration to an estimated 200 mg/L. The filtrate pH ranged from 7.85 to 8.45 during the testing period during fall 2023. Liquid samples were obtained for analysis of nitrogen and phosphorus concentrations. Samples were taken weekly from system influent, bay 1, bay 2, bay 3, and effluent locations (Figure 2a). These locations were also used for weekly pH measurements using an Oakton® WD-35614-20 field pH probe calibrated before each weekly session of data collection. For the month of October, a single sample was taken at each of these locations once a week before harvesting. Analyses of the liquid samples for total nitrogen and total phosphorus were performed using Hach TNT828 and TNT845 kits, respectively (Hach Co., Loveland, CO) (Barlow et al., 2016). Five-point standard curves were used for these analyses.

In addition to liquid pH samples, biofilm pH samples were taken each week before harvesting. The biofilm pH samples were measured in corresponding shelves of the three bays from the same section.

2.6 Light and Temperature Measurements

Light levels were quantified using an Apogee Instruments DLI-500. In addition to a daily light integral (DLI), photosynthetic photon flux density (PPFD) readings were obtained weekly (Goldsberry et al., 2023). These PPFD measurements, obtained from the center of the RABR shelves, were used to determine light attenuation among the three-shelved sections of the RABR.

Air temperature readings were logged using the National Weather Service's climate weather data. The temperature data, taken 8.61 km from the RABR, reported values for

minimum, maximum, and average daily temperatures. These values were obtained using NOAA Online Weather Data (National Weather Service, 2023).

2.7 Biofilm and Ash Constituents

Biofilm and ash constituents were quantified using procedures for nitrogen, phosphorus, and total solids. These constituents were used for analysis of elemental balances and nutrient uptake.

2.7.1 Total Phosphorus and Total Kjeldahl Nitrogen

Measurements for total phosphorus (TP), total Kjeldahl nitrogen (TKN), and total solids (TS) of the biofilm were collected by an independent certified laboratory, located at Central Valley Water Reclamation Facility (CVWRF) in Salt Lake City, Utah. Methods used for TP, TKN, and TS were EPA 365.1, EPA 351.2, and SM 2540G-1997, respectively (APHA, 1997; EPA, 1993a, 1993b). In this study, TKN is used for total nitrogen because the filtrate used in the RABR comes from an anaerobic digester.

In addition, TP and TKN procedures were performed using the AW obtained from the RABR biofilm. These procedures used EPA 365.1 and EPA 351.2 (EPA, 1993a, 1993b). However, the CVWRF laboratory used 100 mL deionized water for suspension of 5-g AW samples. The laboratory then digested the suspended AW, followed by the EPA procedures for TP and TKN (EPA, 1993a, 1993b).

It was assumed that organic phosphorus compounds, like organic nitrogen compounds, have sufficiently low boiling points to be released as gaseous oxides under the combustion conditions used (Vassilev et al., 2023). Hence, the nitrogen and phosphorus elemental balances were closed for the biofilm as follows: $N_{\text{Biofilm}} = N_{\text{Biomass}} + N_{\text{Ash}}$ and

$$P_{\text{Biofilm}} = P_{\text{Biomass}} + P_{\text{Ash}}$$

By quantifying the nutrient concentrations in the biofilm and the AW, the nutrient content in the biomass was calculated. The nitrogen-containing AW, assumed to be primarily struvite, was also interpreted for struvite productivity and struvite mass percentage of the biofilm using simple chemical conversions (Hillman and Sims, 2020). The struvite quantities, calculated using TKN concentrations of AW, were used to calculate struvite-bound inorganic phosphorus. Subsequently, the concentration of struvite-bound inorganic phosphorus was subtracted from the TP concentration in the AW to analyze non-struvite-bound inorganic phosphorus.

2.8 Statistical Analyses

Statistical tests were performed for productivity, ash content, liquid nutrients, and pH measurements. These tests were performed using five analysis groupings: Total, intra-duty-cycle, inter-duty-cycle, intra-month, and inter-month testing. For statistical analysis of both productivity and ash content, one-way analysis of variance (ANOVA) was used. In ANOVA tests of productivity, DW and AF productivity values were analyzed using a footprint basis for comparison of bays, sections, and shelves. For ANOVA testing using shelf productivity or ash values, pairwise comparison was performed using the Tukey Adjustment.

Following ANOVA tests for productivity and ash content, multiple linear regression was performed to investigate the effects of weekly averages of light and temperature. In multiple linear regression tests of productivity, DW and AF productivity values were analyzed using both footprint and substratum bases. For statistical analysis of liquid nutrient concentrations, one-way ANOVA was performed for influent; bays 1, 2, 3; and effluent samples. Lastly, statistical analysis using pH measurements was executed using

one-way ANOVA tests, followed by simple and multiple linear regression. The one-way ANOVA tests compared pH between and across liquid and biofilm pH measurements from various locations in the RABR system. The linear regression tests were performed to establish correlation of pH values with light, temperature, and productivity. All ANOVA tests were performed using a 95% confidence interval (CI). Statistical analyses were performed in SAS® Studio and Microsoft Excel, while data visualization was performed in Python and Microsoft Excel. The statistical analyses employed throughout this study are summarized in Figure 3.

3.1 Power Reduction using Duty Cycle

Results from the power reduction experiments are found in Figure 4. As expected, the lowest instantaneous power draw occurred at the lowest RPM and duty cycle. Because the two lowest power draws occurred at 25% and 50% duty cycles, these two duty cycles were chosen for testing in the fall of 2023. To maintain consistency between duty cycles, both 25% and 50% were both assigned a 20 min continuous cycle. As such, the 25% duty was programmed to rotate for 5 min and remain stationary for 15 min, while the 50% duty was programmed to rotate for 10 min and remain stationary for 10 min. To further reduce power draw, the RPM was held constant at 0.896 RPM.

3.2 Productivity

The complete results for productivity are reported in Table 1. Of note, the harvests associated with 50% duty cycle tests yielded maximum productivity across all productivity bases. The harvests associated with 25% duty cycle tests, conversely, yielded the lowest productivity across all productivity bases. With an additional 5 cyclical minutes of stationary operation compared with a 50% duty cycle, the algae

biofilms were more nutrient starved using a 25% duty cycle. As shown in previous studies, greater algae biomass growth contributed to ash-enhanced productivity (Hillman and Sims, 2020).

3.2.1 Bay Statistical Analysis

One-way ANOVA tests using productivity yielded no statistically significant differences between the three RABR bays using intra-duty-cycle, intra-month, total tests. This lack of statistical significance held true irrespective of DW and AFDW productivity analysis.

The lowest p-value observed of eight ANOVA tests was $p = 0.2744$, observed at the test involving all AFDW bay productivities observed during the fall of 2023. This lack of difference between bays is indicative of continuous flow stirred tank reactor (CFSTR) behavior. The intended purpose of the two polycarbonate sheets serving as dividers between the three bays to retrofit the RABR to plug-flow operations was not realized; the RABR's performance is not indicative of plug-flow reactor (PFR) behavior. Had productivity values between the three bays been statistically distinct, PFR behavior would have been validated. The only statistically results observed from bay comparisons were for inter-duty-cycle tests. In comparing all bays from 25% and 50% duty cycle tests, AFDW productivity yielded a p-value = 0.0255 and DW productivity yielded a p-value = 0.0041. Because duty cycle yielded productivity differences and months tested did not yield productivity differences, it is concluded the duty cycles had a greater effect on productivity.

3.2.2 Section Statistical Analysis

As with bay comparisons, one-way ANOVA tests for section productivity using intra-duty-cycle, intra-month, and total testing yielded no significant differences. These

sections, housing the shelves containing the growth substrata, were exposed to the same liquid medium and the only structural difference was placement on the RABR's rotating shaft. The lack of statistical distinction between sections makes intuitive sense, as the treatment conditions were identical. As in the bay comparisons, section productivity ANOVA yielded statistical significance for inter-duty-cycle testing, while inter-month testing yielded no statistical significance. The tests between 25% and 50% duty cycles showed significance using both DW and AFDW productivity ($p = 0.0005$ and 0.0066 , respectively).

3.2.3 Individual Shelf Analysis

For shelf analysis, the three RABR shelves showed strong statistical differences across total, intra-duty-cycle, and intra-month testing. Within all one-way ANOVA tests, the top shelf showed the highest productivity, followed by the middle and bottom shelves. In most tests, significant differences were observed for both the top and bottom shelves and the middle and bottom shelves. However, for 25% duty cycle testing, the only significant differences observed were between the top and bottom shelves. This lack of distinction between shelves indicates the 25% duty cycle caused the middle and bottom shelves to produce biomass indistinguishably from one another. It is possible the longer evaporation periods associated with the 25% duty cycle testing eliminated significant productivity differences between the middle and bottom shelves.

3.2.4 Light and Temperature Correlation

Multiple linear regression (MLR) of productivity values vs. light and temperature yielded varied correlation for duty cycles and months tested. Grouping productivity values using months produced the least significant correlation. None of the adjusted R-squared values

for these analyses was greater than 0. Conversely, grouping productivity values using duty cycles produced more significant correlation. The 50% duty cycle grouping showed insignificant correlation using DW analysis and slight correlation using AFDW analysis. Correlation was highest using the 25% duty cycle testing period, with the highest fidelity regression occurring using the AFDW analysis. It is likely the AFDW analysis provided slightly higher correlation than the DW analysis because, between the organic and inorganic phases of the biofilm, the organic phase is more directly influenced by light and temperature. The MLR analysis for the 25% duty cycle testing is visualized in Figure 5. As shown by ANOVA testing for productivity, the duty cycle used in operation had a greater effect on productivity than the month tested. For this reason, the duty cycle grouping in MLR had stronger correlation with the data than the month grouping. However, the 50% duty cycle MLR had considerably lower correlation than the 25% duty cycle. This lack of correlation could be attributed to the freezing temperatures. With the onset of freezing temperatures, the RABR was equipped with polycarbonate walls, causing greater light attenuation and heat insulation within the RABR. These factors may have caused the lack of fidelity from the 50% duty cycle MLR testing.

3.2.5 Biofilm Weight

The highest wet biofilm weight harvested from the pilot-RABR was 24 kg. This weight contributed to less than 3% of the total rotating assembly weight. Biofilm weight's insignificance is favorable for scale-up and further optimization. Unlike rotating biological contactors (RBC), the current and future embodiments of the RABR can avoid mechanical fatigue associated with biomass overloading (Mba et al., 1999).

3.3 Ash Content

The overall average ash content values were obtained using AW values, observed from weekly harvests of the 18 shelves of RABR. The total average ash percentage was 42.6%. Since each shelf ash content was monitored, the ash content values were used in further comparisons of RABR bays, sections, and shelves. The highest average ash content, 48.0%, was recorded for the month of December. The lowest average ash content, 38.2%, was recorded for the month of October. The average contents from duty cycle testing fell within this range, with 25% duty cycle testing yielding 40.6% and 50% duty cycle testing yielding 44.2% ash.

3.3.1 Ash Content Statistical Analyses

One-way ANOVA tests of bay ash content percentages yielded no statistically significant differences between bays for total testing, intra-duty-cycle testing, and intra-month testing. This lack of distinction is further evidence of the RABR's CFSTR behavior. For inter-duty-cycle testing, there was statistical significance between the bays ($p = 0.0069$). Likewise, the inter-duty-cycle testing yielded statistical significance between the bays ($p < 0.0001$). In these tests, the 50% duty cycle and December bays exhibited higher ash percentages. These results are indicative of ash-enhanced productivity at a 50% duty cycle. However, with statistical significance from bay comparison tests for both inter-duty-cycle and inter-month testing, it remains unclear if the duty cycle or time of year had greater influence on ash content from this analysis alone. As with the analysis of pH measurements, linear regression was employed to better understand the influences of duty cycle and time of year.

As shown in the bay comparisons, section comparisons yielded no statistically significant differences between sections for total, intra-duty-cycle, and intra-month testing.

Additionally, inter-duty-cycle and inter-month testing yielded statistical significance between sections ($p < 0.0001$ for both). For total and intra-duty-cycle testing, there were no statistically significant differences between individual shelf ash content. Similarly, there were no statistically significant differences between the shelves for October testing. This lack of statistical difference suggests non-freezing temperatures and high light conditions of October yielded uniformity of ash content between the shelves. For intra-month testing of December, however, there was statistically significant differences between the top and middle shelves, and the top and bottom shelves. The top shelves had the highest average ash content, followed by the middle and bottom shelves. Lower light conditions and freezing temperatures were likely the causes for this distinction.

3.3.2 Light and Temperature Correlation

Since all inter-duty and inter-month tests yielded statistical significance, it would seem both duty cycle and month tested were predictors for ash content. Yet, further analysis using MLR showed duty cycle better fit the overall ash content data. The average ash content MLR testing for the month groupings yielded insignificant to moderate correlation. By contrast, the duty cycle grouping yielded high correlation for 25% and 50% duty cycle testing (Adjusted R-squared = 0.9919 and 0.9950, respectively). Hence, month grouping of the average ash content data was not a favorable model for MLR. Grouping with respect to duty cycle provided a higher-fidelity linear model. The duty cycle MLR models, visualized in Python, are shown in Figure 5.

Interestingly, the 50% duty cycle grouping had virtually identical correlation to the 25% duty cycle grouping. This similarity between 50% and 25% duty cycle testing is contrary to what was observed for productivity using MLR. It is noted despite non-linear

productivity values, the 50% duty cycle yielded very linear ash content with respect to light and temperature. Though productivity lacked MLR consistency between duty cycles, ash content proved highly predictable using duty cycle grouping.

3.4 Nutrient Uptake

Nutrient uptake of nitrogen and phosphorus occurred through both biological metabolism and chemical precipitation. The average nitrogen concentration measured from the RABR's influent was 367 mg/L. The average phosphorus concentration in the influent was 15.5 mg/L. Average nutrient removals for nitrogen and phosphorus were 21.4% and 38.0%, respectively. Additionally, maximum nutrient reductions for nitrogen and phosphorus were 58.0% and 76.3%, respectively.

3.4.1 Liquid Nutrient Statistical Analyses

Using the sampling points shown in Figure 2a, five liquid samples were taken weekly for the RABR. These five samples allow overall and bay nutrient reduction analysis. For one-way ANOVA testing of all five samples, no significant differences were observed. This lack of significance was consistent for total, intra-duty-cycle, intra-month, inter-duty-cycle, and inter-month testing. Since no statistical distinctions could be made between nutrient sampling points, statistical analyses compared the bay nutrient reductions with the effluent nutrient reductions. These analyses yielded no statistical significance, strengthening the understanding of the RABR as a CFSTR. Then, the original analyses were repeated combining all bay samples with the effluent samples and comparing these "RABR samples" with the influent samples.

For nitrogen, the RABR samples showed a statistically significant difference from the influent samples ($p = 0.0372$). This statistical significance, shown using all liquid

samples obtained, validated nutrient removal had occurred. Using these RABR samples for nutrient removal, the average nitrogen removal was 30.9%. Further nitrogen analysis yielded no significant differences in inter-duty-cycle and inter-month testing.

As with nitrogen, RABR samples for phosphorus showed a statistically significant difference from the influent samples ($p = 0.0209$). This statistical significance, shown using all liquid samples obtained, validated nutrient removal had occurred. Using these RABR samples for nutrient removal, the average phosphorus removal was 35.0%. As shown using RABR samples for nitrogen, RABR samples for phosphorus yielded no significant differences in inter-month testing. But unlike RABR samples for nitrogen, the RABR samples for phosphorus showed significant differences in inter-duty-cycle testing ($p = 0.0190$). There are multiple interpretations to be made from this statistically significant result. First, the 50% duty cycle had higher phosphorus removal efficiency than the 25% duty cycle. Also, phosphorus removal from the liquid phase proved more predictable than nitrogen. Nitrogen was present in much higher concentrations in the filtrate influent but was unable to chemically precipitate as readily as phosphorus, nitrogen likely only precipitating in struvite. The phosphorus removal presumably occurred through the solid phase precipitation of calcium- and magnesium-phosphate inorganic salts. Additionally, phosphorus removal from the liquid phase could have occurred through biological luxury uptake (see Results and Discussion 3.4.5). Lastly, the significance of inter-duty-cycle testing for phosphorus favors operational effects over seasonal effects of nutrient removal.

3.4.2 Nutrient Uptake Power Requirements

Using power draws required to rotate the RABR assembly, power consumption for nutrient removal using 25% and 50% duty cycles were summarized in Table 2. For these calculations, liquid nutrient reductions were correlated to power requirements to rotate at the associated duty cycle. Hence, Table 2 offers a representation of power requirements to remove 1 kg liquid nutrient if the RABR were to continue performing as observed during liquid sampling.

Of note, the power consumption was optimized for nitrogen at a 25% duty cycle. Conversely, the power consumption was optimized for phosphorus using a 50% duty cycle. The 25% duty cycle may have efficiently removed nitrogen by operating in a stationary position and thereby encouraging evaporation of NH_3^+ . The 25% duty cycle also failed to remove phosphorus as efficiently as the 50% duty cycle. Phosphorus would likely require more contact with the filtrate to be taken up or precipitated; it is therefore plausible, relative to the 25% duty cycle, the 50% duty cycle's prolonged contact with the filtrate facilitated this enhanced phosphorus uptake.

Overall, the optimal expected power consumption for nitrogen, 1.36 kWh/kg_{TKN}, occurred during 25% duty cycle testing. Likewise, the optimal expected power consumption for phosphorus, 20.1 kWh/kg_{TP}, was observed during the 50% duty cycle testing. In relation to the only other study to specify power requirements for nutrient removal using an attached-growth algae cultivation system, this system proved very comparable. The RABR used in this study removed nitrogen slightly more efficiently (1.36 kWh/kg vs. 2.6 kWh/kg) and removed phosphorus slightly less efficiently (20.1 kWh/kg vs. 17.5 kWh/kg) under best-case operation (Christenson and Sims, 2012). If

further studies report analogous power requirements, there is strong potential for innovation in power optimization of attached-growth algae cultivation systems.

3.4.3 Inorganic Salt Quantification

Struvite quantities from within the algae biofilm are summarized in Table 3. Due to inconsistencies in the digestion of the ash for TKN, the results for struvite quantities obtained for the 25% duty cycle were imprecise. Hence, Table 3 summarizes struvite quantities for the 50% duty cycle only. As shown in Table 3, the average struvite percentage of the biofilm DW was 0.68%. The average theoretical struvite productivity, assuming all shelves of the RABR produced struvite as efficiently as the shelf sampled for struvite analysis, was 0.049 g/m²-day. This value is meaningful because it translates the RABR from strictly a water remediation tool to a veritable biorefinery for production of struvite-rich biofilm. Struvite percentages, obtained from 50% duty cycle tests, were converted to struvite-bound inorganic phosphorus. The average inorganic phosphorus percent as struvite was 4.92%. Using AW phosphorus content, the remaining inorganic phosphorus content was calculated to be 3.48% of biofilm DW.

By quantifying total inorganic nitrogen- and phosphorus-containing salts, the analysis accounts for all nutrient uptake of nitrogen and phosphorus through chemical precipitation. While non-struvite-bound phosphorus is not empirically measured, this analysis provides an understanding of total inorganic phosphorus compounds. Results from this study suggest an increase of ash productivity using a 50% duty cycle. Further studies can explore operating parameters to enhance mineral productivity as algae systems are integrated as biologically induced chemical reactors.

3.4.4 Nitrogen and Phosphorus Balances

Elemental balances, summarized in Table 4, offer validation of the elemental composition of the algae biomass harvested from the RABR. As shown in Table 4, the elemental balance for nitrogen was within one percent of the known algae stoichiometry. This precision is favorable for validation of AW nutrient concentrations discussed previously. Because the elemental balance closed favorably for nitrogen, the analysis successfully accounted for all nitrogen found in the organic and inorganic phases of the biofilm.

The phosphorus elemental balance did not match the algae stoichiometry as favorably as the nitrogen elemental balance. The biomass percentage of phosphorus observed was 3.3% w/w, while the stoichiometry percentage of phosphorus is approximately 1% w/w. However, this elevated level of phosphorus could be evidence of luxury phosphorus uptake (Solovchenko et al., 2019). This would be the first pilot-scale observation of luxury phosphorus uptake using an outdoor attached-growth algae cultivation system. However, with influent phosphorus levels well above K_m for microalgae, it seems unlikely the microalgae would store excess polyphosphate (Ermis and Altinbas, 2019). With high levels of bioavailable phosphorus, it is not possible to know definitively if luxury phosphorus uptake occurred. The possibility of luxury phosphorus uptake is favorable for attached-growth microalgae cultivation, and further studies should seek to validate these findings using outdoor pilot-scale systems.

3.5 pH Measurements

The average pH of the influent of the RABR was 8.14 (standard deviation = 0.20). Due to lack of statistical significance between bay and effluent pH samples, these pH samples were combined, constituting liquid “RABR samples,” as used in the liquid nutrient

analysis (see Results and Discussion 3.4.2). The lack of distinction between bays and effluent pH values are further evidence of CFSTR behavior. The average liquid pH for RABR samples ranged from 7.73 to 8.35, while the average biofilm pH ranged from 7.16 to 8.08. The observed decrease of pH from influent to liquid and biofilm pH could be attributed to evaporation of ammonia (NH_3^+). As ammonia exits the aqueous phase, the pH becomes more acidic. The pH change is not fully counteracted by the algae's absorption of CO_2 , which would cause the filtrate within the RABR system to become more basic.

3.5.1 pH Statistical Analyses

For ANOVA testing of all liquid samples taken from the five sampling points of the RABR (see Figure 2a), there was little statistical significance observed. Only pH samples from the month of October showed distinction between liquid samples from within the RABR and the influent (p-value = 0.0069). However, ANOVA testing between biofilm pH and influent pH showed statistical significance for total, October, and 25% intra-duty-cycle testing. In these statistically significant tests, it was shown that influent pH was consistently higher than the biofilm pH. Additionally, ANOVA testing between liquid and biofilm pH samples yielded highly significant results. In all tests performed, the average liquid pH was higher than the average biofilm pH. This difference suggests precipitation of organic salts such as struvite was more likely to occur in the liquid phase of the RABR, if only pH parameters are considered.

As with statistical analyses used for ash content, the inter-duty-cycle and inter-month testing both yielded statistical significance. For inter-duty-cycle testing, both the liquid and biofilm pH of the 50% duty cycle testing were higher than the liquid and biofilm pH

of the 25% duty cycle testing. Similarly, both the liquid and biofilm pH of the December testing were higher than the liquid and biofilm pH of the October testing. During the 50% duty cycle testing, it is likely the biofilm was more biologically active. Both the liquid and biofilm pH were significantly raised as more CO₂ was absorbed for biological metabolism by the algae biomass.

3.5.2 Light and Temperature Correlation

Total testing of pH values showed low to moderate correlation using MLR for both liquid and biofilm pH. Additionally, 25% duty cycle and October groupings showed insignificant to low correlation for both liquid and biofilm pH. By contrast, 50% duty cycle and December groupings showed high correlation for both liquid and biofilm pH. For 50% duty cycle testing, the adjusted R-squared values for liquid and biofilm pH were 0.8430 and 0.9159, respectively. For December testing, the adjusted R-squared values for liquid and biofilm pH were 0.8710 and 0.9930, respectively. Greater fluctuations in light and temperature, as seen in October testing, may have caused the inconsistency seen in pH. Ammonia evaporation may have also skewed results. By contrast, the walls installed in December, coupled with more consistent light and temperature conditions, may have eliminated drastic pH fluctuations. This normalization likely contributed to more predictable pH results using the multiple linear regression model. Additionally, the 50% duty cycle testing may have fostered more consistent biological activity in the biofilm, contributing to more predictable pH values using the MLR model. Interestingly, for the December and 50% duty cycle testing, the testing periods that appear to have best fit the MLR model, the correlation is higher for biofilm pH averages. This difference from

liquid pH averages suggests the algae biomass was more predictable in its response to light and temperature than was the liquid filtrate.

4. Conclusions

An outdoor pilot-scale RABR was implemented for nutrient uptake and productivity testing. The 25% and 50% duty cycles showed minimal power draw. Optimal power consumptions for nutrient uptake were 1.36 kWh/kg_{TKN} (nitrogen) and 20.1 kWh/kg_{TP} (phosphorus). Maximum footprint productivity was 7.09 g/m²-day. Statistical analysis distinguished operating parameters from seasonal effects and quantified productivity differences due to light attenuation. MLR established correlation between light/temperature levels and productivity, ash content, and pH. Nitrogen content was within 1% of microalgae stoichiometry, and phosphorus was elevated, suggesting luxury phosphorus uptake. Analysis of inorganic salts showed 0.68% w/w of the dry biofilm was struvite.

References

- APHA, 1997. Standard Methods for the Examination of Water and Wastewater.
- Barlow, J., Sims, R.C., Quinn, J.C., 2016. Techno-economic and life-cycle assessment of an attached growth algal biorefinery. *Bioresour. Technol.* 220, 360–368.
<https://doi.org/10.1016/j.biortech.2016.08.091>
- Boelee, N.C., Janssen, M., Temmink, H., Shrestha, R., Buisman, C.J.N., Wijffels, R.H., 2014. Nutrient Removal and Biomass Production in an Outdoor Pilot-Scale Phototrophic Biofilm Reactor for Effluent Polishing. *Appl. Biochem. Biotechnol.* 172, 405–422.
<https://doi.org/10.1007/s12010-013-0478-6>
- Cheah, Y.T., Chan, D.J.C., 2021. Physiology of microalgal biofilm: a review on prediction of adhesion on substrates. *Bioengineered* 12, 7577–7599.
<https://doi.org/10.1080/21655979.2021.1980671>
- Choudhary, S., Tripathi, S., Poluri, K.M., 2022. Microalgal-Based Bioenergy: Strategies, Prospects, and Sustainability. *Energy Fuels* 36, 14584–14612.
<https://doi.org/10.1021/acs.energyfuels.2c02922>
- Christenson, L., Sims, R., 2011. Production and harvesting of microalgae for wastewater treatment, biofuels, and bioproducts. *Biotechnol. Adv.* 29, 686–702.
<https://doi.org/10.1016/j.biotechadv.2011.05.015>
- Christenson, L.B., Sims, R.C., 2012. Rotating algal biofilm reactor and spool harvester for wastewater treatment with biofuels by-products. *Biotechnol. Bioeng.* 109, 1674–1684.
<https://doi.org/10.1002/bit.24451>

- Ennaceri, H., Ishika, T., Mkpuma, V.O., Moheimani, N.R., 2023. Microalgal biofilms: Towards a sustainable biomass production. *Algal Res.* 72, 103124. <https://doi.org/10.1016/j.algal.2023.103124>
- EPA, 1993a. Method 365.1, Revision 2.0: Determination of Phosphorus by Semi-Automated Colorimetry.
- EPA, 1993b. Method 351.2, Revision 2.0: Determination of Total Kjeldahl Nitrogen by Semi-Automated Colorimetry.
- Ermis, H., Altinbas, M., 2019. Determination of biokinetic coefficients for nutrient removal from anaerobic liquid digestate by mixed microalgae. *J. Appl. Phycol.* 31, 1773–1781. <https://doi.org/10.1007/s10811-018-1671-3>
- Espinosa-Ortiz, E.J., Gerlach, R., Peyton, B.M., Roberson, L., Yeh, D.H., 2023. Biofilm reactors for the treatment of used water in space: potential, challenges, and future perspectives. *Biofilm* 6, 100140. <https://doi.org/10.1016/j.biofilm.2023.100140>
- Gerardo, M.L., Van Den Hende, S., Vervaeren, H., Coward, T., Skill, S.C., 2015. Harvesting of microalgae within a biorefinery approach: A review of the developments and case studies from pilot-plants. *Algal Res.* 11, 248–262. <https://doi.org/10.1016/j.algal.2015.06.019>
- Goldsberry, P., Jeppesen, P., McLean, J., Sims, R., 2023. An attached microalgae platform for recycling phosphorus through biologically mediated fertilizer formation and biomass cultivation. *Clean. Eng. Technol.* 17, 100701. <https://doi.org/10.1016/j.clet.2023.100701>
- Hillman, K.M., Sims, R.C., 2020. Struvite formation associated with the microalgae biofilm matrix of a rotating algal biofilm reactor (RABR) during nutrient removal from municipal wastewater. *Water Sci. Technol.* 81, 644–655. <https://doi.org/10.2166/wst.2020.133>
- Johnson, M.B., Wen, Z., 2010. Development of an attached microalgal growth system for biofuel production. *Appl. Microbiol. Biotechnol.* 85, 525–534. <https://doi.org/10.1007/s00253-009-2133-2>
- Kannah, R.Y., Kavitha, S., Banu, J.R., Sivashanmugam, P., Gunasekaran, M., Kumar, G., 2021. A Mini Review of Biochemical Conversion of Algal Biorefinery. *Energy Fuels* 35, 16995–17007. <https://doi.org/10.1021/acs.energyfuels.1c02294>
- Katarzyna, L., Sai, G., Singh, O.A., 2015. Non-enclosure methods for non-suspended microalgae cultivation: literature review and research needs. *Renew. Sustain. Energy Rev.* 42, 1418–1427. <https://doi.org/10.1016/j.rser.2014.11.029>
- Kesaano, M., Sims, R.C., 2014. Algal biofilm based technology for wastewater treatment. *Algal Res.* 5, 231–240. <https://doi.org/10.1016/j.algal.2014.02.003>
- Lutzu, G.A., Ciurli, A., Chiellini, C., Di Caprio, F., Concas, A., Dunford, N.T., 2021. Latest developments in wastewater treatment and biopolymer production by microalgae. *J. Environ. Chem. Eng.* 9, 104926. <https://doi.org/10.1016/j.jece.2020.104926>
- Mba, D., Bannister, R.H., Findlay, G.E., 1999. Mechanical redesign of the rotating biological contactor. *Water Res.* 33, 3679–3688. [https://doi.org/10.1016/S0043-1354\(99\)00086-X](https://doi.org/10.1016/S0043-1354(99)00086-X)
- Mendoza, J.L., Granados, M.R., De Godos, I., Acién, F.G., Molina, E., Banks, C., Heaven, S., 2013. Fluid-dynamic characterization of real-scale raceway reactors for microalgae production. *Biomass Bioenergy* 54, 267–275. <https://doi.org/10.1016/j.biombioe.2013.03.017>
- Morales, M., Bonnefond, H., Bernard, O., 2020. Rotating algal biofilm versus planktonic cultivation: LCA perspective. *J. Clean. Prod.* 257, 120547. <https://doi.org/10.1016/j.jclepro.2020.120547>
- National Weather Service, 2023. NOWData - NOAA Online Weather Data.
- Patwardhan, S.B., Pandit, S., Ghosh, D., Dhar, D.W., Banerjee, S., Joshi, S., Gupta, P.K., Lahiri, D., Nag, M., Ruokolainen, J., Ray, R.R., Kumar Kesari, K., 2022. A concise review on the cultivation of microalgal biofilms for biofuel feedstock production. *Biomass Convers. Biorefinery.* <https://doi.org/10.1007/s13399-022-02783-9>

- Rezvani, S., Saadaoui, I., Al Jabri, H., Moheimani, N.R., 2022. Techno-economic modelling of high-value metabolites and secondary products from microalgae cultivated in closed photobioreactors with supplementary lighting. *Algal Res.* 65, 102733. <https://doi.org/10.1016/j.algal.2022.102733>
- Richard Kingsley, P., Braud, L., Kumar Mediboyina, M., McDonnell, K., Murphy, F., 2023. Prospects for commercial microalgal biorefineries: Integrated pilot demonstrations and process simulations based techno-economic assessment of single and multi-product value chains. *Algal Res.* 74, 103190. <https://doi.org/10.1016/j.algal.2023.103190>
- Roostaei, J., Zhang, Y., Gopalakrishnan, K., Ochocki, A.J., 2018. Mixotrophic Microalgae Biofilm: A Novel Algae Cultivation Strategy for Improved Productivity and Cost-efficiency of Biofuel Feedstock Production. *Sci. Rep.* 8, 12528. <https://doi.org/10.1038/s41598-018-31016-1>
- Schnurr, P.J., Molenda, O., Edwards, E., Espie, G.S., Allen, D.G., 2016. Improved biomass productivity in algal biofilms through synergistic interactions between photon flux density and carbon dioxide concentration. *Bioresour. Technol.* 219, 72–79. <https://doi.org/10.1016/j.biortech.2016.06.129>
- Sims, R., Peterson, B., 2021. Waste to value: algae-based biofuel utilizing oil and gas extraction wastewater. *Acad. Lett.* <https://doi.org/10.20935/AL4460>
- Solovchenko, A.E., Ismagulova, T.T., Lukyanov, A.A., Vasilieva, S.G., Konyukhov, I.V., Pogosyan, S.I., Lobakova, E.S., Gorelova, O.A., 2019. Luxury phosphorus uptake in microalgae. *J. Appl. Phycol.* 31, 2755–2770. <https://doi.org/10.1007/s10811-019-01831-8>
- Stumm, W., Morgan, J.J., 2012. *Aquatic Chemistry: Chemical Equilibria and Rates in Natural Waters*, 3rd ed. ed. Wiley, Hoboken.
- Ubando, A.T., Felix, C.B., Chen, W.-H., 2020. Biorefineries in circular bioeconomy: A comprehensive review. *Bioresour. Technol.* 299, 122585. <https://doi.org/10.1016/j.biortech.2019.122585>
- Udom, I., Zaribaf, B.H., Halfhide, T., Gillie, B., Dalrymple, O., Zhang, Q., Ergas, S.J., 2013. Harvesting microalgae grown on wastewater. *Bioresour. Technol.* 139, 101–106. <https://doi.org/10.1016/j.biortech.2013.04.002>
- Vassilev, S.V., Vassileva, C.G., Bai, J., 2023. Content, modes of occurrence, and significance of phosphorous in biomass and biomass ash. *J. Energy Inst.* 108, 101205. <https://doi.org/10.1016/j.joei.2023.101205>
- Wang, J., Liu, W., Liu, T., 2017. Biofilm based attached cultivation technology for microalgal biorefineries—A review. *Bioresour. Technol.* 244, 1245–1253. <https://doi.org/10.1016/j.biortech.2017.05.136>
- Zamalloa, C., Boon, N., Verstraete, W., 2013. Decentralized two-stage sewage treatment by chemical–biological flocculation combined with microalgae biofilm for nutrient immobilization in a roof installed parallel plate reactor. *Bioresour. Technol.* 130, 152–160. <https://doi.org/10.1016/j.biortech.2012.11.128>
- Zhuang, L.-L., Li, M., Hao Ngo, H., 2020. Non-suspended microalgae cultivation for wastewater refinery and biomass production. *Bioresour. Technol.* 308, 123320. <https://doi.org/10.1016/j.biortech.2020.123320>

Figure Captions

Fig. 1. Three-dimensional model of the pilot-scale rotating algae biofilm reactor (RABR).

Fig. 2. Complete RABR system, represented by (a) diagram and (b) photograph, located at Central Valley Water Reclamation Facility in Salt Lake City, Utah (40°42'19.9"N 111°54'35.3"W). In (a), "S" represents liquid sampling points.

Fig. 3. Representation of statistical analyses performed using empirical data obtained from the pilot-scale rotating algae biofilm reactor. Asterisks denote repeated tests using total, intra-duty-cycle, inter-duty-cycle, intra-month, and inter-month analysis groupings.

Fig. 4. Power reduction of pilot-scale RABR, obtained by modulating duty cycle and RPM of rotating assembly.

Fig. 5. Visualization of multiple linear regression tests to correlate RABR productivity/ash with average daily light integral (DLI) and average air temperature. Top-left: 25% Duty productivity, substratum basis; top-right: 25% Duty Productivity, footprint basis; bottom-left: 25% ash content, bottom-right: 50% ash content

Fig. 6. Visualization of multiple linear regression tests to correlate RABR ash content with average daily light integral (DLI) and average air temperature. The top two lines show two views of the 25% duty cycle testing and the bottom line shows two views of the 50% duty cycle testing.

Tables and Figures

Table 1. Average productivity values, obtained using mathematical combinations of 18 shelf yields harvested weekly during the fall season of 2023.

	Dry Weight Productivity		Ash-Free Dry Weight Productivity	
	Footprint Basis (g/m ² -day)	Substratum Basis (g/m ² -day)	Footprint Basis (g/m ² -day)	Substratum Basis (g/m ² -day)
Total	5.85	1.88	3.27	1.05
25% Duty Cycle	4.30	1.40	2.58	0.84
50% Duty Cycle	7.09	2.26	3.83	1.22
October	5.49	1.78	3.31	1.07
December	6.29	2.01	3.23	1.03

Table 2. Summary of expected power consumption using empirical liquid-phase nutrient removal data, where the rotating algae biofilm reactor (RABR) was operated at 25% and 50% duty cycles.

Nutrient Power Requirement	Associated Duty Cycle	Expected nitrogen power consumption (kWh/kg _{TKN})	Expected phosphorus power consumption (kWh/kg _{TP})
Minimum for nitrogen removal	25%	1.36	-
Minimum for phosphorus removal	50%	-	20.1
Average values	25%	1.89	106
Average values	50%	6.38	55.7
Percent Reduction using Average Power Consumption	25 to 50%	-	47.5%
	50 to 25%	70.4%	-

Table 3. Biofilm struvite (NH_4MgPO_4) quantification, using DW values for RABR shelves and TKN values of ashed biofilm from the same location of the rotating algae biofilm reactor (RABR) operating at a 50% duty cycle.

	Struvite Weight Harvested (g)	Struvite Percent of Dry Weight (%)	Theoretical Struvite Productivity ($\text{g/m}^2\text{-day}$) [^]
50% Duty Cycle Tests	0.152	0.22	0.018
	0.176	0.42	0.020
	0.816	1.14	0.093
	0.292	0.94	0.051
	0.507	0.71	0.062
Average	0.389	0.68	0.049
Standard Deviation	0.248	0.33	0.028

[^] - Calculated using struvite percent of total solids multiplied by RABR's overall DW footprint productivity (Hillman and Sims, 2020)

Table 4. Nitrogen and phosphorus balances, calculated using biofilm samples obtained from bay 1 of the outdoor pilot-scale rotating algae biofilm reactor (RABR).

Analyses	Dry Weight (DW)			Ash Weight (AW)			Biomass Nutrient Calculation		Biomass Percent Nutrient		Percent Difference of Average from Algae Stoichiometry	
	TP (mg/kg)	TKN (mg/kg)	DW (%)	TP (mg/kg)	TKN (mg/kg)	AW (%)	TP (mg/kg)	TKN (mg/kg)	TP (%)	TKN (%)	Percent Difference for P (%)	Percent Difference for N (%)
10/5/23	33700	52300	3.6	70800	-	37.0	7478	-	0.7	-		
10/12/23	31500	56200	2.7	-	-	39.4	-	-	-	-		
10/19/23	34000	63200	2.6	11600	51.9	36.1	29813	63181	3.0	6.3		
10/26/23	30600	63500	3.4	25700	226	35.7	21436	63419	2.1	6.3		
11/2/23	69800	57900	2.2	13500	427	44.5	63787	57710	6.4	5.8		
12/7/23	60300	60900	5.5	46900	1160	50.4	36667	60315	3.7	6.0		
12/14/23	52400	53600	4.5	36200	954	47.8	35083	53144	3.5	5.3		
12/20/23	51100	77600	4.7	27700	722	48.9	37555	77247	3.8	7.7		
12/28/2023 [^]	50800	63250	2.9	45200	1450	49.3	28523	62535	2.9	6.3		
Average	46000	61000	3.6	34700	713	43.2	33000	63000	3.3	6.3	273*	-0.9*
Standard Deviation	13300	7110	1.0	18000	471	5.8	15000	6910	1.5	0.7		

[^] - Averages of samples from bay 2 used for dry weight analyses

* - Percent difference compares biomass percent nutrient to algae stoichiometry of $C_{106}H_{263}O_{110}N_{16}P$ (Stumm and Morgan, 2012)

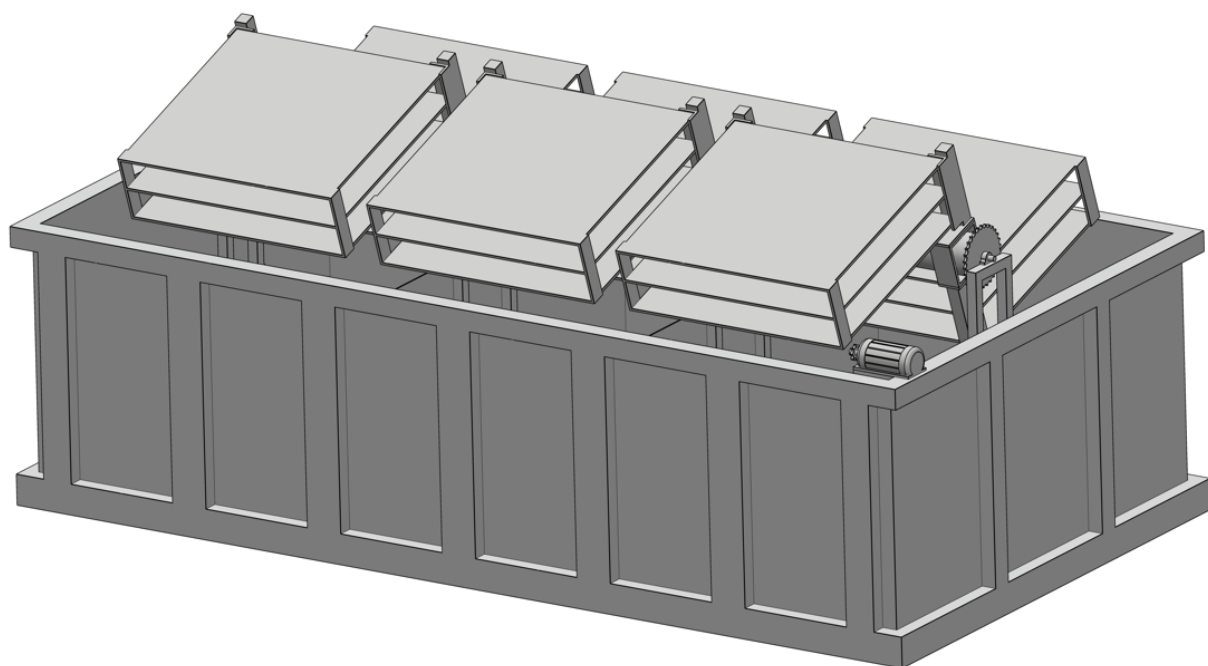
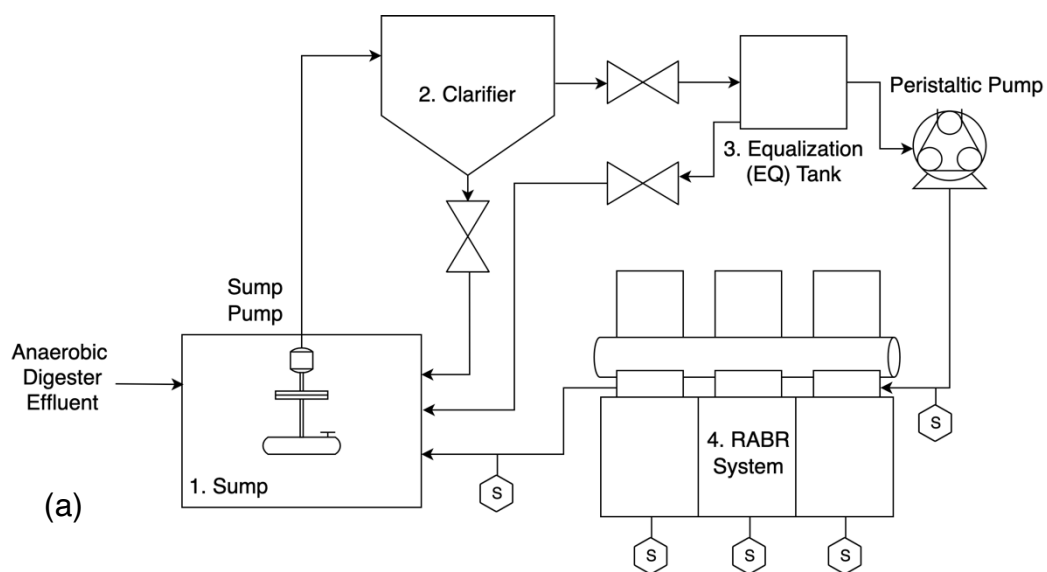


Fig. 1

**Fig. 2**

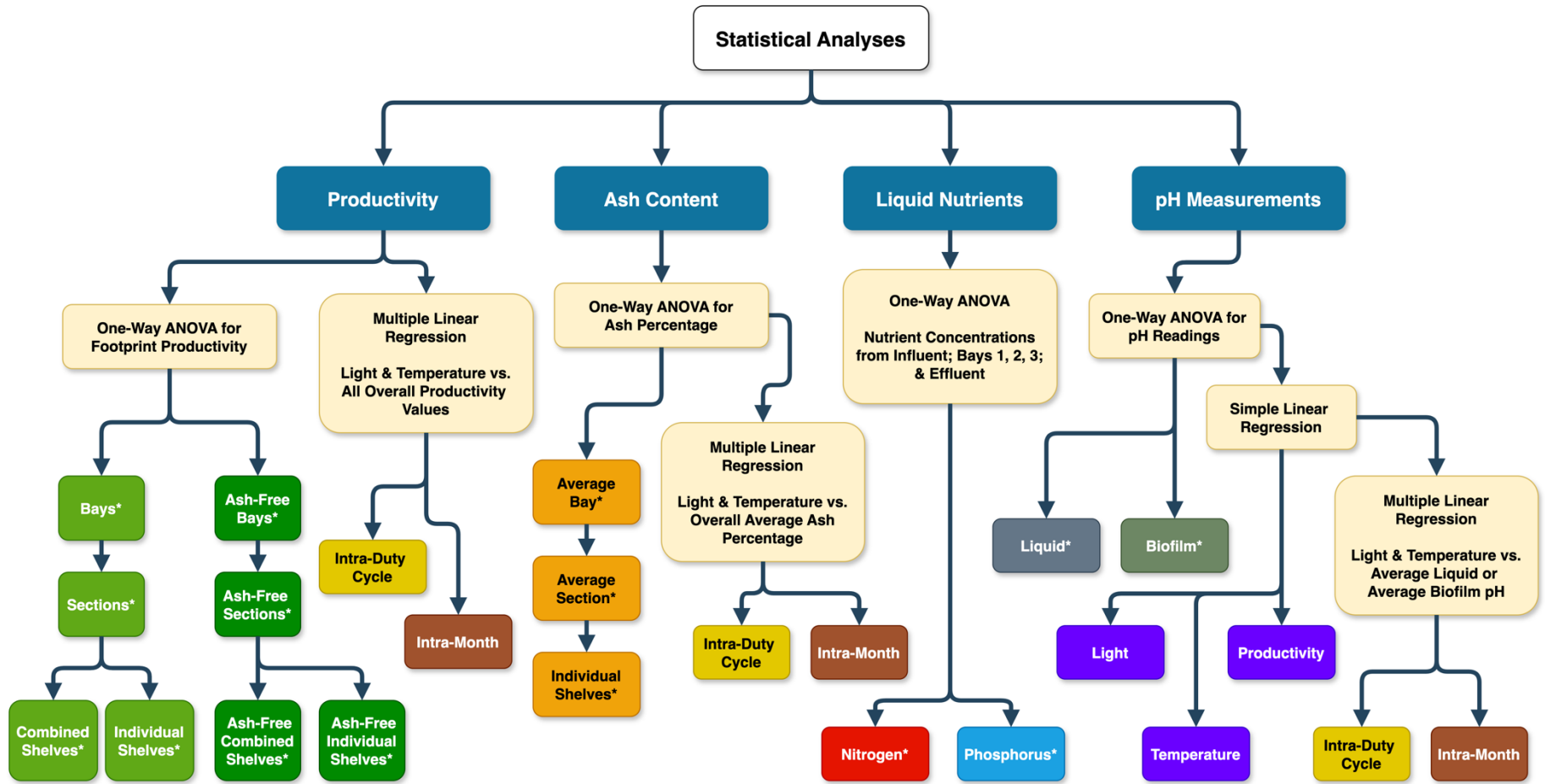


Fig. 3

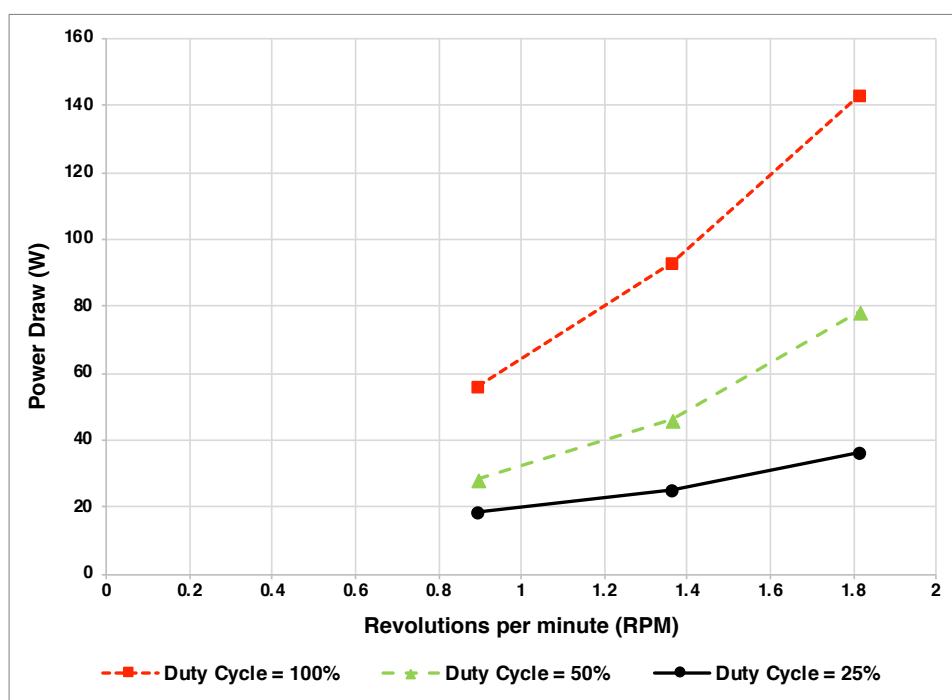


Fig. 4

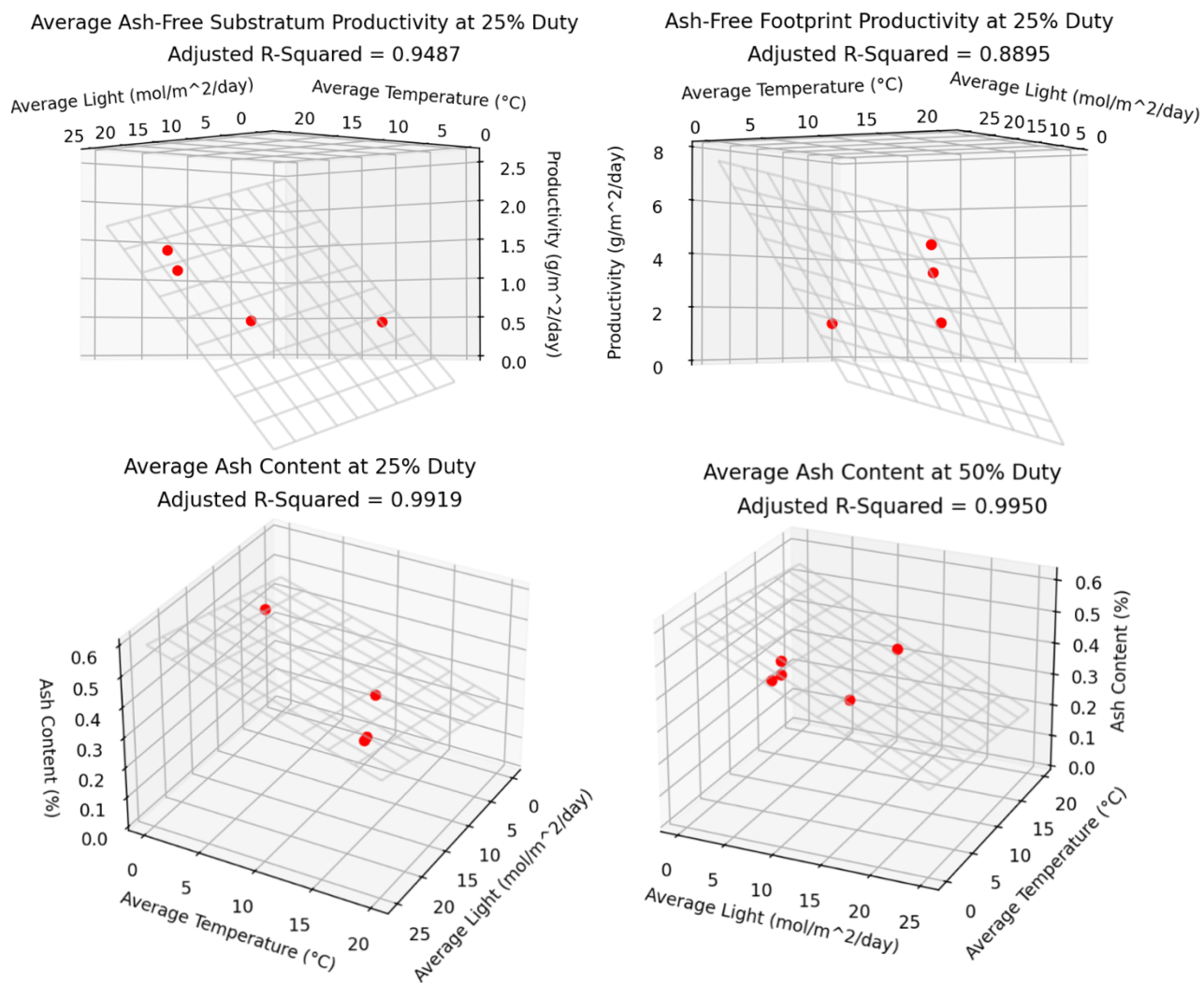


Fig. 5

Power Optimization of an Outdoor Pilot-Scale Rotating Algae Biofilm Reactor for Enhanced Productivity and Nutrient Uptake from Anaerobic Digestate

Authors: Peter F. Jeppesen*, J. Dietrich Storrer, Ronald C. Sims

* - Corresponding author, peter.f.jeppesen@gmail.com

Competing Interests: The authors have no known competing interests to declare.

Power Optimization of an Outdoor Pilot-Scale Rotating Algae Biofilm Reactor for Enhanced Productivity and Nutrient Uptake from Anaerobic Digestate

Authors: Peter F. Jeppesen*, J. Dietrich Storrer, Ronald C. Sims

* - Corresponding author, peter.f.jeppesen@gmail.com

Credit Author Statement:

Peter Jeppesen was responsible for writing the entirety of the manuscript. Dietrich Storrer provided several drafts of the introduction, from which content was used in the final introduction written by Peter F. Jeppesen. Ronald Sims supervised the writing process, offering necessary edits and adjustments to the manuscript.